TECHNICAL REPORTS SERIES NO. 461

Relative Biological Effectiveness in Ion Beam Therapy

Jointly sponsored by the IAEA and ICRU

IAEA
International Atomic Energy Agency

RELATIVE BIOLOGICAL EFFECTIVENESS IN ION BEAM THERAPY

TECHNICAL REPORTS SERIES No. 461

RELATIVE BIOLOGICAL EFFECTIVENESS IN ION BEAM THERAPY

JOINTLY SPONSORED BY THE
INTERNATIONAL ATOMIC ENERGY AGENCY
AND THE INTERNATIONAL COMMISSION
ON RADIATION UNITS AND MEASUREMENTS

INTERNATIONAL ATOMIC ENERGY AGENCY
VIENNA, 2008

COPYRIGHT NOTICE

Sales and Promotion, Publishing Section
International Atomic Energy Agency
Wagramer Strasse 5
P.O. Box 100
1400 Vienna, Austria
fax: +43 1 2600 29302
tel.: +43 1 2600 22417
email: sales.publications@iaea.org
http://www.iaea.org/books

Printed by the IAEA in Austria
February 2008
STI/DOC/010/461

IAEA Library Cataloguing in Publication Data

Relative biological effectiveness in ion beam therapy / jointly sponsored by the International Atomic Energy Agency and the International Commission on Radiation Units and Measurements. — Vienna : International Atomic Energy Agency, 2008.
p. ; 24 cm. — (Technical reports series, ISSN 0074–1914 ; no. 461)
STI/DOC/010/461
ISBN 978–92–0107807–0
Includes bibliographical references.

1. Ion bombardment — Therapeutic use. I. International Atomic Energy Agency. II. Series : Technical reports series (International Atomic Energy Agency) ; 461.

IAEAL 08–00503

FOREWORD

The use of ion beams for radiation therapy was first explored at the University of California's Lawrence Berkeley National Laboratory, in the United States of America, and is currently undergoing investigation at institutions in both Japan and Germany with other facilities which are under development or planned. With respect to a role in radiation therapy, ion beams have two important features arising both from the physical aspects of their dose distribution in the patient and from potentially advantageous biological phenomena resulting from their high rate of energy deposition (high linear energy transfer (LET)) over a portion of the particle track which can often be located in the tumour volume. Probably the most important of these biological phenomena is a markedly increased efficiency of cell killing. The concept of relative biological effectiveness (RBE) has been introduced to account for this increased efficiency. RBE is defined as the ratio of a dose of photons to a dose of any other particle to produce the same biological effect. RBE is a simple concept but its clinical application is complex because it is a function of particle type, energy, dose, dose per fraction, fraction number, cell or tissue type, and varies between early and late reactions following therapy.

Future developments in ion therapy will require a coherent approach to the reporting of therapies and their outcomes for comparison not only with other ion facilities but also with conventional and newly developing photon irradiation techniques. The International Commission on Radiation Units and Measurements (ICRU) has been involved in the production of a series of reports aimed at rationalizing the reporting of various forms of radiation therapy. Collaboration between the IAEA and the ICRU was initiated for proton therapy.

The present publication reflects a continuation of the collaboration between the IAEA and the ICRU, and represents a beginning step in an attempt to standardize the reporting of ion beam radiotherapy using concepts previously developed by the ICRU for reporting other therapies but with special emphasis on the use and reporting of weighting factors related to RBE. Such standardization will facilitate the comparison of therapeutic results obtained with ions not only between centres using this approach but also with centres using other modern forms of radiation therapy, such as proton and intensity modulated radiation therapy with photon beams.

A Technical Meeting on Relative Biological Effectiveness in Ion Beam Therapy, jointly sponsored by the IAEA and the ICRU, was held in Vienna, in June 2004. The meeting dealt primarily with the review of experimental measurements of RBE and approaches to the clinical use of the concept of RBE based on experimental findings, theoretical models and previous clinical

experience with fast neutrons and ions. Four of the papers presented at this meeting appear as Annexes I–IV in this publication. They were selected as examples related to methods used in different research centres.

This publication was prepared by an editorial group comprising E. Blakely of the Lawrence Berkeley National Laboratory, J. Hendry of the IAEA, and P. DeLuca, R. Gahbauer, B. Michael, A. Wambersie and G. Whitmore of the ICRU. The group was chaired by G. Whitmore. The IAEA officer responsible for this publication was J. Hendry of the Division of Human Health.

CONTENTS

1. RELATIVE BIOLOGICAL EFFECTIVENESS IN ION BEAM THERAPY

1.1. INTRODUCTION

1.1.1. Role of radiation therapy in the treatment of cancer

Surgery, radiation therapy and chemotherapy are the standard methods of cancer treatment. Rapid advances are being made in our understanding of the evolution of cancer that may soon translate into more effective treatments. However, radiation therapy will almost certainly continue to be a most important, effective and cost effective treatment modality for all types of solid malignancies. Its importance in the local control of primary solid malignancies will most likely increase in the future if more effective chemotherapeutic or other systemic treatment options become available to treat metastatic disease.

With increased longevity of the population resulting from improved control of epidemics and infectious diseases, the frequency of cancer (and the suffering often associated with it) has raised cancer awareness in the twentieth century [1.1].

In the United States of America, in 1991, more than one million invasive cancers occurred, i.e. an incidence of about 400 per 100 000 per year. In addition, more than 600 000 non-melanoma skin cancers occurred, most of them now curable. In industrialized countries, the probability of dying from cancer is 20–25%. In developing countries, cancer cases have risen from two million in 1985 to five million in 2000, and are projected to number ten million in 2015.

It has been estimated that about 45% of all cancer patients can be cured (excluding those suffering from non-melanoma skin cancers). Since that estimate was presented, cancers may be diagnosed somewhat earlier in industrialized countries, but the overall conclusion is still representative of what can be accomplished.

Radiation therapy contributes to the cure of approximately 23% of all cancer patients, when used alone (12%) or in combination with surgery (6%) or chemotherapy–immunotherapy (5%). Thus, about half of the cancer patients who are cured benefit from radiation therapy. This proportion illustrates the important role of radiation therapy in cancer management.

Sixty-five per cent of cancer patients present themselves for the first consultation with a localized tumour. Of that 65%, about one third fails, i.e. nearly 25% of the total number of cancer patients. One challenge of the coming

years is to improve this situation by increasing the effectiveness of 'local' treatments, i.e. radiation therapy and/or surgery [1.2].

Besides increasing the 'cure rate', it is important to improve treatment tolerance to facilitate combined treatments with systemic treatment options and to reduce the long term sequelae of all treatments.

1.1.2. Present situation and future trends

At present, in industrialized countries, about 70% of cancer patients are referred to a radiation therapy department for at least part of the treatment. The majority is treated with 'conventional' photon beam therapy, which for that reason remains the reference radiation treatment modality.

History has shown that the major improvements in the efficacy of radiation therapy were always associated with significant progress in technology [1.3–1.5]. Improvements in the physical selectivity, from orthovoltage X rays to ^{60}Co and high energy linear accelerators, combined with more effective diagnostic tools and radiation delivery methods have continuously improved the results of photon therapy.

The culmination of these modern developments in photon therapy is intensity modulated radiation therapy (IMRT), which optimizes several parameters: selection of multiple beams and, for each beam, optimization of dose and dose rate, homogeneity, field size, shape, etc. New technologies have emerged to optimally implement IMRT, sometimes in combination with stereotactic techniques. Proton therapy is perhaps the most advanced of these options and is viewed by many as the optimum modality to deliver state of the art low linear energy transfer (LET) radiation therapy (Fig. 1.1).

These new techniques are rapidly becoming available in an increasing proportion of hospitals, at least in industrialized countries.

The impressive development and progress in conformal therapy with photons and protons, however, raises a difficult issue: the extent to which photon or proton beam therapy has reached a plateau in development (at least as far as physical selectivity is concerned). This important question is still controversial. If, with the use of IMRT, photon or proton therapy has indeed reached a plateau in development, little additional clinical benefit can be expected from further technical developments with low LET radiation delivery methods [1.6]. A search for improvement should be directed to alternative radiation modalities such as ion beam therapy [1.7].

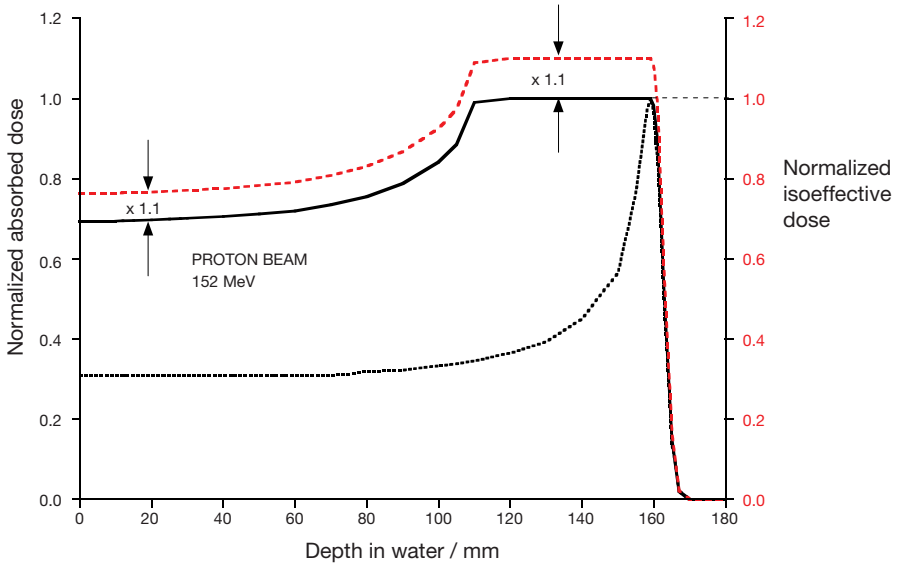

FIG. 1.1. Variation in depth of the absorbed dose of a monoenergetic (dotted line) and a spread out clinical (solid line) proton beam of 152 MeV and the corresponding weighted dose for radiation quality (RQ) (red dotted line, right ordinate). The RQ weighted dose (or RBE weighted dose) is obtained assuming a weighting factor $W_{RQ} = 1.1$ at all depths, protons being delivered with the same fractionation conditions as photons (courtesy P. Andreo).

1.1.3. Rationale for ion therapy

One such development currently under investigation in several centres and under consideration in others is the use of ion beam therapy. Ions, as considered in this report, are charged atoms accelerated to high energies in various types of accelerators. Such particles have a number of potential advantages for use in radiotherapy arising both from the physical aspects of their energy deposition and from biological phenomena resulting from the high density of energy depositions. In contrast to conventional photon radiations where the dose distribution in the patient is primarily characterized by an exponential decline in dose with depth, charged particles demonstrate a phenomenon known as the Bragg peak. Particles at high energy deposit relatively little energy as they enter an absorbing material but tend to deposit extremely large amounts of energy in a very narrow peak, the Bragg peak, as they reach the end of their range (Fig. 1.2). The depth and magnitude of this Bragg peak is determined by the mass and charge, as well as the initial energy of the particle [1.8].

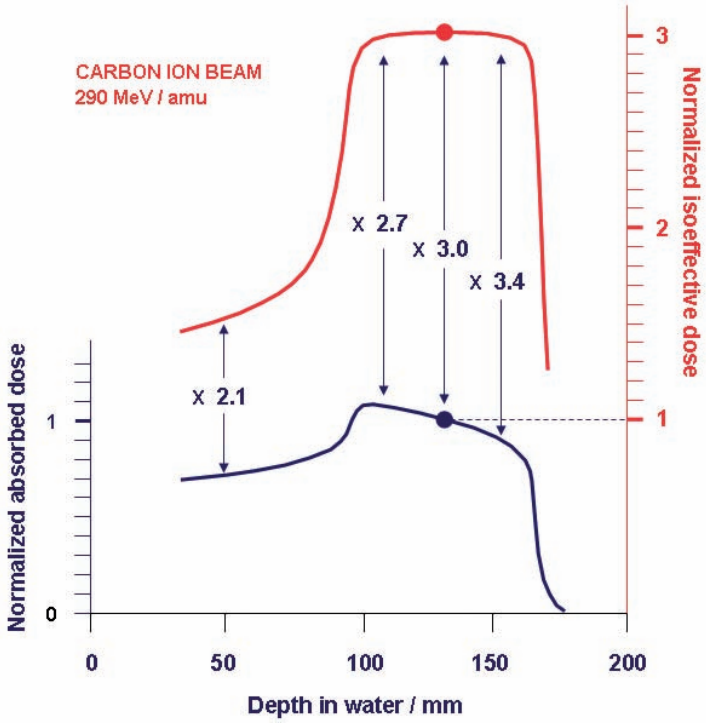

FIG. 1.2. Comparison of the absorbed dose and isoeffective dose variations with depth in a carbon ion beam. Carbon ion irradiation of a PTV located between 100 and 160 mm in depth using a 290 MeV/amu beam. The presentation is similar to Fig. 1.1. However, the RBE of a carbon beam significantly increases with depth. Therefore, in order to obtain a uniform 'isoeffective dose' (plateau) across the SOBP, the absorbed dose needs to be adapted (modulated) and decrease with depth. The weighting factors used to derive the isoeffective dose at different depths are indicated in the figure [1.12] (for more details, see Annex IV).

There is also the question of terminology. Following the terminology of the physics community [1.9], electrons, protons, neutrons (and many other particles) are identified as elementary particles. Ions are the nuclei of atoms with some or all of the atomic electrons removed. Nuclei are made up of the elementary particles neutrons and protons. Different types of ions have been called light ions or heavy ions, and the border between these types is to some extent arbitrary and a matter of convention or consensus. A group from Berkeley [1.10] proposed to call light ions those nuclei with an atomic number equal to, or smaller than, that of neon nuclei (Z = 10), such as carbon ions, leaving the name of heavy ions to heavier charged particles, such as silicon or

argon nuclei. This proposal seems reasonable, is recommended [1.11] and has been adopted in this publication.

In the case of carbon and other ions, the high rate of energy loss towards the end of the particle range results in a dramatic increase of the LET. While the Bragg peak is extremely narrow for a monoenergetic beam of particles, a variety of techniques can be used to moderate the energy and thus the range of the incident particles. The layering of a succession of Bragg peaks of varying intensity can thus result in the spreading of high dose over a sufficiently wide region to encompass a target volume (tumour) at a selected depth — the so-called spread out Bragg peak (SOBP) (Fig. 1.2). Spreading of the Bragg peak results in a lowering of the average LET over the SOBP, but this LET is still much higher than for photons and also for the particles in the entrance region of the beam. The result of all of this is that ions have as good or better distribution of absorbed dose as protons and superior to that of photons, and when the biologically weighted absorbed dose is considered, this superiority is further enhanced.

Not only does the high LET seen at the end of particle ranges affect the absorbed dose distribution, it also has marked consequences for the response of biological systems to that dose. Among these known biological consequences are a reduction in the oxygen enhancement ratio (OER) and a reduction in the variation in cell cycle sensitivity seen with photon radiation. Reduction in the OER may be beneficial in the treatment of certain tumours suspected of possessing radiation resistant regions containing hypoxic cells. Reduction in the variation of cell cycle sensitivity may also be advantageous in the treatment of certain tumour types, notably slowly growing tumours.

In addition to a reduction in the OER and variation in cell cycle sensitivity seen with ion radiation, a major advantage or concern with the use of high LET radiations is their increased efficiency in producing cell kill and a variety of other biological phenomena. This may be an advantage with respect to absorbed dose delivered to the cancer cell population and a disadvantage for dose absorbed in normal tissue. Both issues are of concern. The concept of relative biological effectiveness (RBE) has been introduced to account for the increased efficiency of high LET radiations vis-à-vis photons. The RBE is defined as the ratio of absorbed dose of a reference beam of photons to the absorbed dose of any other radiation, notably high LET radiations, to produce the same biological effect [1.13]. As defined, the RBE is a simple concept, however, its apparent simplicity is deceptive. RBE cannot be uniquely defined for a given radiation. The RBE of a given type of radiation will vary with particle type and energy, dose, dose per fraction, degree of oxygenation, cell or tissue type, biological end point, etc. In the case of ion irradiation, the situation

is particularly complex and the RBE is a strong function of position within the treatment beam [1.14].

Ions are not the only therapeutic radiation characterized by high LET radiation effects. Neutrons were the first high LET radiation to be used therapeutically. Neutrons lack the advantages of ions in terms of improved dose distribution but they have some of the potential biological advantages associated with high LET radiations. Clinical trials with neutrons have indicated their advantage in the treatment of certain types of tumour and this information may be of use in the selection of patients for ion irradiation. For this reason, some of the information gathered from biological experiments and clinical trials will be discussed in Sections 4 and 5.

If radiation oncologists are to benefit from the vast experience with photon radiations and the knowledge gained with respect to doses required for tumour cure and the tolerance of normal tissues, then it becomes mandatory to have the ability to convert doses of photon radiation into equally effective doses of other radiations, namely, ions — hence, the need for the concept of RBE and weighting factors based on RBE. A weighting factor for RBE is, however, only one of several weighting factors required in radiation oncology. Section 2 provides a general discussion of weighting factors and their application in radiation therapy.

REFERENCES

[1.1] LEVIN, V., MEGHZIFENE, A., IZEWSKA, J., TATSUZAKI, H., Improving cancer care: Increased need for radiotherapy in developing countries, Int. At. Energy Agency Bull. **43** 2 (2001) 25–32.

[1.2] WAMBERSIE, A., GRÉGOIRE, V., BRUCHER, J.M., Potential clinical gain of proton (and heavy ion) beams for brain tumours in children, Int. J. Radiat. Oncol. Biol. Phys. **22** 275 (1992).

[1.3] TUBIANA, M., DUTREIX, J., WAMBERSIE, A., Introduction to Radiobiology, Taylor & Francis, London (1990).

[1.4] PÖTTER, R., AUBERGER, T., WAMBERSIE, A. (Eds), Hadrons — A challenge for high-precision radiotherapy, Strahlenther. Onkol. **175** Suppl. II (1999).

[1.5] WAMBERSIE, A., GAHBAUER, R., Hadrons (protons, neutrons, heavy ions) in radiation therapy: Rationale, achievements and expectations, Radiochem. Acta **89** (2001) 245–253.

[1.6] GAHBAUER, R., A challenge for high-precision radiation therapy: The case for photons, Strahlenther. Onkol. **175** (1999) 121–122.

[1.7] WAMBERSIE, A., MENZEL, H.G., GAHBAUER, R.A., DELUCA, P., WHITMORE, G., "RBE and harmonization in prescribing, recording and reporting hadron therapy", in Progress in Radio-Oncology VII (KOGELNIK, H.D., LUKAS, P., SEDLMAYER, F., Eds), Monduzzi Editore, Bologna (2002) 361–371.

[1.8] REGLER, M., BENEDIKT, M., POLJANC, K., Medical accelerators for hadron therapy with protons and carbon ions (with an introduction to the physical advantages of heavy charged-particle radiation), Hephy-PUB-757/023, CERN Accelerator School, Seville, Spain (2002).

[1.9] PERL, M.L., "Hadrons", Encyclopedia of Physics (2nd edn) (LERNER, R.G., TRIGG, G.L., Eds), VCH Publishers, Inc. (1990), 468–469.

[1.10] CHU, W.T., "Hadron therapy", Biomedical Uses of Radiation, Part B Therapeutic Applications (HENDEE, W.R., Ed.), Wiley VCH, New York, Weinheim (1999) 1055–1131.

[1.11] WAMBERSIE, A., DELUCA, P.M., ANDREO, P., HENDRY, J.H., 'Light' or 'heavy' ions: A debate of terminology?, Radiother. Oncol. **73** (Suppl. 2) (2004) iv.

[1.12] TSUJII, H., et al., Overview of clinical experience on carbon ion radiotherapy at NIRS, Radiother. Oncol. **73** (Suppl. 2) (2004) 41–49.

[1.13] INTERNATIONAL COMMISSION ON RADIATION UNITS AND MEASUREMENTS, Quantitative Concepts and Dosimetry in Radiobiology, ICRU Report 30, Bethesda, MD (1979).

[1.14] GUEULETTE, J., OCTAVE-PRIGNOT, M., DE COSTER, B.M., WAMBERSIE, A., GRÉGOIRE, V., Intestinal crypt regeneration in mice: A biological system for quality assurance in non-conventional radiation therapy, Radiother. Oncol. **73** (Suppl. 2) (2004) 148–154.

2. BIOLOGICAL WEIGHTING OF ABSORBED DOSE: THE SPECIFIC ISSUE OF RBE IN ION BEAM THERAPY

2.1. ABSORBED DOSE

Absorbed dose, expressed in joules per kilogram, is a quantity that is rigorously defined [2.1] and used to quantify the dose in any type of material, including biological objects, patients and other humans, to ionizing radiation.

The quantity, 'absorbed dose', was introduced by the International Commission on Radiation Units and Measurements (ICRU) in 1953, with the special unit 'rad'. A new special unit, the 'gray' (Gy), equal to 1 J/kg, was introduced in 1972 to be in accordance with the International System of Units (SI).

Absorbed dose is a fundamental physical quantity that can be used in all fields where ionizing radiations are used. It is related to the physical, chemical and biological effects induced by the radiation. The concept of absorbed dose thus has broad applications and is widely used.

Absorbed dose can be measured with high accuracy and different methods have been developed to measure absorbed dose at the point or in the region of interest. Metrological institutions provide absorbed dose standards and calibration of instruments in terms of absorbed dose.

The required accuracy of dose determination depends on the particular application, and the accuracy achievable is dependent upon the method employed and the experimental conditions. The accuracy requirements in radiation therapy and in radiation protection are obviously not the same. The requirements are far more stringent in radiation therapy, especially when used with curative intent where differences in absorbed dose of 10% — and even 5% — can be detected clinically [2.2, 2.3].

For several decades, the quantity, absorbed dose, has been shown to be useful in radiation therapy, as well as in radiation protection and radiobiology. Most of our current knowledge (and in particular, clinical experience) in radiation therapy, and also in radiation protection, is based on dose–effect relations, documenting that absorbed dose is an effective measure of radiation exposure. There is no doubt that absorbed dose will continue to be the fundamental quantity in radiation dosimetry for all types of applications.

Absorbed dose is the expectation value of a stochastic quantity, energy imparted, and it therefore does not take account of the random fluctuation of the interaction events of the radiation and the energy distributions in cellular and subcellular volumes. If, for a given absorbed dose, the number of energy deposition events in such small volumes is highly variable (low dose and/or

high LET particles), the required averaging may be not meaningful and the concept of absorbed dose has limitations. The dose range in which this limitation is important depends on the size of the microscopic volume considered (and thus, implicitly, which biological reactions are considered to be relevant) and on the LET or ionization density of the charged particles involved. Various pragmatic, empirical approaches have been adopted to overcome this problem. They are outside the scope of this section.

2.2. NEED FOR WEIGHTING FACTORS

Absorbed dose is a fundamental quantity in radiation therapy: the biological–clinical effects are directly related to absorbed dose.

There is, however, no unique relationship between absorbed dose and induced biological effects. The biological effects depend on absorbed dose but also on several other factors, such as fractionation, dose rate, radiation quality, biological system and end points.

In the most general sense, absorbed dose weighting factors are used to correlate an absorbed dose delivered under given conditions with an absorbed dose delivered under another condition to produce the same biological effect.

Weighting factors can serve two functions: either retrospective or prospective. Retrospectively, they can be used to relate a new treatment regime to a reference protocol. Prospectively, they can be used to aid in the prediction of the dose required in a new protocol to achieve the same results as a reference protocol.

A universally agreed approach for the use of weighting factors would facilitate exchange of information and improve collaboration between centres and within the radiation oncology community.

For some well established therapy modalities (e.g. fractionated photon beam therapy, and — to a lesser extent — brachytherapy), there is a general agreement on the methodology to be used in deriving weighting factors. This is discussed in Sections 2.3–2.5. It is based on the linear quadratic model coupled with a repair function [2.4], and the use of agreed numerical values for the involved quantities.

Although the specificity of each therapy modality is recognized, an approach (that is as similar as possible) should be sought to account for the different biological effectiveness when non-conventional radiations such as neutrons and ions are used. So far, the effects of radiation quality are accounted for using a diversity of (almost hospital specific) methods.

2.3. REFERENCE IRRADIATION CONDITIONS

As explained previously, weighting factors can be used in conjunction with any two radiations. The use of weighting factors in several contexts relevant to radiation therapy is discussed in the following sections. Several different weighting factors are described. These contexts include altered fractionation schemes using photon irradiation, altered dose rates during brachytherapy and, finally, the use of weighting factors in particle therapy.

In the case of particle therapy, weighting factors are required to accommodate changes in radiation quality and often major changes in the fractionation scheme and perhaps subjective changes introduced by the oncologist to account for major changes in dose distributions from those seen with photon irradiations. Currently, weighting factors are being applied in various centres using particle radiations, but they are being applied in an often inconsistent manner leading to confusion in interpretation and possible risk to patients.

In order to reduce the possibility of confusion, to aid in the prospective determination of doses when changing to a new radiation protocol and to aid in the comparison of efficacies of various radiation therapy protocols, it is desirable to have a reference radiation protocol to which all other protocols would be referred. There is currently common agreement on the nature of a reference protocol for external beam therapy. The delineation of this reference protocol leads to the requirement for weighting factors which relate doses for non-conventional radiation protocols to the reference protocol.

The term 'isoeffective dose weighting factor', with the symbols W_{IsoE} or W(IsoE), is recommended in Section 3, to be used for such weighting factors, but only with reference to the reference therapy protocol.

2.3.1. Radiation quality

Fractionated irradiation with external photon beams is currently applied to more than 80% of the patients referred to radiotherapy departments, at least for part of the treatment. Photon beams are, therefore, taken as the reference radiation quality and the benefit of any new technique has to be evaluated relative to fractionated photon beam therapy. There is no evidence of a significant RBE difference between ^{60}Co γ rays and 2–30 MV photons.

2.3.2. Reference fractionation scheme

The reference fractionation scheme consists of fractions of 2 Gy/d, five times per week, specified in the planning target volume (PTV).

2.4. FRACTIONATED EXTERNAL PHOTON THERAPY

The influence of the amount of dose per fraction on the effects on tumour and normal tissues is well documented and, when a non-conventional fractionation is used, a weighting factor has to be applied to the absorbed dose to allow for the related difference in biological effect.

The influence of overall time (total duration of treatment in days) on the biological effect is discussed briefly in Section 2.6. A discussion of combinations of radiation and drugs is outside the scope of this section.

2.4.1. Weighting factor for differences in dose per fraction

There is now widespread agreement to base the weighting for differences in fraction size on the linear quadratic (α/β) model, in order to weight absorbed dose for differences in fraction size (see Ref. [2.5]). In the model, the fraction of surviving cells, S, after a dose, d, is given by:

$$S = \exp - (\alpha d + \beta d^2) \tag{2.1}$$

When a non-conventional fractionation is applied, in order to obtain the same clinical effect as with 2 Gy per fraction, a weighting factor, $W_{\alpha/\beta} = D'/D$, can be derived from the equation:

$$D[1 + d/(\alpha/\beta)] = D'[1 + d'/(\alpha/\beta)] \tag{2.2}$$

where D and D′ and d and d′ are the total doses and the doses per fraction for the 'reference' fractionation and the test fractionation, respectively. In the absence of more specific information, the ratio α/β is currently often taken to be equal on average to 10 Gy for early responding tissues, and 3 Gy for late responding tissues. It is assumed that, for many tumours, the ratio α/β is the same as for early responding tissues.

The product, $D_{\alpha/\beta} = D'W_{\alpha/\beta}$, expressed in gray, is the isoeffective dose for the modified fractionation scheme. Subscripts (e.g. $D_{\alpha/\beta = 3}$ or $D_{\alpha/\beta = 10}$) may be useful to indicate whether the dose weighting is done for late or early effects, and to avoid confusion between the (physical) absorbed dose and the isoeffective dose, both being expressed in gray [2.6, 2.7].

2.4.2. Example

A planned treatment of 70 Gy given in 2 Gy fractions is to be replaced by a treatment delivered at 3 Gy per fraction. Applying Eq. (2.2) and assuming $\alpha/\beta = 3.5$ Gy (for a specific late effect):

$$70(1 + 2/3.5) = D'(1 + 3/3.5) \quad (2.3)$$

The total dose, D′, to give an equal probability of late fibrosis in normal tissue would be 59 Gy, i.e. an approximately 15% lower total dose. Thus $W_{\alpha/\beta} = 1.19$ for late effects. The total dose, D′, would be 65 Gy for equal early effects, or equal effects on the tumour ($\alpha/\beta = 10$ Gy). Thus $W_{\alpha/\beta} = 1.08$ for early effects. The difference between 59 and 65 Gy (≈10%) illustrates how fractionation protects selectively against late effects as compared to early effects (and tumour response).

In other words, a dose of 59 Gy delivered with 3 Gy per fraction corresponds to an isoeffective dose for late effects $D_{\alpha/\beta = 3.5}$ of 70 Gy. Similarly, a dose of 65 Gy delivered with 3 Gy per fraction corresponds to an isoeffective dose for early effects (and effects on tumour) $D_{\alpha/\beta = 10}$ of 70 Gy.

2.5. BRACHYTHERAPY AND DIFFERENCES IN DOSE RATE

While brachytherapy is outside the scope of this report, a brief mention of the use of weighting factors in brachytherapy is included for completeness and also to indicate that the approach is also based on the α/β model.

In brachytherapy, there is a dramatic increase in the use of high dose rate (HDR) and pulsed dose rate (PDR) techniques. This was made possible by technological developments.[1]

An important issue is to establish weighting factors W_{IsoE} for the various dose rates, fraction numbers and sizes, and separation between fractions as used in modern brachytherapy. These factors are needed to derive the isoeffective dose D_{IsoE}, and thus treatment prescription (Section 3).

Similar to the case of external beam therapy, selection of the weighting factor is based on the α/β model, using the same respective numerical values for the α/β ratio for early and late effects. There is also an agreement on the reference conditions to derive the W_{IsoE} and D_{IsoE} values: they are taken the

[1] Prescribing, Recording and Reporting Intracavitary Brachytherapy, ICRU Report, in preparation.

same as for external photon beam therapy (i.e. 2 Gy per fraction, 5 times per week).

However, when interpreting the clinical outcomes, the similarities listed above should not obscure the huge differences in dose distribution between external beam therapy and brachytherapy. For example, in brachytherapy for cervix treatment, due to the inverse square law, ~40% of the PTV (around the sources) receives 150% of the specified (peripheral) dose.

Another point specific to brachytherapy is that cell repair kinetics have to be taken into account in two current situations encountered, for example, in gynaecology.

Firstly, for HDR applications, repair during the fractions needs to be taken into account when the duration of one fraction is significant compared to the half-time for repair processes $T_{1/2}$.

Secondly, for PDR applications, repair may be incomplete between the numerous fractions when the interval is as small as 1–4 hours.

An assumption must then be made concerning the half-time for repair processes, $T_{1/2}$, and a value of 1.5 h is widely accepted for most clinical conditions (but with larger uncertainty than the α/β values) [2.8, 2.9].

2.6. INFLUENCE OF OVERALL TIME

In some special external photon beam techniques, in a large proportion of the brachytherapy applications and in many protocols using particle beam therapy, there is a reduction in the overall time.

Thorough discussion of the influence of overall treatment time and of combinations of radiation and drugs on treatment effect is complex and outside the scope of this document. Only a few points are made here related to treatment time to stress the importance of cell proliferation and repopulation. A more complete discussion can be found in Refs [2.5, 2.10–2.12].

Reduction in the overall duration of treatment will increase the effect of irradiation in many tumours and normal tissues. Therefore, in these cases, reducing overall treatment time will aid in increasing tumour response but will exacerbate early reactions in normal tissues.

In human oral mucosa, accelerated proliferation begins 2–3 weeks after initiation of treatment and in human skin after 3–4 weeks. Towards the end of a standard course of radiation therapy, daily proliferation may compensate in large measure for the loss of cells caused by daily dose fractions.

In the case of tumours, accelerated repopulation probably does not commence until approximately 3–4 weeks after the start of treatment. After this time, Withers et al. [2.13] have estimated that in the case of head and neck

tumours, this repopulation may be sufficient to overcome the killing of cells resulting from a dose of as much as 0.6 Gy/d (using daily 2 Gy fractions), assuming a potential doubling time of clonogenic cells of 3–4 days.

2.7. RADIATION QUALITY AND RBE

2.7.1. The RBE concept

At equal absorbed doses, radiations of different quality produce different levels of biological and clinical effects. Radiation quality is related to the type of particles and their energy spectrum. The differences in effectiveness are related to differences in energy deposition at the level of the particle tracks and subcellular structures, see Fig. 2.1 [2.14]. In radiation biology, it has become customary to use RBE values to quantify differences in biological effectiveness of different radiation qualities.

The concept of RBE was discussed by the International Commission on Radiological Protection (ICRP) and the ICRU [2.15, 2.16]. The RBE is defined as a ratio, between two absorbed doses delivered with two radiation qualities, one of which is a 'reference radiation', that result in the same effect in a given biological system, under identical conditions.

The RBE is a clear, unambiguous and well defined radiobiological concept. An RBE value is the result of an experiment and is thus associated with an experimental uncertainty. Also because RBE depends upon the biological system and the type and level of effect, the dose and the experimental conditions in which a given RBE value has been obtained must be specified [2.17]. Predominately, ^{60}Co γ rays are taken as the reference radiation quality [2.18, 2.19].

The RBE of a given radiation quality varies markedly with dose, biological system and effect. The data presented as examples for neutrons in Fig. 2.2 show that, as a general rule, RBE increases with decreasing dose and is sometimes higher for late effects than for early effects, especially at low doses [2.20]. In addition, the RBE of the clinical fast neutron beams varies significantly with energy (Fig. 2.3) [2.21].

2.7.2. Application of the RBE concept in radiation therapy

When applying the radiobiological concept of RBE in clinical practice, the fact that RBE is a function of radiation type, dose and cell or tissue type

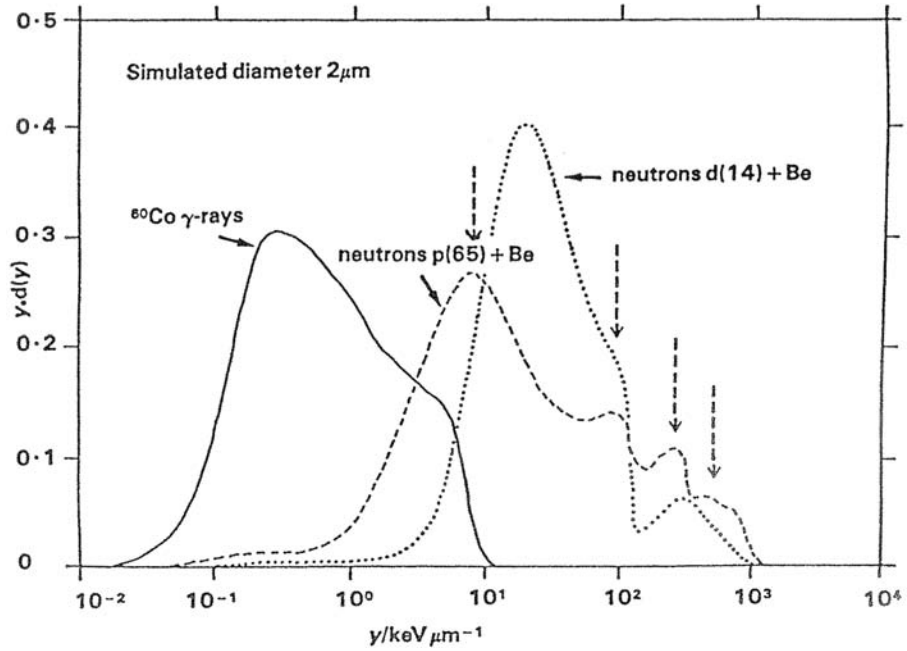

FIG. 2.1. Comparison of the microdosimetric spectra y.d(y) versus y obtained for γ rays, d(14)+Be neutrons and p(65)+Be neutrons, the lowest and highest neutron energies used for therapy, respectively. y is the lineal energy and d(y) is the probability density of absorbed dose in y. For γ rays, the maximum of the spectrum is at 0.3 keV μm^{-1} and for d(14)+Be neutrons it is obtained at 20 keV μm^{-1}. Four peaks are observed for p(65)+Be neutrons (vertical arrows): at 8, 100, 300 and 700 keV μm^{-1}, corresponding to high energy protons, low energy protons, α particles and recoil nuclei, respectively [2.14].

raises complex problems for the application of the principle to therapy with particles, such as neutrons and ions.

2.7.2.1. RBE and dose prescription

When deciding on a dose prescription for a new ion beam, the radiation oncologist will have to weigh a variety of factors and information sources:

(a) The RBE variation within various regions (depths) in the ion beam.
(b) The effect of any alteration in fractionation scheme, compared to the reference fractionation.

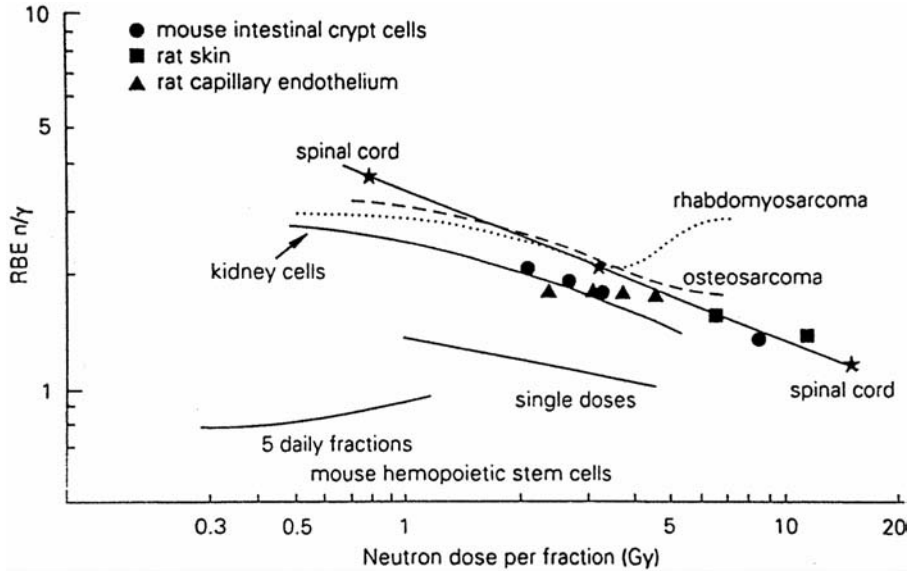

FIG. 2.2. RBE–dose relationships for 15 MeV neutrons produced by a (d,T) generator. Different biological end points in normal tissues and tumours were investigated. For late tolerance on spinal cord, the RBE increases from 1.2 to 3.7 when the neutron dose per fraction decreases from 16 to 0.8 Gy. Higher RBE values were found subsequently for spinal cord at lower doses [2.20].

(c) The fact that, for the same prescribed dose, the dose distributions in the tumour (PTV) and critical normal tissues with ion beams may be significantly different from those seen with photons.
(d) The impact of past personal clinical experience and information reported from other treatment centres.

These factors, and possibly others, could influence the clinical outcome and thus have an impact on dose prescription. The net impact of this is that the weighting factor to be applied is almost certainly never a 'true RBE' (or RBE in the strict sense) and should, therefore, be designated W_{ion} to indicate that the weighting factor takes into account factors other than simply RBE. In specific cases, W_{ion} could be replaced by W_{C+}, for example, to indicate the use of a carbon beam.

The product of the (total) absorbed dose, D, with W_{ion} is the (total) weighted absorbed dose for the particular ion therapy protocol, D_{ion} or D_{C+}, expressed in Gy. It is important to clearly specify the reference protocol to which the weighting is done. For example, in many proton therapy centres, the

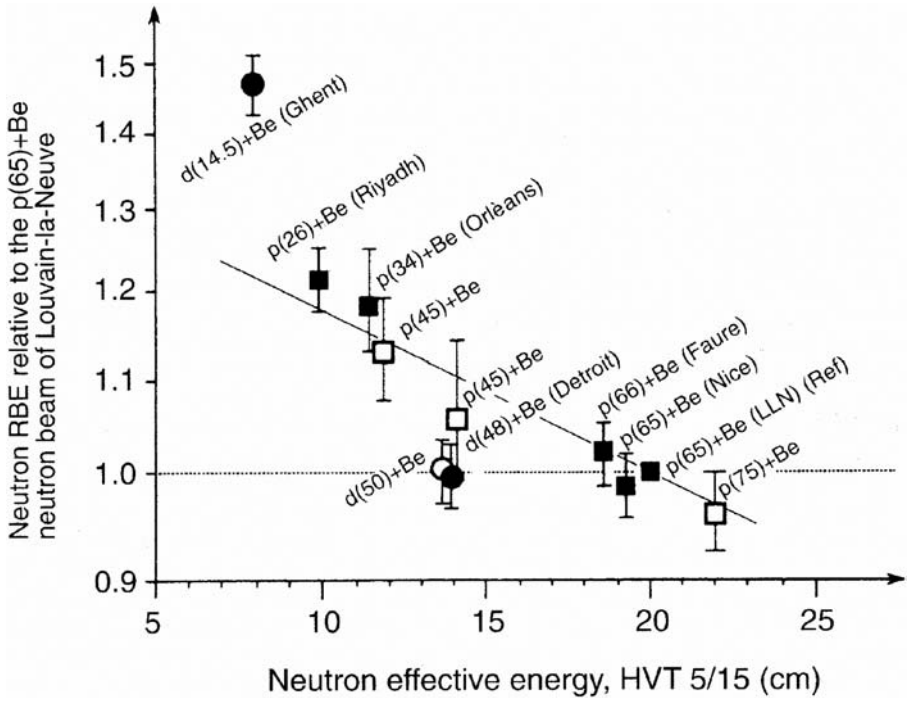

FIG. 2.3. RBE variation of neutron beams as a function of energy. The p(65)+Be beam of Louvain-la-Neuve is taken as reference (RBE = 1). The filled squares and circles correspond to six different neutron facilities. The open squares and circles correspond to beams produced at the variable energy cyclotron of Louvain-la-Neuve. In the abscissa, the 'effective energy' of the neutron beams is expressed by their half-value thickness (HVT 5/15) measured in specified conditions. Intestinal crypt regeneration in mice, after a single fraction irradiation, is taken as the biological system. The 95% confidence intervals are shown. A straight line is fitted through the points (squares) corresponding to neutron beams produced by the (p+Be) reaction. For comparison, the neutron beams produced by the (d+Be) reaction are represented by circles [2.21].

weighting is done with respect to photons applied with the same fraction number and overall time as the ions (see the discussion in Section 3).

In the recommended case where the weighting of the ion beam is done with respect to the reference protocol (photons, 2 Gy per fraction, 5 times per week), W_{ion} would be identical to W_{IsoE}, as defined and recommended in Section 3.

2.7.2.2. Selection of the most clinically relevant RBE or weighting factors for ions

Several approaches have been utilized to predict a value for W_{ion}. A purely experimental approach might use the exposure of various animal tissues to the reference radiation and the new radiation under a variety of conditions in an attempt to predict a likely value of W_{ion}. Some such approaches are outlined in the following:

— *Local radiobiological experimental programme:* When a new non-conventional beam becomes available for therapy it is current practice to carry out, locally, a variety of laboratory experiments to determine RBE values and RBE–dose relationships for a variety of experimental systems and a variety of end points. Commonly, these experiments involve the determination of cell survival curves or the determination of dose–effect relationships for various end points in various tissues in experimental animals. Since in an ion beam the RBE is a function of position or depth in the beam, it may also be necessary to carry out experiments at various positions within the treatment beam. In choosing experimental systems for laboratory studies, these should include model systems typical of late responding normal tissues that are often the critical normal tissues during therapy. In attempting to arrive at a value for W_{ion} for a carbon ion beam, the group at the National Institute of Radiological Sciences (NIRS) in Chiba, Japan, has used a method which combined radiobiological data obtained from cell survival and animal tissue response data coupled with a large clinical experience with neutrons to predict values of RBE for various positions in their carbon beams used for therapy. This approach is described in detail in Annex IV. Besides radiobiological experiments, microdosimetry provides independent additional information on radiation quality of the beam [2.22]. To the extent that RBE versus LET or RBE versus y spectra are known for a specific biological system, microdosimetry may also be used to predict the RBE values for that system. It is an independent approach which improves confidence in both the biological and physical approaches for determining RBE as a function of position in the beam [2.6, 2.23].
— *Theoretical approach:* Alternatively, RBE values may be predicted from theoretical approaches which also incorporate data obtained from laboratory experiments (see Annexes I and II). RBE is a function of the microscopic distribution of energy (LET) in irradiated materials. Therefore, it is not surprising that attempts are being made to predict RBE or W_{ion} values based on biophysical models coupled with cell

survival data obtained from in vitro or in vivo experiments. One such approach is described in Annex II, and is in use at the heavy ion research centre in Darmstadt, Germany, known as the Gesellschaft für Schwerionenforschung mbH (GSI).

— *Past personal clinical experience:* RBE values used for therapeutic prescription may also be based on previous clinical experience with other types of high LET particles such as neutrons, bolstered by information from experimental systems. As mentioned, this approach has been utilized at NIRS and is described in Annex IV.

— *Exchange of information between centres:* Finally, useful information can be obtained from other centres using the same (or similar) type of particle.

In determining appropriate RBE values for therapeutic applications, the reference radiation should be ^{60}Co or high energy photons, and the reference fractionation should be 2 Gy per fraction, 5 fractions per week.

2.7.2.3. Selection of W_{ion} based on the linear quadratic model

Sections 2.4 and 2.5 describe approaches for the derivation of weighting functions for altered fractionation schemes and altered dose rates. Both approaches make use of the linear quadratic relation for cell survival with the implicit assumption that therapeutic responses are related to cell survival and that the α/β and half time for repair could be derived from studies of in vitro and in vivo responses to radiation. In the absence of other more specific information, it is assumed that for photon irradiation the α/β ratio for early responding tissues is on average 10 Gy and that for late responding tissues is 3 Gy, and also that the half time for repair is 1.5 h.

Given that cell survival is the likely determinant of response to therapeutic ion irradiation, it seems likely that the linear quadratic relation can be used as the basis for predicting values of RBE and W_{ion} for such radiations using appropriate values of α/β derived specifically for each ion type and energy. Based on this assumption, Joiner and Marples (see Annex I) have devised a relationship which allows prediction of the RBE for any pair of radiations at any dose provided that the α and β values for each radiation are known. In their formulation, RBE can be expressed as a function of either a chosen dose per fraction of the reference radiation d_x or of a chosen dose of a test radiation d_{ion}.

Their relationships are repeated in the following discussion and in each relationship $K = \alpha_{ion}/\alpha_x$, $V = \alpha_x/\beta_x$ and $C = \alpha_{ion}/\beta_{ion}$. Expressed in terms of d_x, RBE is given by:

$$RBE = \frac{K + \sqrt{K^2 + 4Kd_X\left(1 + d_X/V\right)/C}}{2\left(1 + d_X/V\right)} \tag{2.4}$$

and when expressed in terms of d_{ion} RBE is given by:

$$RBE = \frac{-V + \sqrt{V^2 + 4VKd_{ion}\left(1 + d_{ion}/C\right)}}{2d_{ion}} \tag{2.5}$$

Equations (2.4) and (2.5) are expressed in terms of dose per fraction. In the case of multiple fractions (n), the total doses D_x and D_{ion} would be given by nd_x and nd_{ion}, respectively. In the case where the number of fractions was identical for both radiations, W_{ion} would be equal to the RBE for the chosen fraction sizes.

In many instances when using ion beams for treatment, the number of fractions administered is chosen to be significantly less than the number of fractions used for the reference radiation. In this case, Eqs (2.4) and (2.5) cannot be used to predict W_{ion} but the same general approach as that used by Joiner and Marples can be applied. To obtain equal effects for X ray and ion treatment:

$$n_x\left(\alpha_x d_x + \beta_x d_x^2\right) = n_{ion}\left(\alpha_{ion} d_{ion} + \beta_{ion} d_{ion}^2\right) \tag{2.6}$$

$$n_x d_x\left(\alpha_x + \beta_x d_x\right) = n_{ion} d_{ion}\left(\alpha_{ion} + \beta_{ion} d_{ion}\right) \tag{2.7}$$

Solving for d_{ion}:

$$d_{ion} = -\frac{C}{2} + \sqrt{\left(\frac{C}{2}\right)^2 + \frac{n_x d_x C(V + d_x)}{n_{ion} VK}} \tag{2.8}$$

where (as per Joiner and Marples):

$$C = \frac{\alpha_{ion}}{\beta_{ion}}, \quad V = \frac{\alpha_x}{\beta_x} \quad \text{and} \quad K = \frac{\alpha_{ion}}{\alpha_x}$$

and the weighting factor, W_{ion} is given by:

$$W_{ion} = \frac{n_x d_x}{n_{ion} d_{ion}} = \frac{\alpha_{ion} + \beta_{ion} d_{ion}}{\alpha_x + \beta_x d_x} \tag{2.9}$$

when $n_x = n_{ion}$, then $W_{ion} = RBE_{ion}$. Furthermore, if $n_x = n_{ion}$ and $d_x = 2$ Gy, then $W_{ion} = W_{IsoE}$.

Table 2.1 illustrates the use of the above relationships for a hypothetical situation using the assumed parameter values given to the right of the table. Table 2.1(a) shows the ion doses as a function of fraction number which would be required to produce the same biological effect as various numbers of 2 Gy fractions of photon radiation shown in the column to the far left. Table 2.1(b) shows the value of the weighting factor, W_{ion}, which would be obtained using the values in the upper half of the table. The shaded boxes showing W_{ion} for equal numbers of fractions for both radiations are in fact equal to the RBE for 2 Gy photon fractions for the hypothetical situation illustrated and in this situation $W_{ion} = W_{IsoE}$.

TABLE 2.1(a) ION DOSE PER FRACTION FOR VARIOUS NUMBERS OF ION FRACTIONS VERSUS THE NUMBER OF 2 Gy FRACTIONS OF PHOTONS TO PRODUCE THE SAME BIOLOGICAL EFFECT

	Ion dose per fraction d_{ion}/Gy						
	5	10	15	20	25	30	N_{ion}
15	1.93	0.98	0.66	0.50	0.40	0.33	
20	2.54	1.30	0.87	0.66	0.53	0.44	
25	3.14	1.61	1.09	0.82	0.66	0.55	
30	3.72	1.93	1.30	0.98	0.79	0.66	
35	4.30	2.23	1.51	1.14	0.92	0.77	
40	4.86	2.54	1.72	1.30	1.04	0.87	
N_X							

$d_X = 2$ Gy
$K = \alpha_{ion}/\alpha_x = 5$
$V = \alpha_X/\beta_X = 3$ Gy
$C = \alpha_{ion}/\beta_{ion} = 50$ Gy

TABLE 2.1(b) VALUE OF THE WEIGHTING FACTOR W_{ion} FOR THE TOTAL DOSE. IT IS EQUAL TO $n_x\ d_x/n_{ion}\ d_{ion}$ (Eq. (2.9))

	Weighting factor for ions W_{ion}						
	5	10	15	20	25	30	N_{ion}
15	3.12	3.06	3.04	3.03	3.02	3.02	
20	3.15	3.08	3.05	3.04	3.03	3.03	
25	3.19	3.10	3.07	3.05	3.04	3.03	
30	3.22	3.12	3.08	3.06	3.05	3.04	
35	3.26	3.13	3.09	3.07	3.05	3.05	
40	3.29	3.15	3.10	3.08	3.06	3.05	
N_X							

RBE @ d_X = 2 Gy

2.7.2.4. Evaluation of W_{IsoE} from clinical considerations or outcomes

Section 2.7.2.2 proposes several approaches for the prospective estimation of W_{IsoE} based on biological and biophysical modelling approaches. However, as has been mentioned, the ion dose chosen for a therapeutic application may be determined by clinical as well as biological considerations. Such considerations might include changes in the organs at risk, changes in volumes of tissues irradiated, the presence of radiation 'hot spots' or other factors. In these situations, the determination of W_{IsoE} will include additional factors and/or clinical judgements not accounted for by the modelling approaches described. In these circumstances, the radiation oncologist should document all of the considerations that went into the choice of W_{IsoE}.

Ultimately, the best choice of W_{IsoE} will only come from determinations of the ion and photon doses required to achieve equivalent clinical results based on either tumour control or normal tissue morbidity using a given protocol for comparison with the reference photon protocol. An example of such an approach is described in Annex IV.

In the present section, the use of the symbol W_{IsoE} implies that the reference protocol is for photons 2 Gy per fraction, 5 fractions per week. If this would not be the case, the reference protocol should be specified and a symbol such as W_{Ion} (or W_{C+}) be used.

2.7.3. Ion RBE in therapy applications: Summary

As pointed out in Section 2.7.2.3, there is currently no agreement on the methodology to be used in the determination of W_{ion} or W_{IsoE} values to be used in ion therapy. Various institutions are currently using different approaches and some of these are described in Annexes II and IV. Because different institutions are currently using different fractionation schemes, the dimensionless weighting factors W_{Ion} or W_{IsoE} not only include assumptions about RBE but also assumptions about the effects of different fractionation schemes and whether the weighting factor is applied to tumour or various normal tissues.

The situation is further confused by the fact that the term 'RBE' is often used not in its rigorous sense as the ratio of two doses given under identical conditions, but as the ratio of total doses given under two different fractionation schemes. Often the same weighting factor is applied to different tissue types where the parameters determining response may not be identical. For these reasons, the concepts of isoeffective dose D_{IsoE} and W_{IsoE} have been recommended to remove the confusion with RBE and to indicate that a variety of factors including altered fractionation may have been included in its determination.

The uncertainty in the factors that may impinge on any quoted value of W_{ion} or W_{IsoE} requires that every effort be made to describe the methodology used to define its value, and to specify the reference conditions. Such a description might refer to models and the values of the parameters contained therein or to the results of clinical trials comparing outcomes following ion irradiation or use of the reference radiation.

REFERENCES

[2.1] INTERNATIONAL COMMISSION ON RADIATION UNITS AND MEASUREMENTS, Fundamental Quantities and Units for Ionizing Radiation, ICRU Report 60, Bethesda, MD (1998).

[2.2] INTERNATIONAL COMMISSION ON RADIATION UNITS AND MEASUREMENTS, Determination of Absorbed Dose in a Patient Irradiated by Beams of X or Gamma Rays in Radiotherapy Procedures, ICRU Report 24, Bethesda, MD (1976).

[2.3] MIJNHEER, B.J., BATTERMANN, J.J., WAMBERSIE, A., What degree of accuracy is required and can be achieved in photon and neutron therapy?, Radiother. Oncol. **8** (1987) 237–253.

[2.4] DALE, R.G., The application of the linear-quadratic formula dose–effect equation to fractionated and protracted radiotherapy, Br. J. Radiol. **58** (1985) 515–528.

[2.5] HALL, E.J., GIACCIA, A.J., Radiobiology for the Radiologist, 6th edn, Lippincott Williams & Wilkins, Philadelphia (2006).
[2.6] WAMBERSIE, A., et al., Biological weighting of absorbed dose in radiation therapy, Radiat. Prot. Dosim. **99** (2002a) 445–452.
[2.7] WAMBERSIE, A., MENZEL, H.G., GAHBAUER, R.A., DELUCA, P., WHITMORE, G., "RBE and harmonization in prescribing, recording and reporting hadron therapy", Progress in Radio-Oncology VII (KOGELNIK, H.D., LUKAS, P., SEDLMAYER, F., Eds), Monduzzi Editore, Bologna, Italy (2002b) 361–371.
[2.8] FOWLER, J.F., MOUNT, M., Pulsed brachytherapy: The conditions for no significant loss of therapeutic ratio compared with traditional low dose rate brachytherapy, Int. J. Radiat. Oncol. Biol. Phys. **23** (1992) 661–669.
[2.9] FOWLER, J.F., VAN LIMBERGEN, E.F., Biological effect of pulsed dose rate brachytherapy with stepping sources if short half-times of repair are present in tissues, Int. J. Radiat. Oncol. Biol. Phys. **37** 4 (1997) 877–883.
[2.10] FOWLER, J.F., "Fractionation and therapeutic gain", The Biological Basis of Radiation Therapy, 2nd edn (STEEL, G.G., ADAMS, G.E., HORWICH, A., Eds), Elsevier, Amsterdam and New York (1989) 181–207.
[2.11] BAUMANN, M., SAUNDERS, M., JOINER, M.C., "Modified fractionation", Basic Clinical Radiobiology, 3rd edn (STEEL, G., Ed.), Arnold, London (2002) 147–157.
[2.12] DALE, R.G., et al., Practical methods for compensating for missed treatment days in radiotherapy, with particular reference to head and neck schedules, Clin. Oncol. **14** (2002) 382–393.
[2.13] WITHERS, H.R., TAYLOR, J.M.G., MACIJEWSKY, B., The hazard of accelerated tumour clonogen repopulation during radiotherapy, Acta Oncol. **27** (1988) 131–146.
[2.14] PIHET, P., GUEULETTE, J., MENZEL, H.G., GRILLMAIER, R.E., WAMBERSIE, A., Use of microdosimetric data of clinical relevance in neutron therapy planning, Radiat. Prot. Dosim. **23** (1989) 471–474.
[2.15] INTERNATIONAL COMMISSION ON RADIOLOGICAL PROTECTION, Report of the RBE Subcommittee to the International Commission on Radiological Protection and the International Commission on Radiation Units and Measurements, Health Phys. **9** (1963) 357–386.
[2.16] INTERNATIONAL COMMISSION ON RADIATION UNITS AND MEASUREMENTS, Quantitative Concepts and Dosimetry in Radiobiology, ICRU Report 30, Bethesda, MD (1979).
[2.17] WAMBERSIE, A., MENZEL, H.G., RBE in fast neutron therapy and on boron neutron capture therapy. A useful concept or a misuse?, Strahlenther. **169** (1993) 57–64.
[2.18] INTERNATIONAL COMMISSION ON RADIATION UNITS AND MEASUREMENTS, Prescribing, Recording and Reporting Photon Beam Therapy, ICRU Report 50, Bethesda, MD (1993).

[2.19] INTERNATIONAL COMMISSION ON RADIATION UNITS AND MEASUREMENTS, Prescribing, Recording and Reporting Photon Beam Therapy (Suppl. to ICRU Report 50), ICRU Report 62, Bethesda, MD (1999).
[2.20] VAN DER KOGEL, A.J., Late Effects of Radiation on the Spinal Cord: Dose Effect Relationships and Pathogenesis, Thesis, Radiobiological Institute TNO, Univ. Amsterdam, Rijswijk, Netherlands (1979).
[2.21] GUEULETTE, J., MENZEL, H.G., PIHET, P., WAMBERSIE, A., "Specification of radiation quality in fast neutron therapy: Microdosimetric and radiobiological approach", Fast Neutrons and High-LET Particles in Cancer Therapy, Recent Results in Cancer Research, Vol. 150 (ENGENHART-CABILLIC, R., WAMBERSIE, A., Eds), Springer-Verlag, Heidelberg (1998) 31–53.
[2.22] INTERNATIONAL COMMISSION ON RADIATION UNITS AND MEASUREMENTS, Microdosimetry, ICRU Report 36, Bethesda, MD (1983).
[2.23] MENZEL, H.G., PIHET, P., WAMBERSIE, A., Microdosimetric specification of radiation quality in neutron radiation therapy, Int. J. Radiat. Biol. **57** (1990) 865–883.

3. QUANTITIES AND UNITS

In addition to quantities and units, this section discusses the definitions of some terms and recommended symbols.

3.1. ABSORBED DOSE, D

The quantity, absorbed dose, is the energy deposited per unit mass in the irradiated medium, at the point of interest [3.1]. It is expressed in joules per kilogram. The special unit is the gray (Gy) and:

$$1 \text{ Gy} = 1 \text{ J/kg} \tag{3.1}$$

Absorbed dose is a fundamental quantity in radiation therapy (Section 2.1). Regardless of the type of radiation and the nature of the biological effect, the radiobiological and clinical effects are directly related to the quantity, absorbed dose.

When prescribing and reporting a therapeutic irradiation, the absorbed dose shall always be indicated together with the specification of the point(s) or volume(s) where the absorbed dose is delivered and the irradiation conditions (Section 6).

Even when observing a single biological system or effect, however, the relation between absorbed dose and the radiobiological effect is not unique but depends on several factors (Section 2.2), such as:

— Dose per fraction;
— Dose rate;
— Overall time and other time–dose relations;
— Radiation quality;
— Irradiation conditions (e.g. degree of oxygenation or temperature).

Therefore, weighting of the absorbed dose is necessary when comparing or combining radiation treatments performed under different technical conditions, and weighting factors (or functions) have to be introduced.

3.2. BIOLOGICAL WEIGHTING FACTOR, W_B

In radiation therapy, the dimensionless 'isoeffective dose weighting factor', W_{IsoE}, is the ratio of the dose given under the reference treatment conditions to the dose given under the actual treatment conditions to produce the same effects in a given biological system (all other conditions being identical).

For conventional external beam therapy, the reference conditions consist of daily fractions of 2 Gy to the PTV, 5 fractions per week delivered with ^{60}Co or 2–30 MV photons (see Table 2.1). For brachytherapy, the reference dose rate is 0.5 Gy/h. To date, specific reference conditions have not been defined for special techniques, such as treatment of uveal melanoma, radiosurgery, etc. Further discussion of brachytherapy and these special techniques is outside the scope of this section.

The symbol W_{IsoE} is recommended, but parentheses can also be used W(IsoE). It must be stressed that the symbols W_{IsoE} and D_{IsoE} should be used only when doses given under any other circumstance are referred to the reference condition, i.e. 2 Gy per fraction, 5 fractions per week.

W_{IsoE} depends on the biological system and end point, absorbed dose, dose per fraction and radiation quality (as listed in Section 3.1) and is, therefore, meaningful only to the extent that all these factors are specified.

The numerical value selected for W_{IsoE} shall always be reported together with the biological end point and irradiation conditions for which the W_{IsoE} value has been selected (e.g. late versus early biological effects, dose per fraction, depth in a carbon ion beam, as discussed in Section 2.2). Because the selection of W_{IsoE} is not an exact science and may involve a number of assumptions, variables or model parameters, the rationale and methodology followed for the selection of W_{IsoE} should be reported.

Examples of selection and reporting of the weighting factor W_{IsoE} are presented below for fractionated external beam therapy with photons using non-conventional fractionation and for beams of non-conventional radiation quality.

3.2.1. Fractionated photon beam therapy

For fractionated photon radiation therapy, selection of the isoeffective dose weighting factor, W_{IsoE}, is based on the linear quadratic (LQ) model (Section 2.4). In addition to the actual (non-reference) dose per fraction, the numerical value selected for α/β should be reported, for example, W_{IsoE}(3 Gy, $\alpha/\beta = 3$) or W_{IsoE}(3 Gy, $\alpha/\beta = 10$) for late or early effects, respectively. The ratio α/β has the Gy as a special unit.

When the actual overall treatment time is different from that of the reference treatment technique, and if the total isoeffective dose is adjusted to take into account this difference in overall time, the magnitude of the correction should also be indicated. As pointed out in Section 2.7, the effect of overall treatment time on clinical outcome is difficult to predict [3.2–3.6]. Although protracted treatments are not recommended, a simple suggestion to compensate for a difference in overall treatment time for head and neck tumours when calculating equivalent doses is to add 0.6 Gy to the total photon dose for each additional day difference in schedules beyond 3–4 weeks, when using 2 Gy fractions [3.7]. When other fraction sizes, other tumour types or normal tissues are being considered, the compensated dose will be different. If such a correction is made, its magnitude should be specified. If the correction is specified as a fraction of the total photon dose, it may be included in the value of W_{IsoE}.

For example, regarding tumour responses ($\alpha/\beta = 10$) and assuming an adjustment for overall time of 0.6 Gy/d, a notation for the isoeffective dose weighting factor might be:

W_{IsoE} ($\alpha/\beta = 10$; 0.6 Gy/d)

3.2.2. Brachytherapy

Section 2.5 contains a brief discussion of weighting factors as applied to brachytherapy; further discussion is outside the scope of this section.

3.2.3. External beam therapy with non-conventional radiation quality

When radiation qualities other than photons are used, for example, protons, ions and neutrons, the isoeffective dose weighting factor, W_I, includes several components:

(a) A factor related to radiation quality to account for altered radiation effectiveness;
(b) Factors resulting from differences in fractionation and overall time. Fractionation schemes and overall times used in ion therapy are often very different from those specified in the reference conditions. When evaluating the weighting factors for differences in fractionation, it must be kept in mind that the α/β values are significantly different for photons and carbon ions and depend on the biological effects (early/late effects). In addition, when adjusting for differences in overall time, the additional dose (in Gy) per additional day is also significantly different for photons

and carbon ions, and has been established only for photons and a few tumour types and normal tissues.

(c) Other factors (as discussed in Section 2.6).

While it is tempting to think of these components independently, they are in fact often interrelated. RBE is a function of α and β for both the reference and test radiation and of the tissue type, and therefore a value of RBE cannot be chosen independently of α and β and/or tissue type, unless the RBE is very small and variations in it cannot be detected accurately. Total dose, dose per fraction, number of fractions and total treatment time are obviously related and therefore cannot be treated independently in any calculation of the weighting factors. The net effect of this is that one cannot neatly specify separate correction factors for radiation quality, dose per fraction, total treatment time, etc.

3.3. BIOLOGICALLY WEIGHTED ABSORBED DOSE, D_B

In radiation therapy, the 'isoeffective dose', D_{IsoE}, is the product of the absorbed dose, D, by the isoeffective dose weighting factor W_{IsoE}:

$$D_{IsoE} = D\, W_{IsoE} \tag{3.2}$$

The isoeffective dose is the absorbed dose that, if delivered under the reference treatment conditions (see Section 2, Table 2.1), would produce the same effects on a given biological system as the dose delivered under the actual treatment conditions, all other conditions being identical.

As W_{IsoE} and D_{IsoE} depend on radiation quality, dose per fraction and overall time, as well as on the biological system and effects for which they are selected (Section 3.1), these should be specified as well as the numerical values of any parameters used in any calculations. In some instances (see Annexes III and IV), values for W_{IsoE} may be based on experience with other radiations, for example, neutrons, in which case the rationale and approach should be clearly described.

As W_{IsoE} is dimensionless, the isoeffective dose, D_{IsoE}, is expressed in joule per kilogram. Its special unit is the gray (Gy).

Use of the terms 'isoeffective dose weighting factor' and 'isoeffective dose' implies a comparison with a dose delivered under reference conditions (see Section 3.2).

For specific treatment techniques or studies, reference conditions different from those stated above (Section 3.2) could be defined. However,

when collaborative studies are initiated, these specific selected reference treatment conditions should be accepted by all participating centres and clearly reported.

3.4. RECOMMENDATIONS FOR REPORTING

3.4.1. Reporting the isoeffective dose weighting factor, W_{IsoE}

The isoeffective dose weighting factor, W_{IsoE}, depends on the biological system, the effects (e.g. early versus late) radiation type (e.g. carbon ions versus photons) and fractionation scheme for which it has been selected. W_{IsoE} is, therefore, meaningful only to the extent that these factors are reported.

To aid in understanding, W_{IsoE} may be followed in parentheses by other relevant information, such as:

— Selected numerical value for RBE if appropriate (Sections 2.6 and 3.2.3);
— Selected α/β values (for photons and other involved radiation qualities) to take into account differences in dose per fraction (Section 3.2.1);
— Method adopted for dose adjustment for differences in overall time (Section 3.2.1).

For example, for a carbon ion beam treatment using an SOBP of 6 cm, an RBE value of 3 is selected for the carbon ions in the actual fractionation conditions, relative to photons delivered with the same fractionation. Then, for photons, an α/β value of 10 Gy for early effects and 0.6 Gy per additional day of treatment are assumed. A notation for the isoeffective dose weighting factor might then be:

$$W_{IsoE}(C+; SOBP = 6\ cm; RBE = 3; \alpha/\beta_{photons,\ early} = 10\ Gy; 0.6\ Gy/d)$$

Note that the value of the additional dose per day of treatment protraction is near zero for late reactions, varies for different tumour types, and is up to 1–2 Gy/d for some early reacting normal tissues. Also, the presence of ‘consequential’ late reactions, arising as a consequence of severe early reactions, can increase the time factor for these late reactions.

3.4.2. General recommendations for reporting radiation therapy

For any radiation therapy modality, it is ICRU policy to recommend that full technical description and irradiation conditions of the treatment be reported [3.7, 3.8].

In particular, absorbed dose and dose per fraction shall always be reported for relevant point(s) or volume(s).

3.4.3. Review of some current practices for weighting and reporting weighted dose and isoeffective dose in centres using particle irradiations

3.4.3.1. Proton beam therapy

In proton beam therapy, it is current practice in the majority of centres to assume an RBE value of 1.1 for protons, relative to photons, for all clinical conditions. A 'generic' RBE value of 1.1 is recommended.[2]

Due to the modest LET (thus RBE) variation involved, recommendation of a generic RBE weighting factor W (RBE) of 1.1 for protons seems logical for most clinical situations. However, in the distal part of the SOBP, a small increase of RBE has often been observed as a result of the LET increase in that region (see footnote 2). In the dose fall-off region, one consequence of LET increasing where dose is decreasing on the distal edge of the SOBP is the extension of the biologically effective range of the proton beam by ~2 mm for 160–250 MeV and ~1mm for 60–85 MeV proton beams.

The 'generic' RBE value of 1.1 is the RBE weighting factor, W_{RBE} or W(RBE), and its product with the absorbed dose is the RBE weighted dose, D_{RBE} or D(RBE).

This weighting factor of 1.1 would be equal to the 'isoeffective dose weighting factor' W_{IsoE} and (1.1 × D) would be equal to the 'isoeffective dose' D_{IsoE} only if fractionation, overall treatment time and all other conditions would be those defined for the reference treatment conditions (Section 3.2). Otherwise, additional weighting factors would have to be introduced to obtain the isoeffective dose.

In contrast to the majority of centres in the USA and Europe, some Japanese centres adopt an RBE value of 1.0 in proton beam therapy [3.10, 3.11].

[2] Proton Report No. 78, IAEA/ICRU publication, in preparation.

3.4.3.2. The Darmstadt–Heidelberg approach in carbon ion therapy

In the Darmstadt–Heidelberg programme using carbon ion beams, the RBE is computed taking into account the radiation quality (LET) and dose per fraction at any point of interest, relative to photons delivered at 3 Gy per fraction, 3 fractions per week. It must, of course, be pointed out that, in the case of carbon ions, the RBE values are much higher and exhibit more variation throughout the target volume than those assumed for protons. No adjustment was made so far for differences in overall time in current protocols as mainly slowly growing tumours are treated (for more details, see Scholz et al. in Annex II).

3.4.3.3. The Chiba approach in carbon ion therapy

The weighting factor, W_I, for carbon ion therapy adopted in Chiba is based on a combination of radiobiological experimentation and a large amount of clinical experience with neutron therapy (see Annexes III and IV). The clinical experience with neutron therapy indicated that a 'clinical RBE' value of 3 was appropriate when clinical results obtained with neutrons were compared with those obtained with photons. Based on a series of radiobiological experiments in various cellular systems and determinations of LET in both the neutron and carbon ion beams, a nominal RBE value of 3.0 was assigned to the distal part of each SOBP, irrespective of its size, used in the therapy programme (for more details, see Annex IV).

This nominal RBE value of 3.0, defined at the distal part of the SOBP, was then used in a series of dose escalation trials, as well as in trials in which hypofractionation schemes were applied. For prescription and reporting, it was thus assumed to be the 'isoeffective dose weighting factor', W_{IsoE}, as no other weighting factor was introduced.

3.4.3.4. Equivalent dose

Unfortunately, it has become common practice worldwide, in most of the proton and ion therapy centres, to report the 'RBE weighted dose', D(RBE), and the 'isoeffective dose', D_{IsoE}, in terms of gray equivalent (symbol GyE). The term 'cobalt gray equivalent' (CGE) has also been used. Neither of these approaches is in agreement with the recommendations of the International System of Units (SI) as indicated in the following discussion [3.12].

In addition, the terms 'equivalent dose' and 'effective dose' have specific definitions for radiation protection purposes in the low dose range [3.13]. They are now accepted and used by several national and international commissions

and regulatory authorities. To use the terms 'effective' or 'equivalent' in radiation therapy opens up further possibilities for confusion.

3.4.4. ICRU/IAEA recommendations for reporting the isoeffective dose, D_{IsoE}

Because the unit Gy is used for two quantities (absorbed dose and isoeffective dose, D_{IsoE}), there is an obvious risk of confusion that could be harmful (and potentially lethal) for the patient.

When the treatment is delivered using reference conditions, the numerical values for the absorbed dose and the isoeffective dose are equal: there is no risk of confusion. In contrast, when the treatment is delivered under non-reference conditions, two dose values need to be reported: (1) the absorbed dose, D; and (2) the isoeffective dose, D_{IsoE}.

Reporting both absorbed dose and isoeffective dose reduces the possibility of confusion as to which dose is being reported. The isoeffective dose is useful, for example, in the interpretation of clinical outcome, but also is needed for preparing new cancer therapy protocols and for combining two radiation protocols in the same patient, for example, an ion boost therapy after a first photon course.

According to the SI, the names of the quantities should be given together with the number of grays. No additional indication (subscript, asterisk, etc.) is allowed to be added to the name of the unit to specify the quantity that is involved [3.12]. For example, in the clinical record one should write: 'The patient received an absorbed dose of 20 Gy with carbon ions, isoeffective to a photon dose of 60 Gy using 2 Gy fractions (assuming $W_{IsoE} = 3$).'

Experience has shown that it is often difficult to comply with this recommendation, i.e. to specify both absorbed and isoeffective doses together with the names of the corresponding quantities in current radiation therapy clinical practice (e.g. in patient records, protocol discussion or correspondence with the referring physicians).

Taking into account the difficulty related to the fact that both absorbed dose and isoeffective dose have the same unit (Gy), and the present lack of uniformity/harmonization in reporting the weighted dose and isoeffective dose, the ICRU and the IAEA, in discussion with the proton and ion therapy communities, are currently evaluating the need, usefulness and feasibility of introducing a new unit for the quantity isoeffective dose. The major concern is to avoid or at least reduce, in clinical practice, the risk of confusion between the quantities that could be harmful for the patients.

Meanwhile, the following was agreed between the four groups listed previously. For reporting, the absorbed dose should always be given first in Gy,

followed by the isoeffective dose, Gy (IsoE), with the indication (IsoE for isoeffective) after Gy to draw attention to the fact that one is dealing with the isoeffective dose D_{IsoE}, and not with the absorbed dose. The space between Gy and (IsoE) is necessary to comply with the requirements of the SI.

For example, one can write 'the patient received 20 Gy (60 Gy (IsoE))' with the implicit understanding that the 20 Gy absorbed dose from ions produces a biological effect equivalent to that produced by an absorbed dose of 60 Gy of photons given under reference conditions of 2 Gy/d of photon radiation over the same treatment time.

Additional relevant information can be added in parentheses when considered useful. For example, for carbon ion therapy, selecting a constant RBE value of 3 and assuming no other weighting factor is included in W_{IsoE}, one can write 'the patient received 20 Gy [60 Gy (IsoE; C+; RBE = 3)].' However, this would be valid only if the RBE value of 3 had been determined, taking as reference photon irradiation delivered at 2 Gy per fraction to correspond to reference conditions.

The definition and use of the isoeffective dose weighting factor and the isoeffective dose, as defined in this publication, are restricted to the field of radiation therapy applications.

REFERENCES

[3.1] INTERNATIONAL COMMISSION ON RADIATION UNITS AND MEASUREMENTS, Fundamental Quantities and Units for Ionizing Radiation, ICRU Report 60, Bethesda, MD (1998).

[3.2] WITHERS, H.R., TAYLOR, J.M.G., MACIEJEWSKI, B., The hazard of accelerated tumour clonogen repopulation during radiotherapy, Acta. Oncol. **27** (1988) 131–146.

[3.3] FOWLER, J.F., "Fractionation and therapeutic gain", The Biological Basis of Radiotherapy, 2nd edn (STEEL, G.G., ADAMS, G.E., HORWICH, A., Eds), Elsevier Science Publishers (Biomedical Division), Amsterdam (1989) 181–207.

[3.4] BAUMANN, M., SAUNDERS, M., JOINER, M.C., "Modified fractionation", Basic Clinical Radiobiology, 3rd edn (STEEL, G., Ed.) Arnold, London (2002) 147–157.

[3.5] BENTZEN, S.M., BAUMANN, M., "The linear–quadratic model in clinical practice", ibid., 134–146.

[3.6] HALL, E.J., GIACCIA, A.J., Radiobiology for the Radiologist, 6th edn, Lippincott Williams & Wilkins, Philadelphia (2006).

[3.7] DALE, R.G., et al., Practical methods for compensating for missed treatment days in radiotherapy, with particular reference to head and neck schedules, Clin. Oncol. **14** (2002) 382–393.

[3.8] INTERNATIONAL COMMISSION ON RADIATION UNITS AND MEASUREMENTS, Prescribing, Recording and Reporting Photon Beam Therapy (Suppl. to ICRU Report 50), ICRU Report 62, Bethesda, MD (1999).
[3.9] INTERNATIONAL COMMISSION ON RADIATION UNITS AND MEASUREMENTS, Prescribing, Recording, and Reporting Electron Beam Therapy, ICRU Report 71, Bethesda, MD (2004).
[3.10] SHIOYAMA, Y., et al., Clinical evaluation of proton radiotherapy for non-small-cell lung cancer, Int. J. Radiat. Oncol. Biol. Phys. **56** (2003) 7–13.
[3.11] IGAKI, H., et al., Clinical results of proton beam therapy for skull base chordoma, Int. J. Radiat. Oncol. Biol. Phys. **60** (2004) 1120–1126.
[3.12] BUREAU INTERNATIONAL DES POIDS ET MESURES, The International System of Units (SI), (BIPM, Ed.), Pavillon de Breteuil, Sèvres, France (1998).
[3.13] INTERNATIONAL COMMISSION ON RADIOLOGICAL PROTECTION, 1990 Recommendations of the International Commission on Radiological Protection, ICRP Publication 60, Annals of the ICRP, Vol. 21, Pergamon Press, Oxford (1991).

4. RADIOBIOLOGY OF HIGH LET RADIATION: NEUTRONS AND IONS

4.1. RADIOBIOLOGICAL RATIONALE FOR THE USE OF HIGH LET RADIATION

This publication discusses an alternative radiation modality, ion beam therapy. Ion beams possess the outstanding physical selectivity of proton beams and, in addition, exhibit several biological features related to their high LET which have an impact on patient selection, treatment planning and outcome. Neutron beams were the first high LET radiation to be used for radiation therapy. Although neutron beams do not exhibit the physical selectivity of proton and ion beams, they exhibit many of the same biological features related to high LET. The results of both experimental and clinical studies with neutrons provide information relevant to the use of ion beams for therapy, particularly with respect to the types of tumours which may be expected to demonstrate the greatest advantage from treatment with ion beams [4.1]. Some of the relevant biological features of high LET irradiations derived from experience with both neutrons and ions are discussed in the following sections.

4.1.1. Increased RBE

As described in Section 2.6.1, RBE is defined as the ratio between two absorbed doses delivered with two radiation qualities, one of which is the reference radiation, that result in the same effect in a given biological system irradiated under the same conditions. RBE values for various high LET radiations have been determined for a great many biological systems and a number of generalizations can be drawn from the results.

The first of these generalizations is that RBE tends to increase with increasing LET. In the case of neutrons, LET increases with decreasing energy and Fig. 2.3 (see Section 2) shows a comparison of RBE values for neutron beams of various energies with a reference neutron radiation using survival of intestinal crypt cells as the biological indicator. As neutron energy decreases, both LET and RBE increase. Because LET increases for all particles as energy decreases, a second generalization is that, for any particle, RBE generally increases as particle energy decreases, except in the region of 'overkill' described in the following discussion.

Figure 4.1 shows RBE values as a function of LET for cell survival measured for two cell lines using three different ion beams at different points in SOBPs. Once again, RBE increases with LET but appears to reach a maximum

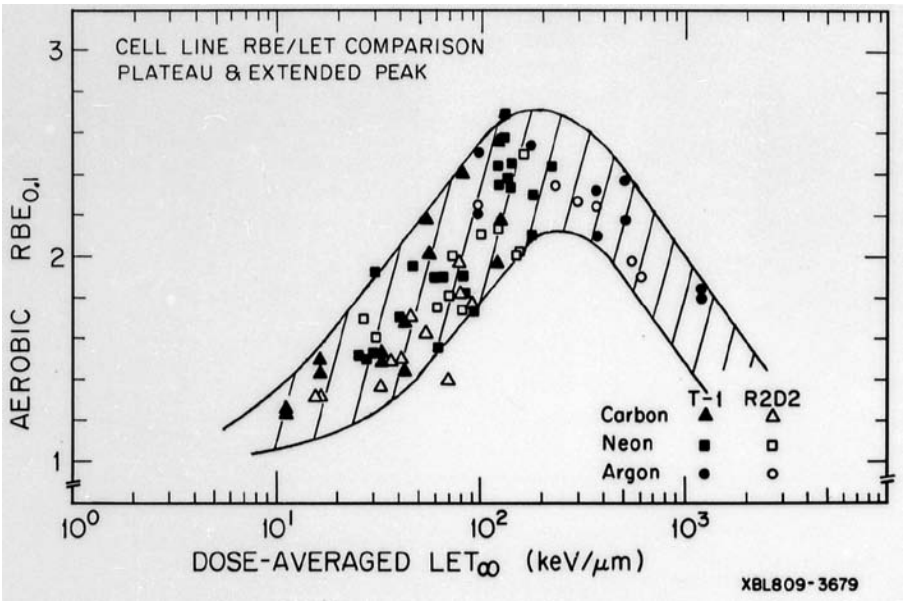

FIG. 4.1. RBE of cell survival for T-1 and R2D2 cells as a function of LET measured at various points in SOBPs for carbon, neon and argon ions. The cells were irradiated under aerobic conditions and the end point was 10% cell survival [4.2].

at LET values of approximately 100–200 keV/μm before declining in the 'overkill' region where the amount of energy deposited in a cell by a single particle traversal is in excess of the amount required to kill the cell. Figure 4.2 also shows variations in RBE as a function of LET at various points in SOBPs of carbon, neon, silicon and argon ions. Once again, RBE is seen to peak for LET values of approximately 100–300 keV/μm.

Figures 4.1 and 4.2 both demonstrate that even at the same value of LET_{∞}, RBE is a function of ion type. This is a result of differences in the fine structure of energy deposition for different particle types even at the same LET and indicates that LET, while often adequate, is not a perfect predictor of RBE.

In addition to increasing with LET and decreasing particle energy, RBE also increases with decreasing dose per fraction. This is illustrated in Fig. 2.2 (Section 2.6.1) and in Fig. 2.3, which show RBE versus neutron dose per fraction for a variety of tissues in experimental animals. Figure 2.2 (see Section 2) and Fig. 4.3 also illustrate one other finding: in some cases, the RBE of late responding tissues is greater than that of rapidly responding tissues and tumours.

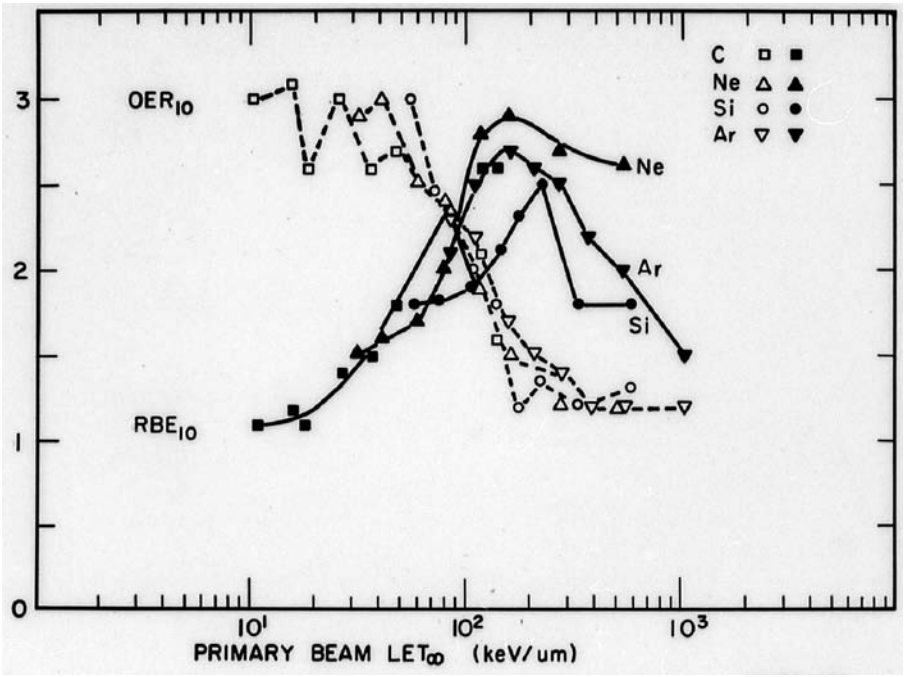

FIG. 4.2. Variation of OER as a function of LET measured at various points in SOBPs of carbon, neon, silicon and argon ions (courtesy of E. Blakely).

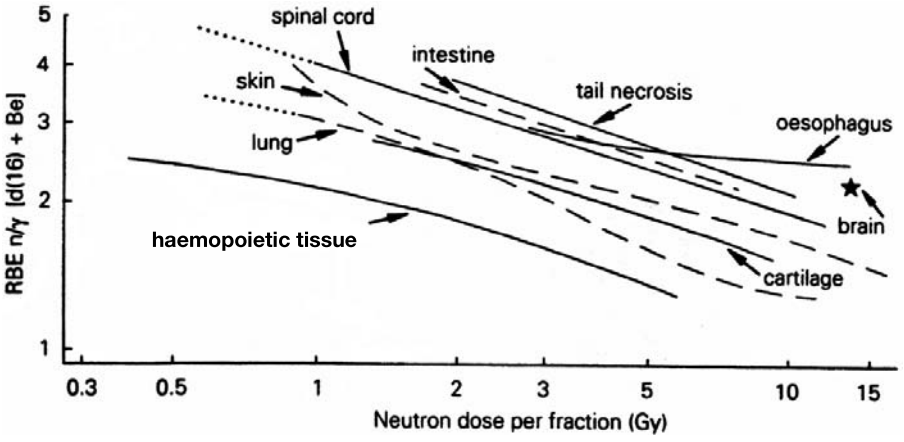

FIG. 4.3. RBE relationships for different normal tissues. The increase of RBE with decreasing dose per fraction is evident [4.3].

The previous discussion points out several generalities with respect to RBE. RBE increases with LET, decreases with increasing particle energy, increases with decreasing fraction size and is higher for some late versus early responding tissues. These findings can be assumed to apply to all tissues irradiated with high LET radiations and in particular to apply, to a greater or lesser extent, to all tumour or normal tissues in the SOBP region of an ion beam. There are, however, several consequences of high LET irradiation that may aid in the selection of tumour types which are likely to selectively benefit from treatment with high LET radiations. These are discussed in the following sections.

4.1.2. Reduction in the oxygen enhancement ratio with increasing LET

Historically, a reduced oxygen effect was the rationale for introducing fast neutrons in radiotherapy. The rationale for choosing neutrons over photons was based on the following observations:

(1) Hypoxic cells are present in most malignant tumours; they result from the fast and anarchic proliferation of the cancer cells;
(2) Hypoxic cells are ≈3 times more radioresistant than well oxygenated cells when exposed to low LET radiations. The presence of even a small percentage of hypoxic cells (1% or even 0.1%) can make the tumour resistant to radiation therapy;
(3) The oxygen enhancement ratio (OER) decreases when LET increases (Fig. 4.4) [4.4]. It decreases to approximately 1.6 for fast neutrons, and is close to unity for α particles. OER = 1.3 and 1.0 for α particles of 4 and 2.5 MeV (i.e. for LETs of 110 and 160 keV/μm, respectively). Essentially, this means that the effect of hypoxic cells in controlling tumour response will be much less for high LET radiations.

Figure 4.2 also shows that with ion irradiation, the OER decreases with increasing LET and that the decrease in OER versus LET is almost the mirror image of the increase in RBE achieving an OER of approximate unity for LET values greater than 200 keV/μm. One effect of the reduced OER seen with neutrons and ions is that the RBE of hypoxic cells in general will be greater than that for aerobic cells.

In principle, a reduction in OER is always an advantage. However, as discussed in the following sections, not all patients may benefit from high LET radiations and, therefore, careful patient selection is important.

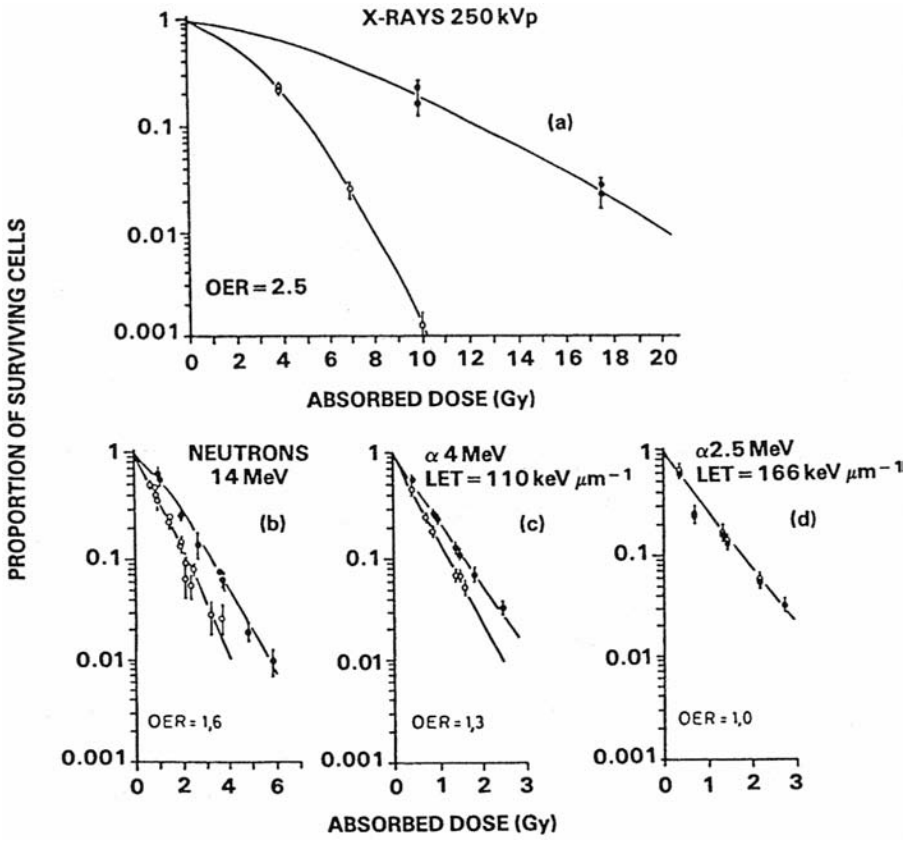

FIG. 4.4. Survival curves of human kidney cells T1 irradiated under hypoxic and aerobic conditions with different qualities of radiation: (a) 250 kV X rays (LET about 1.3 keV μm^{-1}); (b) 14 MeV neutrons produced by the (d,T) reaction (LET about 12 keV μm^{-1}); (c) 4 MeV α particles (LET = 110 keV μm^{-1}); (d) 2.5 MeV α particles (LET = 166 keV μm^{-1}) [4.4].

4.1.3. Reduction of the variation in radiosensitivity related to the position of the cell in the mitotic cycle

Increasing LET reduces the differences in radiosensitivity related to the position of cells in the mitotic cycle (Fig. 4.5) [4.5]. Particularly with low LET radiation, cells in stationary phase and in S phase are significantly more radioresistant than mitotic cells.

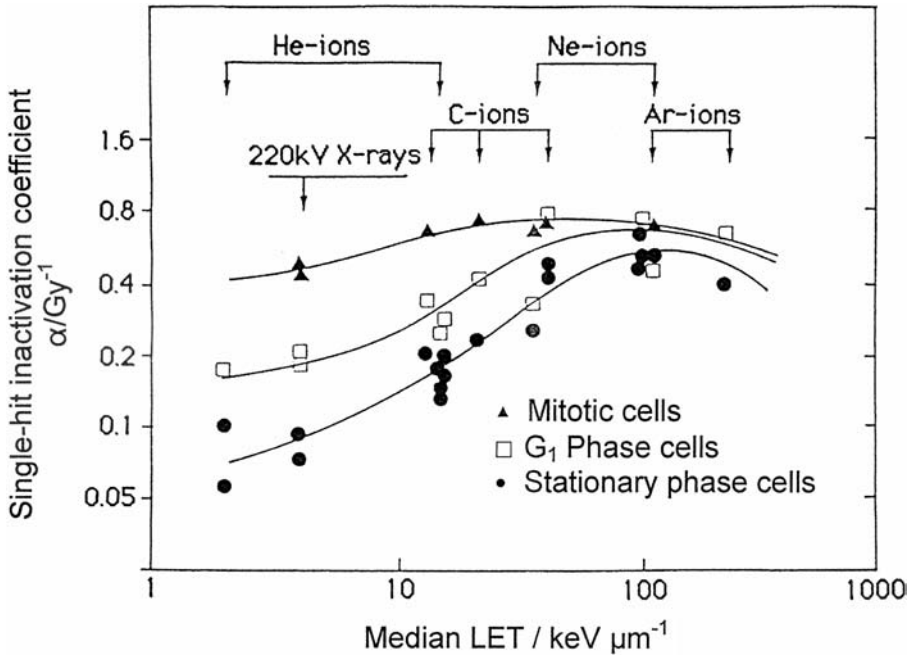

FIG. 4.5. Differences in radiosensitivity with the position of cells in the mitotic cycle. The differences are reduced with increasing LET. The ordinate shows the single hit inactivation coefficient, α, for homogeneous populations of mitotic, G1 phase and stationary phase Chinese hamster cells irradiated with 220 kV X rays and various charged particle beams, as a function of median LET (in keV/µm) [4.5].

4.1.4. Reduced repair with high LET radiation

Tissues exposed to fractionated photon irradiation exhibit repair between fractions so that the effect of a therapeutic regimen is highly dependent on the number of fractions and the dose per fraction. Because of the large amount of energy deposited in the critical cellular target by a single high LET particle track (Fig. 2.1 in Section 2 and Fig. 4.6) repair phenomena are less prominent. Therefore, the effect of fractionation is much less with high LET radiation.

The effects of fractionation with both low LET radiations (X rays) or high LET radiations (ions) are illustrated in Fig. 4.7. In the figure, the dashed lines represent survival curves for cells exposed to single doses of X rays (upper dashed curve) or ions (lower dashed curve). The solid lines represent survival curves obtained after fractionated exposures for each radiation assuming that the shoulder regions of the survival curves are repeated for each fraction as has

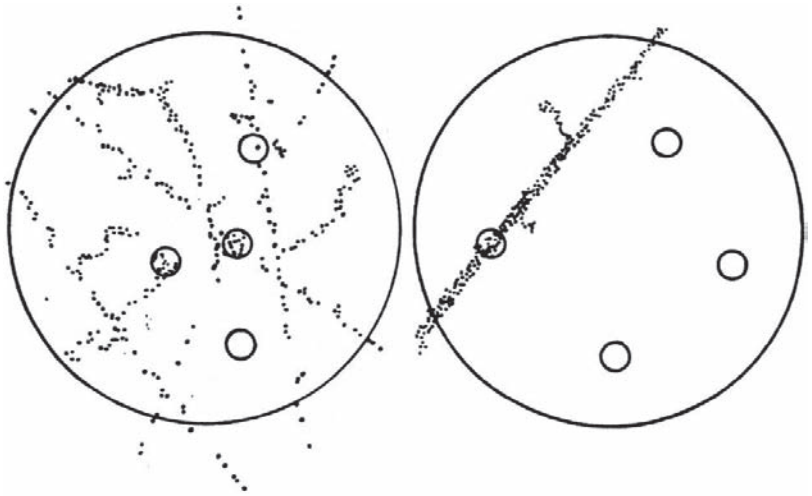

FIG. 4.6. Ionization density in a medium irradiated by (a) X rays and (b) high LET particles (neutrons). The small circles represent biological targets and the dots represent ionizations produced along the tracks of electrons set in motion by photons or protons set in motion by neutrons. When a sensitive structure is crossed by a high LET particle track (protons), there is a high probability of cell death regardless of position in the cell cycle, degree of oxygenation or the repair capacity of the cell [4.6].

been experimentally demonstrated. It is apparent that the effect of fractionation is large for X rays but much smaller for ion irradiation.

The effect of fractionation is reduced after neutron or ion irradiation compared to X rays. This is illustrated in Fig. 4.8 for mouse intestinal crypt cells. The ratio of the doses of fractionated and single exposures to X rays to achieve the same level of surviving clonogenic cells is significantly greater than the comparable ratio for neutrons and heavy ions in the proximal, middle and distal portions of the SOBP. The ratio for the unmodulated carbon beam is intermediate, reflecting a somewhat lower LET than is seen in the SOBP.

Because high LET radiations permit less cellular repair than low LET radiations, they can be expected to be selectively more efficient against tumour cells with a high repair capacity, for example, prostate cancer which has a low value of α/β. On the negative side, the sparing of late normal tissue reactions by the use of low dose fractions (the feature that underpins the use of hyperfractionation photon therapy) is reduced in the case of high LET therapy. There is also less long term repair, and more residual injury, in normal tissues after high rather than after low LET irradiations. Finally, because the effects of fractionation are less with high LET than with low LET radiation, the clinical effects

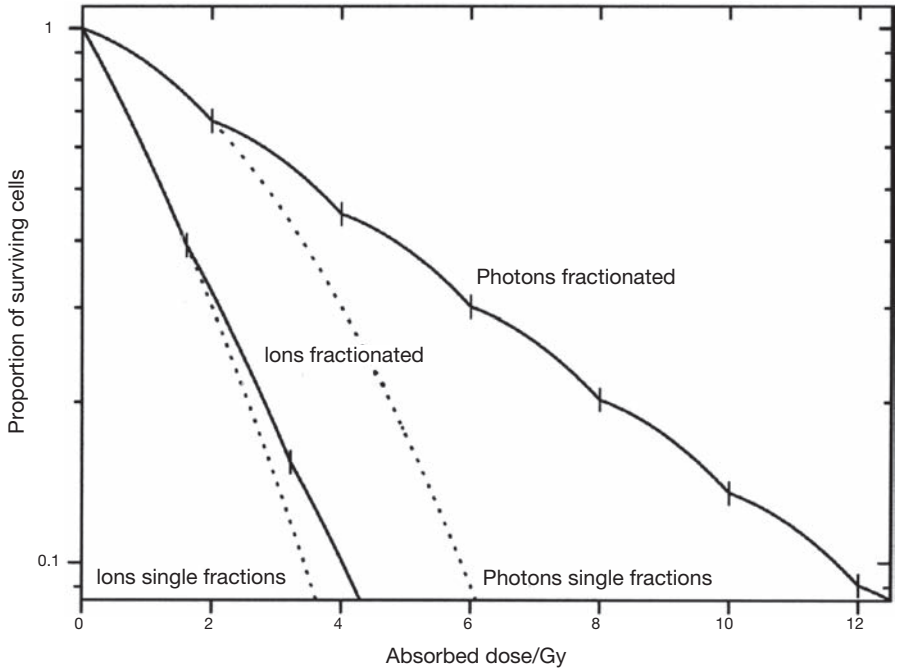

FIG. 4.7. Illustration of the effects of fractionation after photon (upper solid curve) and ion irradiation (lower solid curve). The dotted lines represent cell survival after exposures to single doses. Note the much greater sparing effect seen with photons compared to ions.

seen with particle radiations are likely to be less dependent upon fractionation. This may permit treatment with reduced fraction numbers with ions leading to increased efficiency of machine utilization and patient convenience.

4.1.5. Effect of tumour differentiation and growth rate

The observations of Battermann [4.8] on the treatment of lung metastases indicate that slowly growing tumours benefit from high LET irradiation (Fig. 4.9). Slow growth is associated with resistance to photons because of the few cells in radiosensitive cell cycle phases, and the longer time available for cellular repair. By classifying tumours according to their degree of histological differentiation, Battermann also reached the conclusion that 80–90% of the well differentiated tumours had a doubling time >100 days and, therefore, would be likely to benefit from high LET. The clinical results accumulated over more than 25 years confirmed these predictions as shown below.

For the 15 MeV neutrons used in this study (produced by a (d,T) generator), the RBE for the tolerance of the most important normal tissues is

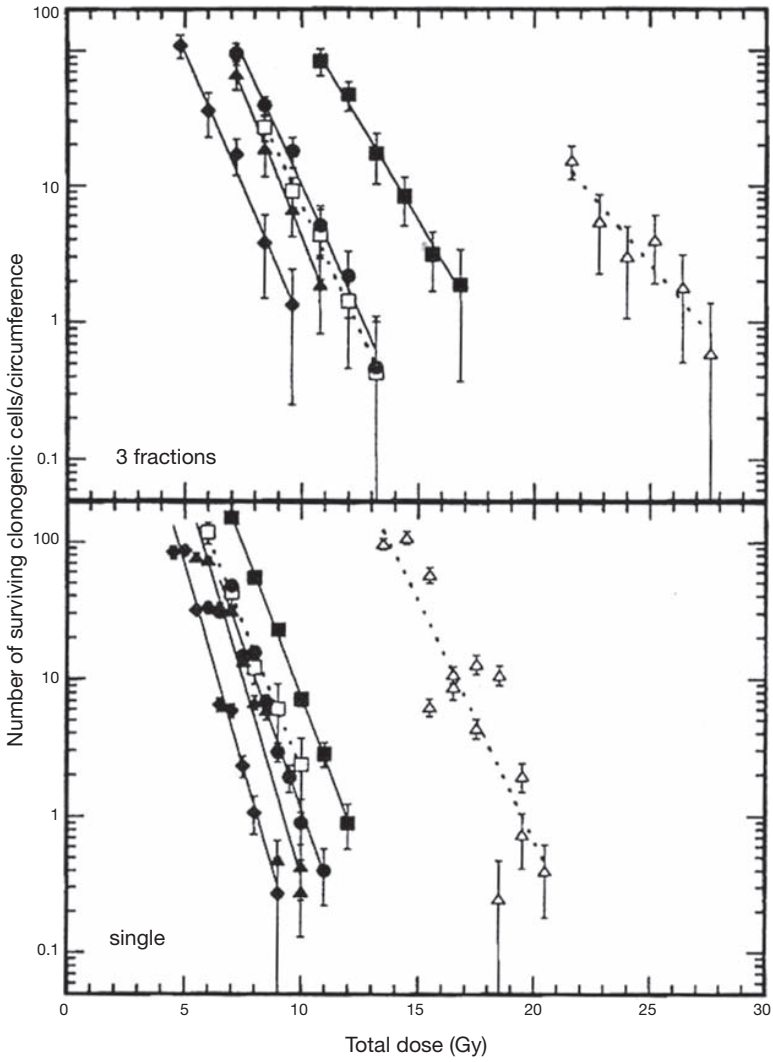

FIG. 4.8. Relationship between the total dose and survival of jejunal crypt clonogenic cells in mice exposed to single or three fraction irradiation. γ rays (△); neutrons (□); proximal (•), middle (▲) and distal (♦) peak of the SOBP carbon ion beam; unmodulated carbon ion beam (■) (mean +/- SE). The data were fitted by a least squares regression analysis [4.7].

about 3. As a consequence, neutrons are a good indication (RBE > 3) for tumours having a doubling time greater than ≈100 days. In contrast, they should not be used for rapidly growing tumours. For details on the technical irradiation conditions, see Ref. [4.8].

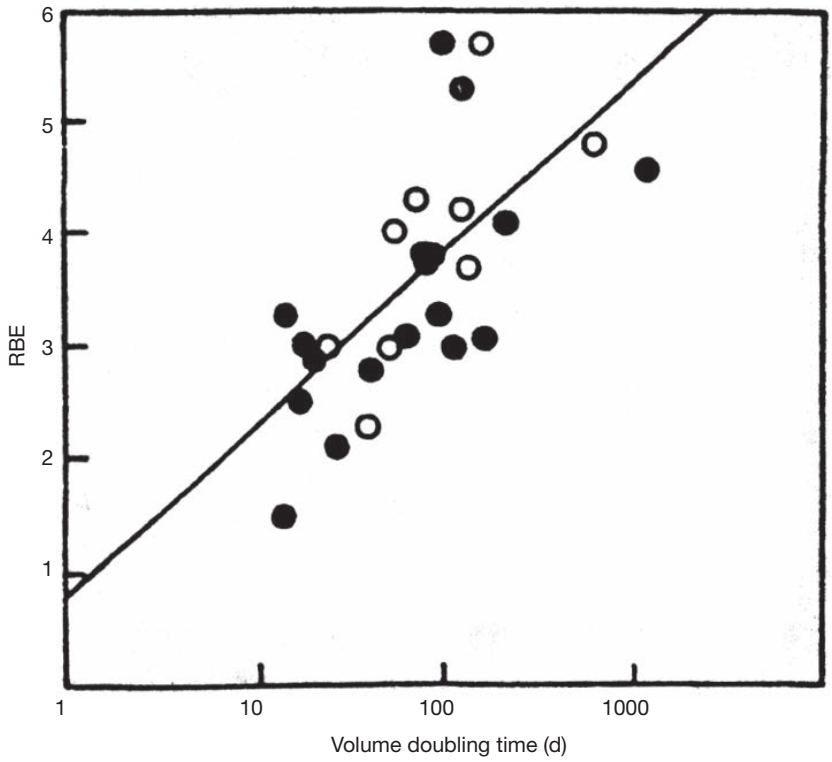

FIG. 4.9. Relation between the RBE of neutrons for regression of lung metastases in patients and tumour volume doubling time [4.8].

4.2. PATIENT SELECTION FOR HIGH LET RADIOTHERAPY

Radiobiological data suggest that high LET radiations may have a potential benefit for the treatment of some cancer types or sites. These data, obtained in the 1960s with neutrons, are still valid and consistent with more recent radiobiological and clinical findings [4.9]. Consequently, they imply the need to identify those patients that are likely to benefit from high LET radiation.

A reduction in OER should, in principle, always be an advantage. However, it is still necessary to identify those patients where hypoxia is the main factor of radioresistance and who could significantly benefit from a reduction in OER.

In contrast, a reduction of differences in radiosensitivity related to cell line, position in the mitotic cycle and repair capacity could be an advantage or a disadvantage, depending on the relative characteristics of the cancer cell population and the surrounding normal cell population.

Schematically, the clinical situations may be described with three possible scenarios, illustrated in Fig. 4.10, which shows (a) the differences in radiosensitivity to photons protect the normal tissues at risk. Replacing photons by neutrons, resulting in a reduction in the differences in radiosensitivity would thus be detrimental. Some typical examples are seminomas, lymphomas and Hodgkin's disease. The opposite situation is represented in Fig. 4.10(b) and (c) where the normal tissues are more sensitive to photons than tumour cells. High LET brings a benefit by reducing the difference in radiosensitivity, which protects selectively the malignant cell population. A third more favourable situation, Fig. 4.10(c), can be considered where the relative radiosensitivities are reversed in the case of high LET. This could be the case when the greater radioresistance of the cancer cell population to photons is due, for example, to the presence of hypoxic cells. The possibility of altering the sequence of intrinsic radiosensitivities is suggested by the data of Fertil et al. (Fig. 4.11) [4.11].

This very schematic presentation based on experimental observations illustrates why high LET radiation cannot be expected to bring a benefit in all cases and again stresses the importance of patient selection.

4.3. RATIONALE FOR ION THERAPY

The potential advantages of ions can be summarized in four points:

(1) The physical selectivity of ion beams is comparable to, or better than, the best low LET therapy techniques. The penumbra is narrow and the dose ratio between the SOBP and entrance plateau is better than with the best low LET radiation (protons). Nuclear fragmentation of the ion beams is a potential disadvantage because some energy is deposited beyond the Bragg peak. However, this aspect is probably not clinically significant because the dose is low and the fragments are lower LET particles.

(2) The LET in the ion beam, and consequently the RBE, increases with depth, and this increases the ratio of the biologically weighted doses between the SOBP and the entrance plateau. The RBE is comparable to neutrons, but the physical dose selectivity is vastly improved for ions.

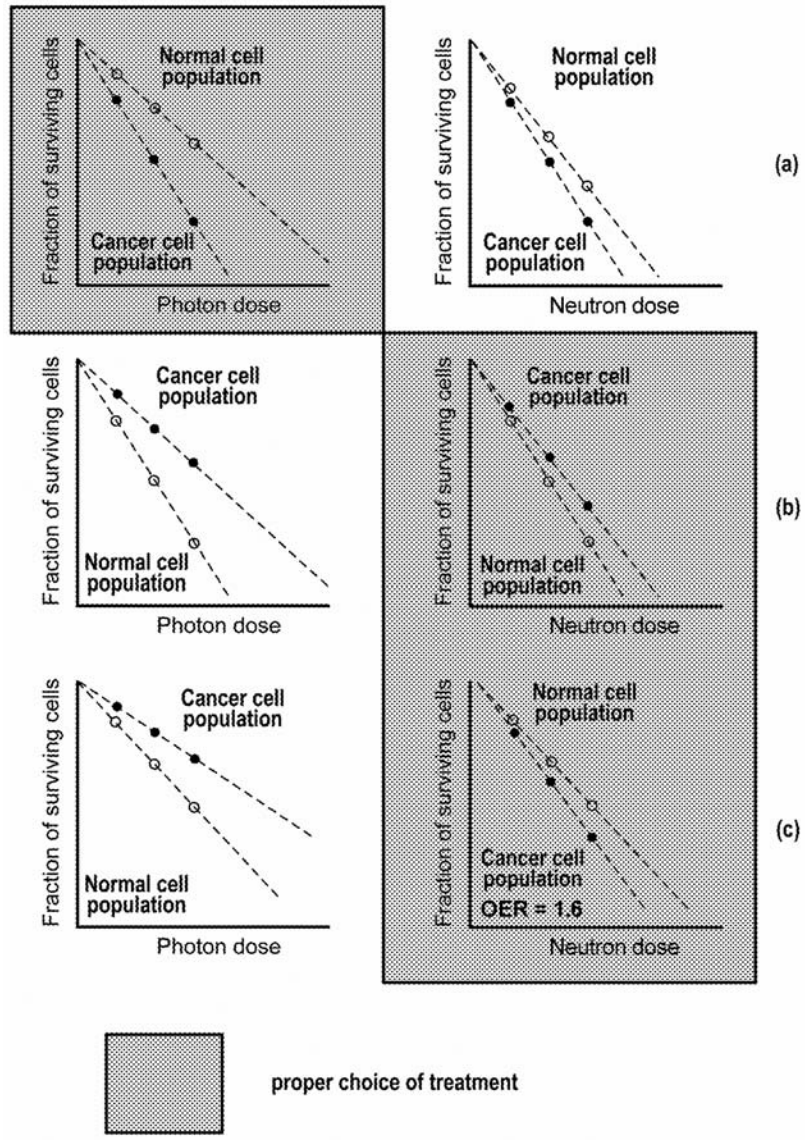

FIG. 4.10. Importance of patient selection for high LET therapy. Three possible scenarios are considered [4.10]: (a) the cancer cells are more sensitive to X rays than the critical normal cells and there is no argument for using high LET radiation, which would reduce this favourable differential effect; (b) high LET brings a benefit by reducing a difference in radiosensitivity, which would selectively protect the cancer cell population; (c) the relative radiosensitivities are reversed (see the following sections). It is assumed in the figure that the survival curves are exponential after fractionated irradiation [4.10].

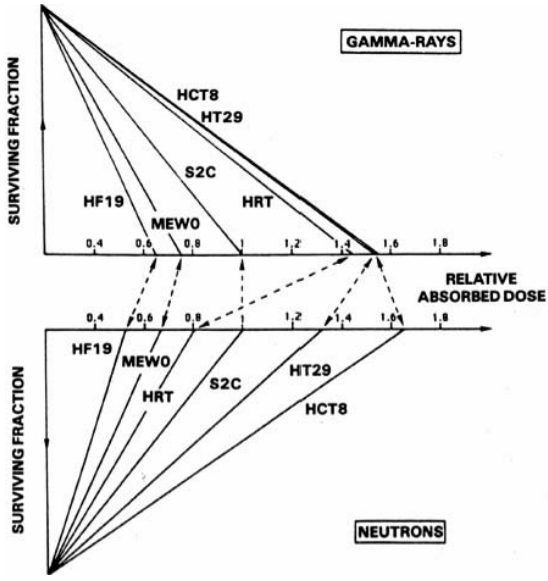

FIG. 4.11. Surviving fractions for six cell lines irradiated with γ rays or d(50)+Be fast neutrons. The effective Do ($_{eff}D_o$) values are computed for fractionated irradiation at 2 Gy per fraction (photons or equivalent). To facilitate comparison, the relative doses are given in the abscissa after normalization for RBE. The variations of radiosensitivities are as large with neutrons as with photons but the order of radiosensitivities is modified [4.12, 4.11].

(3) At the level of the SOBP, where the PTV (see Section 6) is located, high LET makes heavy ion beams specifically effective for the treatment of some tumour types that are resistant to low LET radiation.

(4) After fractionated irradiation, there is reduced possibility for repair for cells in the PTV located in the SOBP, because the LET is highest there. In contrast, the normal tissues located outside the SOBP, in the entrance plateau region, are exposed to lower LET radiation and thus may benefit from an increased repair opportunity. Therefore, from a radiobiological point of view, fractionation in ion therapy should bring a significant advantage and should be exploited. It is recognized, however, that this radiobiological advantage may be balanced by the advantage of reducing treatment times to reduce the effect of tumour cell repopulation and also by some economic considerations [4.13].

Based on the arguments and the accumulated clinical experience with protons and neutrons, ions appear to be a very promising radiation therapy

modality for selected tumour types or tumour sites. Section 5 discusses some clinical data that support this conclusion.

While ions appear to have potential advantages for the treatment of many tumour types, it seems wise to insert a word of caution. It has been pointed out that the physical dose in the SOBP is significantly greater than in the entrance plateau and that, because of the high LET in the SOBP, the biological weighting factor will increase the effect of this dose. It has also been pointed out that LET increases with depth in the SOBP. All of the above would appear to be advantageous for the treatment of tumours wholly contained within the SOBP. However, it cannot be assumed that the radiobiological effects seen in the entrance plateau, where the LET may be in excess of 20 keV/μm, are characteristic of low LET radiations. Figure 4.1 suggests that RBE begins to increase for LET values above 20 keV/μm. Table 4.1 [4.14] shows RBE values measured for several biological systems at several points in a spread out beam of carbon ions as well as at the entrance. The table indicates that RBE increases with depth in the SOBP but also shows a very high value for RBE in the entrance region. The apparently high RBE value shown in the entrance region was derived from a preliminary skin experiment and more recent experiments suggest that the RBE in the entrance region is approximately 1.5, in agreement with the data shown in Fig. 4.1. The data in Fig. 4.1 and Table 4.1 indicate that care must be taken in assuming values of RBE in the entrance region of an ion beam. In addition, the RBE in the entrance plateau may be a function of the type of scattering and beam modulation used with any ion beam.

TABLE 4.1. RBE VALUES OF MODULATED 290-MEV/AMU CARBON ION BEAMS OF THE HEAVY ION MEDICAL ACCELERATOR RELATIVE TO PHOTON RADIATION

Position	LET[a] (keV/μm)	RBE values		
		Single fraction		Four fractions
		Cell culture	Skin reaction	Skin reaction
Entrance SOBP (6 cm)	22	1.8	2.0	—
Proximal	42	2.1	2.1	2.3
	45	2.2	2.2	—
Middle	48	2.2	2.3	—
	55	2.4	2.3	—
Distal	65	2.6	2.3	2.9
	80[a]	2.8	2.4	3.1
Distal fall-off	100	—	—	3.5

[a] LET value of fast neutrons used in cancer treatment at the National Institute of Radiological Sciences (Chiba, Japan) is also 80 keV/μm [4.14].

REFERENCES

[4.1] WAMBERSIE, A., et al., Radiobiological rationale and patient selection for high-LET radiation in cancer therapy, Radiother. Oncol. **73** Suppl. 2 (2004) 1–14.

[4.2] BLAKELY, E.A., NGO, F.Q.H., CURTIS, S.B., TOBIAS, C.A., Heavy-ion radiobiology: Cellular studies, Adv. Radiat. Biol. **11** (1984) 195–389.

[4.3] FIELD, S.B., HORNSEY, S., High-LET Radiations in Clinical Radiotherapy (BARENDSEN, G.W., BROERSE, J.J., BREUR, K., Eds), Pergamon Press, Oxford (1979).

[4.4] BARENDSEN, G.W., Responses of cultured cells, tumours and normal tissues to radiations of different linear energy transfer, Curr. Top. Radiat. Res. **4** 293 (1968).

[4.5] CHAPMAN, J.D., "Biophysical models of mammalian cell inactivation by radiation", Radiation Biology in Cancer Research (MEYN, R.E., WITHERS, H.R., Eds), Raven Press, New York (1980).

[4.6] BARENDSEN, G.W., The relationship between RBE and LET for different types of lethal damage in mammalian cells: Biophysical and molecular mechanisms, Radiat. Res. **139** (1994) 257–270.

[4.7] FUKUTSU, K., KANAI, T., FURUSAWA, Y., ANDO, K., Response of mouse intestine after single and fractionated irradiation with accelerated carbon ions with a spread-out Bragg peak, Radiat. Res. **148** 2 (1997) 168–174.

[4.8] BATTERMANN, J.J., BREUR, K., HART, G.A.M., VAN PEPERZEEL, H.A., Observations on pulmonary metastases in patients after single doses and multiple fractions of neutrons and cobalt-60 gamma rays, Eur. J. Cancer **17** 539 (1981).

[4.9] ENGENHART-CABILLIC, R., WAMBERSIE, A. (Eds), Fast Neutrons and High-LET Articles in Cancer Therapy, Recent Results in Cancer Research 150, Springer Verlag, Heidelberg (1998).

[4.10] TUBIANA, M., DUTREIX, J., WAMBERSIE, A., Introduction to Radiobiology, Taylor & Francis, London (1990).

[4.11] FERTIL, B., et al., In vitro radiosensitivity of six human cell lines. II. Relation to RBE of 50 MeV neutrons, Radiat. Res. **90** (1982) 526–537.

[4.12] FERTIL, B., DESCHAVANNE, P., GUEULETTE, J., WAMBERSIE, A., MALAISE, E.P., Dependence of the quadratic model parameters on dose rate (gamma rays) and 50 Mev neutrons: An analysis based on the in vitro survival curves of 6 human cell lines, Radiat. Environ. Biophys. **17** 315 (1980).

[4.13] WAMBERSIE, A., GUEULETTE, J., JONES, D.T.L., GAHBAUER, R., "Ion-beam therapy: Rationale, achievements and expectations", Particle and Photon Interactions with Matter (HATANO, MOZUMBER, Eds), Marcel Dekker, New York (2003) 743–784.

[4.14] TSUJII, H., MORITA, S., MIYAMOTO, T., et al., Preliminary results of phase I/II carbon ion radiotherapy, Int. J. Brachytherapy **13** (1997) 1–8.

5. CLINICAL EXPERIENCE WITH NEUTRONS AND IONS

Many of the clinical data available today for high LET radiations were obtained with fast neutrons. A short review of the neutron data is presented here. As some of the neutron results may be subject to controversy, the review concentrates on information derived from randomized trials.

5.1. CLINICAL EXPERIENCE WITH FAST NEUTRONS

5.1.1. Salivary gland tumours

For inoperable, incompletely resected or recurrent salivary gland tumours, a significant advantage for neutron versus photon therapy was recognized. The European data [5.1] are pooled in Table 5.1: the local control averaged 65% for neutrons versus 25% for comparable historical series treated with low LET techniques.

A randomized cooperative study, initiated by the Radiation Therapy Oncology Group (RTOG) and the Medical Research Council (MRC), at two years showed a significant advantage for neutrons compared to photons for locoregional control (76% versus 17%, $P < 0.005$) and a trend towards improved survival (62% versus 25%). From Fig. 5.1 it can be seen that analysis after ten years continued to show a striking difference in locoregional control

TABLE 5.1. POOLED EUROPEAN DATA OF LOCAL CONTROL IN ADVANCED SALIVARY GLAND TUMOURS AFTER FAST NEUTRON IRRADIATION [5.1]

Reference	No. of patients	Local control
Catterall (1987)	65	48 (74%)
Battermann and Mijnheer (1986)	32	21 (66%)
Duncan et al. (1987)	22	12 (55%)
Prott et al. (1996)	64	39 (61%)
Kovács et al. (1987)	15	13 (87%)
Krüll et al. (1995)	74	44 (59%)
Skolyszweski et al. (1982)	3	2
Overall	275	179 (65%)

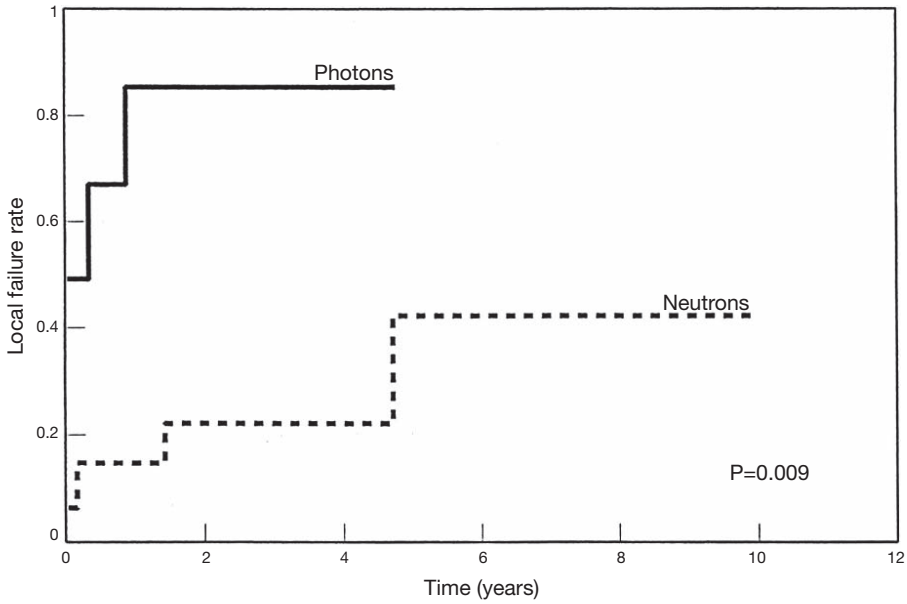

FIG. 5.1. Neutron therapy of salivary gland tumours. Probability of local–regional failure for unresectable salivary gland tumours. Starting values of the curves represent initial local–regional failure rates [5.2].

(56% for neutrons versus 17% for photons, P = 0.009), but both groups experienced a high rate of metastatic failure [5.2].

Neutron beam therapy has been recognized as the treatment of choice in patients with unresectable or recurrent malignant salivary gland tumours or in patients where radical resection would require facial nerve sacrifice. The fact that salivary gland tumours are rather superficial probably explains why the inferior physical selectivity of the neutron beams was not a significant handicap. These observations remain relevant from the radiobiological point of view with respect to possible benefits of high LET radiations even if modern surgical or low LET irradiation techniques may reduce the clinical use of neutrons.

5.1.2. Prostatic adenocarcinomas

The typical slow growth rate and low cycling fraction of prostatic adenocarcinoma provide a logical radiobiological rationale for exploring neutrons or other high LET radiations in the treatment of this disease. Among the

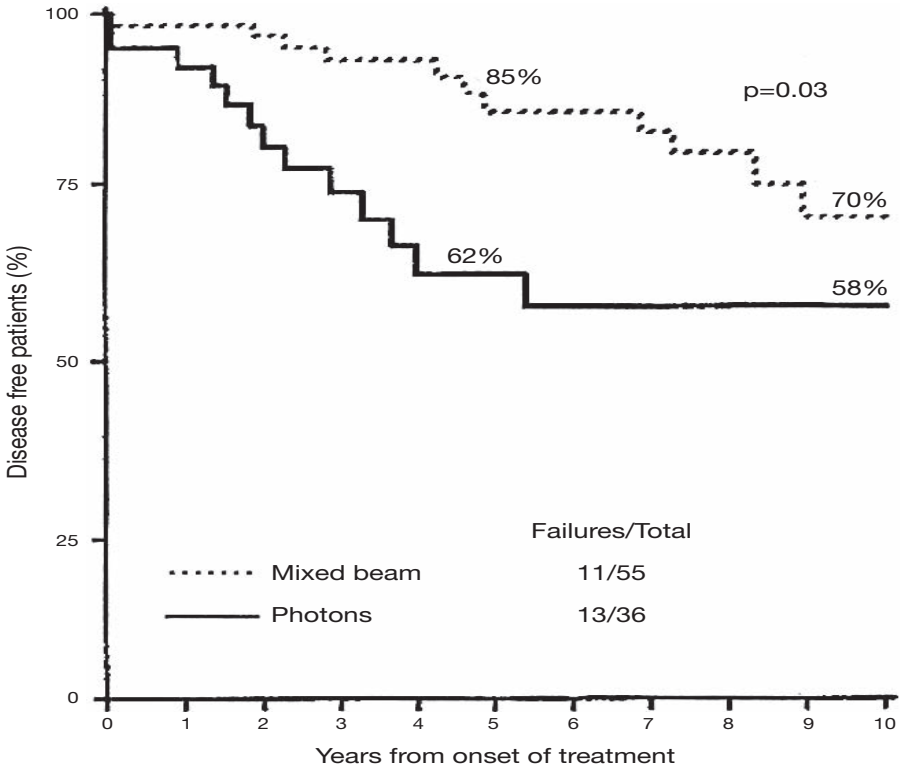

FIG. 5.2. Clinical locoregional control in patients treated with mixed (neutron–photon) beams or photons only (RTOG randomized trial) for locally extended prostatic adenocarcinoma [5.2].

numerous published data, two randomized trials initiated for locally advanced prostate tumours are considered here.

In the USA, the RTOG [5.3] compared 'mixed beams' (a combination of photons and neutrons) to conventional photons. Locoregional control, as well as survival, were significantly superior after mixed beam irradiation (Fig. 5.2) [5.2].

In 1986, the Neutron Therapy Collaborative Working Group (NTCWG) compared neutrons (alone) and conventional photons. A significant difference ($P < 0.01$) was observed in 'clinical' locoregional failure, with actuarial five year failure rates of 11% versus 32% after neutrons and photons, respectively (Fig. 5.3). Inclusion of routine post-treatment biopsies resulted in five year 'histological' locoregional failure rates of 13% and 32%, respectively ($P = 0.01$) [5.2, 5.4].

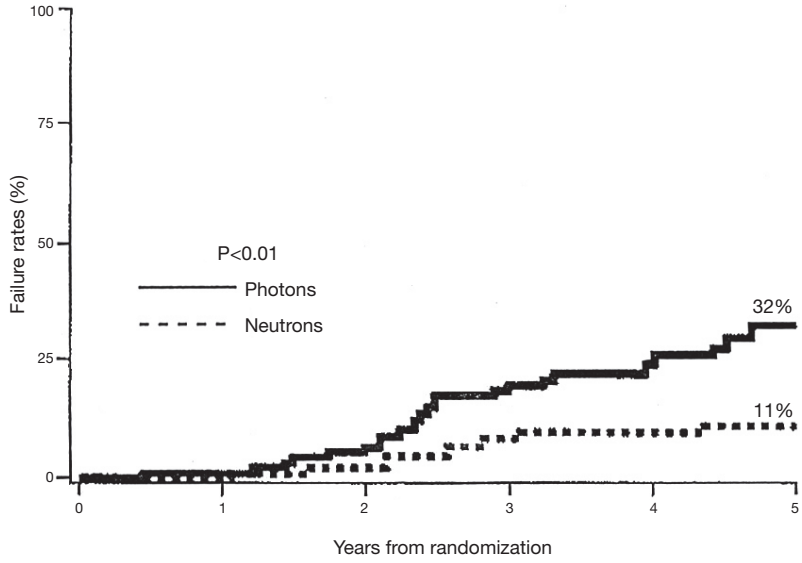

FIG. 5.3. Actuarial clinical locoregional failure in patients with locally advanced prostate cancer. For results of NTCWG trial on prostate, see Ref. [5.2].

Due to the long natural history of recurrent prostate cancer, longer follow-up is required to assess the ultimate impact of the improved local control on survival. However, differences in prostate specific antigen (PSA) levels confirm the apparent advantage of neutrons.

Late sequellae, mainly large bowel complications, were similar in the neutron and photon groups when the technical irradiation conditions with neutrons were improved and reached a level comparable to that with photons. In particular, the introduction of a multileaf collimator in one neutron centre dramatically reduced the complication rate [5.2].

Since these results were obtained, a number of novel techniques have been developed for the treatment of prostatic adenocarcinoma at different stages. They may influence the proportion of patients treated by high LET techniques, but the radiobiological conclusions of these clinical trials on the advantage of high LET radiation remain valid and strengthen arguments for the potential usefulness of high LET ions.

5.1.3. Other tumour sites or types

For other tumour sites or types, such as slowly growing soft tissue sarcomas, fixed lymph nodes in the cervical area, locally advanced paranasal sinus tumours and some bronchus carcinomas, the available data show a

benefit for neutrons for trials where neutron therapy was applied under appropriate technical conditions. Randomized studies are needed to confirm the benefit of high LET for these disease sites [5.5–5.9].

5.2. CLINICAL EXPERIENCE WITH ION BEAMS

5.2.1. The Berkeley ion programme

The Berkeley ion programme utilizing both helium and neon ions was limited by the availability of the machine and its complexity, which resulted in many unscheduled downtimes. As a consequence, there was a patient recruitment problem. Nevertheless, a great deal of valuable radiobiological and clinical information was obtained. Table 5.2 [5.10] summarizes the results obtained with the neon beams. The results obtained with the then current photon techniques are shown for comparison. While these data are not compiled from formal clinical trials, they do suggest an advantage for neon ions. Reported results for neon treatments of bronchus carcinomas gave local control of 39%. For brain tumours, median survival was 17 months. The results for lung and brain showed no improvement over conventional photon treatments [5.11].

TABLE 5.2. TREATMENT OUTCOME COMPARING NEON IONS AND CONVENTIONAL X RAY THERAPY FOR SELECTED TYPES OF TUMOURS [5.10]

Tumour and end point	Neon beam (%)	X rays (%)
Salivary gland cancer (N = 18)		
Long term local control	61	25–35
Paranasal sinus cancer (N = 10)		
Long term survival	69	32–40
Long term local control	69	n.a.[a]
Soft tissue sarcoma (N = 12)		
Long term local control	56	30–50
Sarcoma of bone (N = 18)		
Long term local control	59	21–33
Locally advanced prostate cancer (N = 12)		
5 year actuarial control	75	30–50

[a] n.a.: not applicable.

In an attempt to compare the results obtained with the two high LET modalities, Table 5.3 compares the neon data from Berkeley with the average results obtained with fast neutrons [5.12]. All of the comparisons shown in Tables 5.2 and 5.3 should be taken with care because they are based on the best available photon series and are not randomized trials. Despite this, it should be pointed out that tumour types or sites for which an advantage was found with neon ions are those for which an advantage was also found with fast neutrons. This suggests a specific 'high LET' effect.

Similarly, the clinical experience gained with fast neutrons at NIRS in Chiba was used as the basis for identifying patients suitable for high LET therapy with carbon ions. The neutron experience was also used to help select the best 'isoeffective dose weighting factor' for the carbon ion clinical trials (see Section 3, Annex IV, and Ref. [5.13]).

5.2.2. The Chiba programme

A summary of the clinical experience with carbon ions gained at the NIRS is presented in Table 5.4 [5.13]. A more complete review is given in Annex IV.

Between June 1994 and August 2003, a total of 1601 patients with various types of malignant tumours were enrolled in phase I/II dose escalation studies and clinical phase II studies. All but malignant glioma patients received carbon ion radiotherapy alone with a fraction number and overall treatment time being fixed for each tumour site. One field per day and 3–4 fractions per week were given. In dose escalation studies, the total dose was escalated by 5% or 10% increments to ensure safe treatments and to determine appropriate dose levels.

TABLE 5.3. COMPARISON OF SOME CLINICAL RESULTS OBTAINED WITH FAST NEUTRONS, NEON IONS AND CONVENTIONAL PHOTON RADIATION THERAPY

	Neutrons[a] (%)	Neon ions[b] (%)	Conventional[c] (%)
Salivary gland (local control)	67	61	25–35
Paranasal sinus (survival)	67	69	20–40
Sarcoma (local control)	53	56	30–50
Prostate (5 year actuarial control)	77	75	30–70

[a] See Ref. [5.12].
[b] See Ref. [5.10].
[c] Ranges derived from Refs [5.10, 5.12].

TABLE 5.4. NIRS RESULTS OF CARBON ION THERAPY FROM JUNE 1994 TO AUGUST 2003 [5.13]

Protocol	Phase	Stage	Dose (GyE)	No. of fractions	No. of weeks	No. of patients	3 year local control (%)	3 year survival (%)
H&N -1	1/2	T3–4	48.6–70.2	18	6	17	86	53
H&N -2	1/2	T3–4	52.8–64.0	16	4	19	76	42
H&N -3	2	T3–4		16	4	182+2	78	46
H&N -4	2	Melanoma		16	4	26		
Lung-1	1/2	Stage 1 peripheral	59.4–95.4	18	6	47+1	65	66
Lung-2	1/2	Stage 1 peripheral	72.0–79.2	9	3	34	90	56
Lung-3	2	Stage 1 peripheral	72.0	9	3	49+1	98	68
Lung-4	1/2	Stage 1 peripheral	52.8–60.0	4	1	71+1	93	73
Lung-5	1/2	Stage 1 peripheral	28.0	1	1 d	24		
Lung-6	1/2	Stage 1 hilar	57.6–61.2	9	3	20	95	50
Liver-1	1/2	T2–4	49.5–79.5	15	5	24+1	77	50
Liver-2	1/2	T2–4	48.0–69.6	12 or 8	3 or 2	82+4	87	48
Liver-3	2	T2–4	48.0	4	1	44+3	90	88
Liver-4	1/2	T2–4	32.0	2	2 d	6		
Prostate-1	1/2	B2–C	54.0–72.0	20	5	35	100	94
Prostate-2	1/2	B2–C	60.0–66.0	20	5	61	100	97
Prostate-3	2	T1c–C	66.0	20	5	151	100	92
Uterus-1	1/2	Stage 3–4a (squamous)	52.8–72.0	24	6	30	49	40
Uterus-2	1/2	Stage 2b–4a (squamous)	68.9–72.8	24	6	14	79	43
Uterus-3	1/2	Stage 2b–4a (squamous)	64.0	20	5	15	58	58
Uterus	1/2	Adenoca	62.4–68.0	20	5	22	55	68
Bone/ST	1/2	Unresectable	52.8–73.6	16	4	57+7	67	47
Bone/ST	2	Unresectable	70.4	16	4	98+10	88	54

For patients with prostate, cervix and oesophageal cancer, severe late complications were observed at the level of the recto-sigmoid colon and oesophagus during the initial dose escalation studies. Such adverse effects were greatly reduced following both dose and field size reductions and improvements in radiation techniques.

Carbon ion radiotherapy was shown to provide an improvement in the results for:

(a) Locally advanced head and neck tumours, in particular those with non-squamous cell histology, such as adenocarcinoma, adenoid cystic carcinoma and malignant melanoma;
(b) Early stage and locally advanced non-small cell lung cancer (NSCLC);
(c) Locally advanced bone and soft tissue sarcomas not suited for surgical resection;
(d) Locally advanced hepatocellular carcinomas;
(e) Locally advanced prostate carcinomas, in particular for high risk patients;
(f) Chordoma and chondrosarcoma of the base of the skull and cervical spine;
(g) Post-operative pelvic recurrence of rectal cancer.

In addition, a dose escalation protocol is being investigated for the treatment of malignant gliomas, pancreatic, cervical and oesophageal cancers.

5.2.3. The Darmstadt programme

Carbon ion therapy has been available at the basic physics research centre of the Gesellschaft für Schwerionenforschung (GSI) in Darmstadt, Germany, since December 1997. Patient treatments were carried out by the Radiation Oncology Team of the University of Heidelberg in cooperation with the Department of Biophysics of GSI, the Division of Medical Physics of the German Cancer Research Centre Heidelberg and the Research Centre Rossendorf.

Patients were treated within 3 beam time block periods of 20 days each per year. The overall treatment capacity per year was 45–50 patients. Since inception of the programme, 196 patients have been treated with carbon ions [5.14].

5.2.3.1. Chordomas and low grade chondrosarcomas of the base of the skull

Between November 1998 and December 2001, 44 patients with chordomas and 23 patients with low grade chondrosarcomas have been included in clinical phase I/II trials. The data were analysed in March 2004; the median follow-up

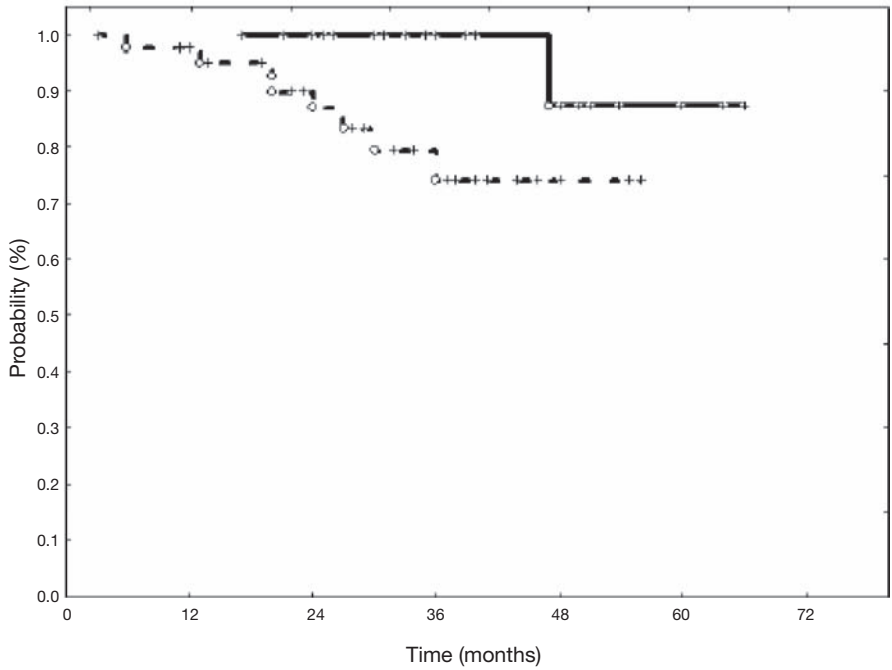

FIG. 5.4. Actuarial local control (Kaplan Meier curve) for 67 patients treated with carbon ion RT for chordomas (dotted line, n = 44) and low grade chondrosarcoma (solid line, n = 23) of the skull base [5.14].

was 32 months (range 3–66 months). Eight patients with chordoma and one patient with chondrosarcoma developed local recurrences. Actuarial four year local control rates were 74% for chordoma and 87% for chondrosarcoma of the base of the skull, respectively (Fig. 5.4). The overall survival rates at four years were 86% for chordomas and 100% for chondrosarcomas, respectively (Fig. 5.5).

These results compare well with those published for protons although no randomized data are currently available. Therefore, no definitive conclusion can be drawn concerning the relative indications for ions versus protons, especially for paediatric tumours [5.15, 5.16].

5.2.3.2. Sacrococcygeal and spinal chordomas and low grade chondrosarcomas

A total of 19 patients with chordomas and chondrosarcomas of the cervical and lumbar spine (9) and sacrum (10) were treated. One patient with sacral chordoma developed a local regional recurrence. One patient with spinal chordoma had a recurrence salvaged by surgery.

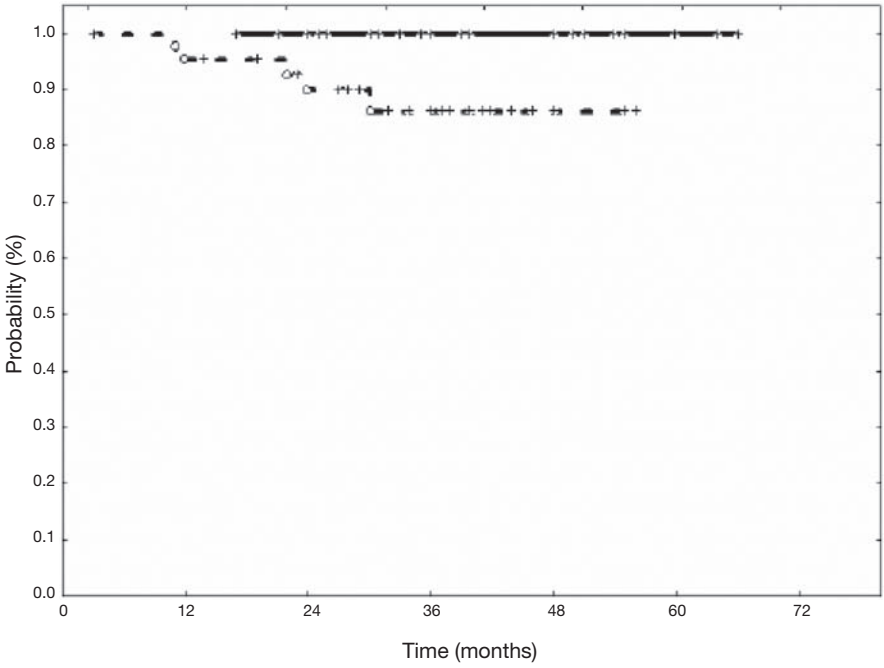

FIG. 5.5. Actuarial overall survival (Kaplan Meier curve) for 67 patients treated with carbon ion RT for chordomas (dotted line, n = 44) and low grade chondrosarcomas (solid line, n = 23) of the skull base [5.14].

Of the 19 patients, two developed distant metastases from which one patient died.

5.3. CONCLUSIONS FROM CLINICAL EXPERIENCE WITH HIGH LET RADIATIONS

5.3.1. Summary of clinical experience

For the last several decades, significant effort has been devoted to improve the efficacy of low LET radiation therapy, for example, conformal therapy, IMRT, tomotherapy, modern brachytherapy and improved fractionation regimes.

The introduction of high LET radiations brings another dimension to the debate: a potential improvement for some tumour types or sites due to a radiobiological differential effect which improves the selectivity of high LET

radiation for these tumours versus normal tissues by their biological mode of action.

Fast neutrons were the first high LET radiations to be used clinically. From randomized trials, a statistically significant benefit of high LET versus low LET radiation was demonstrated for locally advanced salivary gland tumours and prostatic adenocarcinomas. In addition, a number of studies indicate a benefit for the treatment of slowly growing soft tissue sarcomas and some locally advanced head and neck tumours (fixed lymph nodes). It is important to note that these clinical observations are consistent with radiobiological data, predicting a potential benefit for slowly growing and/or hypoxic tumours. However, there is still some controversy on the overall benefit of neutrons.

When using the neutron data to derive the clinical indications for ion therapy, two factors have to be taken into account. Firstly, the poor physical selectivity available in most of the neutron facilities was a great handicap in the initial clinical evaluation of high LET. In contrast, ions achieve a physical selectivity comparable to almost any low or high LET technique.

Secondly, neutrons were compared to the best available photon techniques at that time. The recent and dramatic developments in photon irradiation techniques may, in practice, reduce the clinical gain of ions. However, even if comparable absorbed dose distributions can be obtained with photons and ions, further evidence is needed concerning the radiobiological benefit associated with high LET for some tumour types.

When comparing clinical results obtained with ion and fast neutron beams, it is always difficult to separate the effects resulting from high LET from the effects of large differences in dose distribution. In addition, patient recruitment may have been quite different in the various trials. Nevertheless, comparison of the data from the ion trials at Berkeley with the previous trials with neutrons indicates a clear similarity concerning the tumour types or sites where the best clinical results were obtained (Table 5.5). This seems to suggest a clinical benefit from the use of high LET radiations. Similar conclusions can be drawn from the studies with sarcomas, prostate and lung tumours at the NIRS, Chiba (Table 5.4).

Ongoing studies at NIRS are aimed at reducing the number of fractions employed (see Annex IV). This approach is based on the excellent physical selectivity of the carbon ion beam and the fact that, with high LET, the effects of fractionation are likely to be very much reduced. To date, no reduction of local control or increased morbidity has been detected from this approach.

In Darmstadt, patient selection was strongly influenced by machine availability. Therefore, the selection of tumour sites was intended to exploit the excellent physical selectivity of the carbon beam coupled with a powerful

TABLE 5.5. INDICATIONS FOR ION THERAPY BASED ON HIGH LET CLINICAL EXPERIENCE AND RADIOBIOLOGICAL DATA [5.12]

1. Clinical experience with fast neutrons:
Salivary gland tumours and adenoid cystic carcinoma[a]
Prostatic adenocarcinoma[b]
Soft tissue sarcomas (slowly growing)
Fixed cervical lymph nodes
Some selected (NSCL) series[c]
2. Combination of physical selectivity and high LET radiation:
Uveal melanoma
Base of skull (chordomas[d])
Other brain lesions
3. Tumour characteristics:
Hypoxic tumours (hypoxia can now be detected: PET, etc.)
Slowly growing/well differentiated tumours

[a] Locally extended, inoperable, incompletely resected or recurrent tumours compared to low LET techniques [5.1, 5.2].
[b] Locally extended, compared to fractionated photon beam therapy. RTOG trial; NTCWG trial [5.3, 5.4].
[c] NTCWG 85-22 [5.2]; NIRS, Chiba [5.5].
[d] MGH, Boston [5.16]; CHR, Orléans [5.7]; GSI, Darmstadt [5.14].

treatment planning system. The results obtained for tumours of the base of the skull appear equal to, or better than, that reported for proton therapy. The local control rates for chondrosarcomas are high for both types of beams, but for those with chordomas the results seem slightly better with carbon ions. Although the differences are not significant and the follow-up is short, this could also suggest an advantage for high LET radiations.

5.3.2. Clinical and biological considerations for selecting patients for ion therapy

The overall potential advantages of ions can be summarized in five points:

(1) The physical selectivity of ion beams is comparable to, or better than, the best low LET therapy techniques. The penumbra is narrow and the dose ratio between the SOBP and entrance plateau is better than with the best low LET radiation (protons). Nuclear fragmentation of the ion beams is a potential disadvantage because some energy is deposited beyond the Bragg peak. However, this aspect is probably not a major concern in most instances.

(2) The LET, thus the RBE, at the level of the SOBP, is higher than at the level of the entrance plateau. In addition, within the SOBP, the LET increases with depth. The RBE thus also increases with depth and, as a consequence, increases the ratio of the biologically weighted absorbed doses between the SOBP and the entrance plateau. The RBE is comparable to neutrons, but the physical dose selectivity is vastly improved for ions.

(3) Ideally, the SOBP is delineated to include the whole 'tumour volume' (in the strict sense, the PTV), that is, the whole cancer cell population, and no critical normal structures. This simplified situation may be observed in very small tumours, such as ocular melanoma, some base of skull tumours and some sarcomas. In these rare situations, the SOBP includes mainly the whole malignant cell population, while normal structures are present only in the region of the entrance plateau.

An increase of the RBE from the entrance plateau to the SOBP thus contributes to an increase of the therapeutic gain factor (TGF).

In the discussion above, the SOBP was assumed to contain only malignant cells and no critical normal structures. This is, of course, an oversimplification, as the SOBP needs to include the whole PTV. The 'tumour' may contain, in addition to the cancer cell population, normal tissue structures, such as blood vessels, nerves, volumes of bone and cartilage. Even more important is the fact that the PTV includes a safety margin for subclinical disease and inaccuracy in positioning, that consists mainly of normal structures. This generally is the dose limiting factor.

(4) At the level of the SOBP, where the PTV is located, high LET makes ion beams specifically effective for the treatment of some tumour types that are resistant to low LET radiation.

(5) Fractionation has been shown to protect tissues irradiated with low LET radiation. In contrast, the level of protection is lower or absent with high LET irradiation. Therefore, fractionation would selectively protect the normal tissues in the entrance plateau, where LET is lower than in the region of the SOBP assumed to contain the malignant cells. There is, however, a tendency to reduce the number of fractions used in ion therapy primarily for economic reasons and patient convenience. There could also be some clinical arguments in favour of accelerated treatment to avoid tumour cell repopulation.

Based on the arguments mentioned and the accumulated clinical experience with protons and neutrons, ion beam therapy appears to be a very promising therapy modality for selected tumour types or tumour sites. Table 5.5 summarizes the best estimate of suitable clinical indications for ions based on both dose distribution and biological considerations.

REFERENCES

[5.1] KRÜLL, A., et al., "Neutron therapy in malignant salivary gland tumours: Results at European centres", Fast Neutrons and High-LET Particles in Cancer Therapy (ENGENHART-CABILLIC, R., WAMBERSIE, A., Eds), Springer Verlag, Heidelberg (1998) 88–99.

[5.2] LINDSLEY, K.L., et al., Clinical trials of neutron radiotherapy in the United States, Bull. Cancer Radiother. **83** Suppl. 1 (1996) 78.

[5.3] LARAMORE, G.E., KRALL, J.M., THOMAS, F.J., Fast neutron radiotherapy for locally advanced prostate cancer: Final report of a radiation therapy oncology group randomized clinical trial, Am. J. Clin. Oncol. **16** (1993) 164–167.

[5.4] RUSSELL, K.J., CAPLAN, R.J., LARAMORE, G.E., Photon versus fast neutron external beam radiotherapy in the treatment of locally advanced prostate cancer: Results of a randomized prospective trial, Int. J. Radiat. Oncol. Biol. Phys. **28** (1993) 47–54.

[5.5] TSUNEMOTO, H., et al., Japanese experience with clinical trials of fast neutrons, Int. J. Radiat. Oncol. Biol. Phys. **8** (1982) 2169–2172.

[5.6] TSUNEMOTO, H., MORITA, S., SATOH, S., IINO, Y., Present status of fast neutron therapy in Asian countries, Strahlenther. Onkol. **165** (1989) 330–336.

[5.7] BRETEAU, N., et al., Hadrons in radiation therapy, Bull. Cancer Radiother. **83** Suppl. 1 (1996).

[5.8] ENGENHART-CABILLIC, R., WAMBERSIE, A. (Eds), Fast Neutrons and High-LET Particles in Cancer Therapy, Recent Results in Cancer Research, Springer Verlag, Heidelberg (1998).

[5.9] WAMBERSIE, A., GAHBAUER, R., Hadrons (protons, neutrons, heavy ions) in radiation therapy: Rationale, achievements and expectations, Radiochem. Acta **89** (2001) 245–253.

[5.10] LINSTADT, D.E., CASTRO, J.R., PHELPS, T.L., Neon ion radiotherapy: Results of the phase I/II clinical trial, Int. J. Radiat. Oncol. Biol. Phys. **20** 4 (1991) 761–769.

[5.11] CASTRO, J.R., CHEN, G.T.Y., BLAKELY, E.A., Current considerations in heavy charged particle radiotherapy, Radiat. Res. **104** Suppl. 8 (1985) 263–271.

[5.12] WAMBERSIE, A., et al., Radiobiological rationale and patient selection for high-LET radiation in cancer therapy, Radiother. Oncol. **73** Suppl. 2 (2004) 1–14.

[5.13] TSUJII, H., et al., Overview of clinical experience on carbon ion radiotherapy at NIRS, Radiother. Oncol. **73** Suppl. 2 (2004) 41–49.

[5.14] SCHULZ-ERTNER, D., NIKOGHOSYAN, A., DIDINGER, B., DEBUS, J., Carbon ion radiation therapy for chordomas and low grade chondrosarcomas — current status of the clinical trials at GSI, Radiother. Oncol. **73** Suppl. 73 (2004) 53–56.

[5.15] WAMBERSIE, A., GRÉGOIRE, V., BRUCHER, J.M., Potential clinical gain of proton (and heavy ion) beams for brain tumours in children, Int. J. Radiat. Oncol. Biol. Phys. **22** (1992) 275.

[5.16] MUNZENRIDER, J.E., LIEBSCH, N.J., Proton therapy for tumours of the skull base, Strahlenther. Onkol. **175** Suppl. II (1999) 57–63.

6. RECOMMENDATIONS FOR REPORTING ION BEAM THERAPY

6.1. REPORTING: AN ESSENTIAL TOOL FOR EXCHANGING INFORMATION

As in other medical disciplines, the exchange of clinical information and treatment results is essential for the development of, and progress in, radiation oncology. This goal can be achieved only through a general harmonization of reporting patient data and treatment conditions. It requires uniformity and agreement on methods used to determine the doses and points and/or volumes where these doses are specified [6.1–6.6].

Requirements for reporting ion beam therapy should, in principle, be as similar as possible to those for reporting the current radiation therapy modalities. It is, however, recognized that ion therapy has its own clinical and technical uniqueness that should be taken into account. Ion therapy is a novel and complex irradiation modality, and requires new clinical, radiobiological and technical concepts, and strict quality assurance programmes for efficient and safe clinical application.

6.1.1. Three levels for reporting

The ICRU has recognized three levels of complexity for reporting results of radiation therapy [6.3, 6.6].

Today, ion beam therapy should be reported at level 3. Reporting at level 3 applies to complex treatments and/or new and evolving complex irradiation techniques, therefore, no requirements are formally established as yet. Nevertheless, comprehensive and carefully verified information should be reported.

6.1.2. Reporting radiation treatment

Accurate and complete recording of the treatment parameters is necessary in order to:

— Facilitate further care and follow-up of patients;
— Keep the treatment conditions reproducible and safe;
— Continuously develop clinical experience in the department and systematically improve the techniques;

— Be able to exchange information on treatment conditions with other centres (the amount of information depends on the purpose, for example, participation in clinical trials and follow-up of a patient);
— Be able to 'reconstruct' the treatment conditions when needed, to interpret the treatment outcome(s), and to ensure compliance with a quality assurance programme or a research and development programme.

It is important that adequate information exchange occurs between the medical, physics and radiography/radiotherapy staff, and that there is an agreement on the methods of recording the treatment parameters. The terms and concepts to be used should be clearly defined.

The amount of information that needs to be recorded depends on the technique, the complexity and the purpose of the treatment (cure or palliation). As far as ion therapy is concerned, a large amount of technical and medical information needs to be recorded because it is a new and complex technical modality, used mainly for radical treatment. Recording the treatment involves significant and diverse resources and thus is a departmental responsibility.

6.1.3. Reporting versus prescribing

As stressed above, the need for a consensus and harmonization for *reporting* therapeutic irradiations is no longer questioned. However, the *prescription* should remain the responsibility of the radiation oncologist in charge of the patient.

It is obvious that using the same approach and the same definitions of terms and concepts for prescribing, recording and reporting facilitates the procedures and reduces the risk of confusion and errors.

6.1.4. Points and volumes used for reporting

The ICRU has identified a series of reference points and volumes for reporting radiation therapy treatments. These points and volumes are specified in relation to anatomical structures and organs rather than irradiation beams.

Because of the dramatic development of imaging and radiation delivery techniques, there is an increasing trend in radiation oncology to specify the delivered doses in relation to volumes (or organs) in addition to points. It is thus important to agree on definitions of points and volumes for reporting.

It is possible to envisage three types of volumes. The first group is defined by purely oncological concepts (gross target volume and clinical target volume). The second group is in part defined by the oncological situation and

in part by the treatment modality (planning target volume, organs at risk and planning organ at risk volumes). The final group is mainly defined by the treatment as delivered (treated volume and reference volume). The volumes mentioned are described in ICRU Reports 50, 62 and 71 [6.3, 6.5, 6.6], and recalled only briefly here.

6.1.4.1. Gross target volume

The gross target volume (GTV) is the gross palpable, visible or clinically demonstrable location and extent of the malignant growth. It consists of the primary tumour (GTV-T), metastatic lymphadenopathy (GTV-N) or other metastases (GTV-M), if identified. In the GTV, the tumour cell density is always high ($\geq 10^6/mm^3$). Hence, an adequate dose must be delivered to the whole GTV for radical therapy.

6.1.4.2. Clinical target volume

The clinical target volume (CTV) is a tissue volume that contains the GTV(s) and/or subclinical malignant disease at a certain probability level.

Delineation of the CTV is based on the probability of disease progression of subclinical malignant cells outside the GTV and the probability of side effects of an eventual treatment. It thus requires the judgement of the radiation oncologist in the interpretation of the available clinical data. The relevant data to consider are the probability and magnitude of microscopic extension at different distances around the GTV, and the probability of subclinical invasion of regional lymph nodes or other tissues [6.7, 6.8]. Volumes containing tumour cell densities as high as $10^3/mm^3$ cannot be detected clinically or by current imaging techniques.

The delineations of GTV(s) and CTV(s) constitute part of the basic prescription of treatments; they are essential to the medical record. Their definition should, in principle, precede the selection of the treatment modality and the subsequent treatment planning procedures. However, the possibility of feedback and adjustment should always be kept open and is necessary in some situations [6.9].

6.1.4.3. Planning target volume

The planning target volume (PTV) concept is used as an approach to select the appropriate irradiation conditions to ensure that the prescribed dose is actually delivered to all parts of the CTV.

A volume larger than the CTV must be irradiated to compensate: (1) for expected physiological movements and variations in size, shape and position of the CTV during therapy (internal margin); and (2) for uncertainties (inaccuracies and lack of reproducibility) in patient–machine positioning (set-up margin). The PTV is thus a geometrical concept, introduced for treatment planning [6.5].

With charged particles, such as electrons, protons or ions, the need for adequate coverage implies the selection of the beam dimensions and also the beam penetration in depth. This means that, in addition to all the uncertainties seen with photon beam irradiation, some margin in depth must be left to allow for uncertainties in the position of the distal beam edge [6.6]. As a consequence, the lateral margins and the margin in depth compensate for completely different sources of set-up uncertainties. The goal remains to keep the CTV in the high dose region, taking into account both motion and range uncertainties.

6.1.4.4. Anatomical volumes relating to normal tissues

Issues relating to normal tissues include:

— Organs at risk (OAR);
— Planning organ at risk volumes (PRV).

The OAR ('critical normal structures') are normal tissues (e.g. spinal cord) whose radiation sensitivity may significantly influence treatment planning and/or prescribed dose. The OAR are highly dependent upon the treatment modality and, in particular, an OAR with photons may be avoided with ions. One advantage of ion therapy may be the sparing of the spinal cord, which may not be possible with photon therapy, for example, in the head and neck region.

Any movements of the OAR during treatment, as well as uncertainties in the set-up during the whole treatment course must be considered. This leads, by analogy with the PTV, to the concept of PRV that was introduced in order to protect the OAR from radiation damage.

For the ICRU recommendations for reporting OAR and PRV, see Ref. [6.6].

6.1.4.5. Treated volume

The treated volume is the tissue volume that (according to the approved treatment plan) receives at least the dose selected as the minimum dose to the PTV, and specified by the radiation oncology team as appropriate to achieve

tumour eradication or palliation, within the bounds of acceptable complications [6.5, 6.6].

6.1.4.6. Reference volume

The reference volume has been introduced to compare treatments performed in different centres [6.10]. It is defined as the volume encompassed by a selected and specified reference isodose chosen by consensus among the centres involved in the comparison.

6.2. SPECIFIC RECOMMENDATIONS FOR REPORTING A THERAPEUTIC ION BEAM IRRADIATION

6.2.1. Irradiation conditions

As a general principle, the irradiation conditions should be reported as completely as possible, with some consideration of the purpose of the report, for example, series of patients in a scientific publication or individual medical report.

This general principle applies to ion beam therapy, for which detailed and accurate technical information is especially needed. This should include at least:

— Particle type;
— Energy spectrum;
— Beam delivery system: scattering or scanning;
— Beam number, size and orientation;
— Position and depth of any SOBP;
— Fractionation regime.

6.2.2. Quantities and factors to be reported

6.2.2.1. Absorbed dose

As recommended for any radiation therapy modality, absorbed dose (in Gy) should always be reported for ion beam therapy at specified points or in specified volumes [6.11].

An accuracy on absorbed dose better than 5% is usually required, at the reference point(s) for curative treatments [6.12–6.14].

6.2.2.2. Isoeffective dose weighting factor in radiation therapy

In radiation therapy, the relationship between dose and effect is not unique, and the statement of absorbed dose alone is not sufficient to predict the clinical outcome. In addition to absorbed dose, factors such as dose per fraction, dose rate and radiation quality are known to influence these outcomes. Therefore, weighting factors need to be introduced when comparing and combining different treatment modalities (see Section 2.6).

In ion beam therapy, a weighting factor, W_{IsoE}, must be introduced to take into account differences in radiation quality, as well as to account for altered fractionation or other factors specific to ion beam therapy, relative to the reference treatment modality defined in Section 2.6. The methodology used to determine W_{IsoE} should be fully described. An example of a description for obtaining an appropriate isoeffective dose weighting factor, W_{IsoE}, is given by Mizoe et al. (Annex IV) based on their extensive clinical experience with fast neutrons.

Because of the large variation of RBE with depth and position in the ion beam, the value of W_{IsoE} should be determined at the reference point(s) and volume(s) where the isoeffective dose is to be reported. In addition, the type of effect for which W_{IsoE} is evaluated also needs to be specified, for example, late or early effects for different types of tissues [6.15, 6.16].

6.2.2.3. Isoeffective dose in radiation therapy

The product of the absorbed dose and the dimensionless isoeffective dose weighting factor W_{IsoE} is the isoeffective dose, D_{IsoE}. It is expressed in joule per kilogram, and its unit is the gray (Gy).

Subscripts, $D_{IsoE,\ C+,\ late}$, or parentheses, D(IsoE, C+, late), are useful to avoid confusion between absorbed dose and isoeffective dose by specifying for which treatment modality and tissue effect the weighting is used and whether the weighting refers to the reference conditions (see the discussion in Section 3.5). For example, $D_{IsoE,\ C+,\ late}$ or D(IsoE, C+, late) indicates that the weighting is made for a carbon ion beam and late effects on normal tissues.

The methodology used to choose the appropriate weighting factor may be the result of a consensus between centres and, in that case, the rationale for the consensus should be reported. In some instances, the consensus weighting factor may be different from the one normally used within the particular institution.

Isoeffective dose and absorbed dose are related by the appropriate isoeffective dose weighting factor, W_{IsoE}. For presentation purposes, it is convenient to specify the absorbed dose first followed by the isoeffective dose,

but the value of W_{IsoE} (or any other weighting factor applied) and the methodology used to determine these factors should be clearly specified.

Isoeffective dose is the most relevant quantity to define and report the treated volume and the reference volume in radiation therapy (see Section 6.2.3.2).

Reporting absorbed dose and isoeffective dose together is essential to interpret the clinical observations and to be able to re-evaluate the weighting factors of ions in the future if new and better data become available [6.17].

6.2.3. Reference points and volumes for reporting

6.2.3.1. Reference points

Reference points and/or volumes are currently recommended for reporting the different treatment modalities [6.3, 6.5, 6.6].

For ion beams, when single beams, parallel opposed beams or four orthogonal beams are used, the reference point for reporting should be selected at (or adjacent to) the centre of the PTV. This point would often correspond to the centre of the SOBP or the beam intersection. It is referred to as the ICRU reference point.

This (central) point satisfies four requirements appropriate for selection as a reference point: (1) the dose is representative of the dose distribution in the PTV; (2) the point is easy to identify in an unambiguous way; (3) the dose at that point can be accurately determined; and (4) there is, in general, no important dose gradient in this region.

At the reference point, both the absorbed dose and the isoeffective dose should be reported.

In addition to the dose at the reference point, the best estimates of the maximum and the minimum doses to the PTV should be reported.

6.2.3.2. Volumes for reporting

In the case of scanned beams with photons (IMRT), protons or ions, it is usually difficult to identify points that satisfy the requirements listed above and that could be used as ICRU reference points for reporting. Therefore, the use of volumes for reporting has to be considered [6.18].

The dramatic development of medical imaging and the possibility to delineate accurately the volumes that are clinically relevant make this approach more and more meaningful. Volumes can be used together with, or instead of, reference points for reporting.

The ICRU jointly with the IAEA are now preparing recommendations on dose and volume specifications for reporting scanned beams in IMRT and in proton therapy. The quantities used in these approaches seem suitable for ion therapy with scanned beams and are summarized as follows:

— D_{50} (median dose to the PTV) is defined as the dose received by a volume comprising 50% of the PTV;
— D_{95} (~minimum dose to the PTV) is the minimum dose received by a volume encompassing 95% of the PTV. D_{98} may also be considered;
— D_2 (~maximum dose to the PTV) is the maximum dose received by >2% of the PTV.

D_{50}, D_{95} and D_2 are easily derived from the dose volume histograms (DVH) of the PTV that are now commonly displayed by the treatment planning systems used in the ion beam therapy facilities.

In ion beam therapy, all of the doses described above should be reported as both absorbed doses, D, and isoeffective doses, D_{IsoE}. This also applies to the doses to the treated and reference volumes.

Similarly, when reporting ion doses to the OAR, absorbed doses and isoeffective doses should be reported.

REFERENCES

[6.1] INTERNATIONAL COMMISSION ON RADIATION UNITS AND MEASUREMENTS, Determination of Absorbed Dose in a Patient Irradiated by Beams of X or Gamma Rays in Radiotherapy Procedures, ICRU Report 24, Bethesda, MD (1976).

[6.2] INTERNATIONAL COMMISSION ON RADIATION UNITS AND MEASUREMENTS, Dose and Volume Specification for Reporting Intracavitary Therapy in Gynecology, ICRU Report 38, Bethesda, MD (1985).

[6.3] INTERNATIONAL COMMISSION ON RADIATION UNITS AND MEASUREMENTS, Prescribing, Recording and Reporting Photon Beam Therapy, ICRU Report 50, Bethesda, MD (1993).

[6.4] INTERNATIONAL COMMISSION ON RADIATION UNITS AND MEASUREMENTS, Dose and Volume Specification for Reporting Interstitial Therapy, ICRU Report 58, Bethesda, MD (1997).

[6.5] INTERNATIONAL COMMISSION ON RADIATION UNITS AND MEASUREMENTS, Prescribing, Recording and Reporting Photon Beam Therapy (Suppl. to ICRU Report 50), ICRU Report 62, Bethesda, MD (1999).

[6.6] INTERNATIONAL COMMISSION ON RADIATION UNITS AND MEASUREMENTS, Prescribing, Recording and Reporting Electron Beam Therapy, ICRU Report 71, Bethesda, MD (2004).
[6.7] GRÉGOIRE, V., SCALLIET, P., ANG, K.K. (Eds), "Clinical target volumes in conformal and intensity modulated radiation therapy", A Clinical Guide to Cancer Treatment, Springer Verlag, Berlin, Heidelberg, New York (2003a).
[6.8] GRÉGOIRE, V., DAISNE, J.F., GEETS, X., LEVENDAG, P., Selection and delineation of target volumes in head and neck tumours, Rays **28** (2003b) 217–224.
[6.9] INTERNATIONAL COMMISSION ON RADIATION UNITS AND MEASUREMENTS, Use of Computers in External Beam Radiotherapy Procedures with High-energy Photons and Electrons, ICRU Report 42, Bethesda, MD (1987).
[6.10] PÖTTER, R., VAN LIMBERGEN, E., WAMBERSIE, A., "Reporting in brachytherapy: Dose and volume specification", The GEC ESTRO Handbook of Brachytherapy (GERBAULET, A., PÖTTER, R., MAZERON, J.-J., MEERTENS, H., VAN LIMBERGEN, E., Eds), ESTRO, Brussels (2002) 153–215.
[6.11] INTERNATIONAL COMMISSION ON RADIATION UNITS AND MEASUREMENTS, Fundamental Quantities and Units for Ionizing Radiation, ICRU Report 60, Bethesda, MD (1998).
[6.12] CHAVAUDRA, J., CHAUVENET, B., WAMBERSIE, A., "Medicine and ionizing radiation: Metrology requirements", Comptes Rendus Académie des Sciences, Paris, C.R. Physique, Fascicule 8, Vol. 5 (2004) 921–931.
[6.13] MIJNHEER, B.J., BATTERMANN, J.J., WAMBERSIE, A., What degree of accuracy is required and can be achieved in photon and neutron therapy?, Radiother. Oncol. **8** (1987) 237–253.
[6.14] WAMBERSIE, A., DUTREIX, J., DUTREIX, A., Précision requise en radiothérapie. Conséquences concernant le choix et les performances exigées des détecteurs, J. Belge Radiol. **52** (1969) 94–104.
[6.15] TSUJII, H., et al., Overview of clinical experience on carbon ion radiotherapy at NIRS, Radiother. Oncol. **73** Suppl. 2 (2004) 41–49.
[6.16] WAMBERSIE, A., et al., Radiobiological rationale and patient selection for high-LET radiation in cancer therapy, Radiother. Oncol. **73** Suppl. 2 (2004a) 1–14.
[6.17] WAMBERSIE, A., et al., Biological weighting of absorbed dose in radiation therapy, Radiat. Prot. Dosim. **99** (2002) 445–452.
[6.18] WAMBERSIE, A., GAHBAUER, R.A., MENZEL, H.G., RBE and weighting of absorbed dose in ion-beam therapy, Radiother. Oncol. **73** Suppl. 2 (2004b) 176–182.

Annex I

RESPONSE IN VIVO TO HIGH LET RADIATION

M.C. JOINER, B. MARPLES
Department of Radiation Oncology,
Karmanos Cancer Institute, Wayne State University,
Detroit, Michigan, United States of America

Abstract

Relative biological effectiveness (RBE) increases with increasing linear energy transfer (LET) (below 100 keV μm^{-1}) and decreasing dose (or dose per fraction). The RBE versus dose relationship is well described by equations based on the linear quadratic model, provided this is used in the equivalent photon dose range *above* 1 Gy. The differences in the shape of the RBE versus dose relationships for different cell types and for late responding tissues and acutely responding tissues (and tumours) are accounted for in these equations by incorporating the cell or tissue specific α/β values for the different radiations under comparison, as well as either the ratio of α values for the two radiations or a reference value of RBE at a known dose. With knowledge of these three parameters, RBE can be calculated at any value of dose or dose per fraction of either radiation type, and these calculations could be incorporated into clinical treatment planning procedures that use equal numbers of fractions. When using unequal numbers of fractions, a weighting factor can also be calculated from these same three parameters, which links the total doses of the two radiations to give the same effect (isoeffect). *Below* equivalent photon doses of 1 Gy, adjustments to these equations are required to account for low dose hyper-radiosensitivity, which is largely a process associated with the response to lower LET radiations. The effect of low dose hyper-radiosensitivity is to reduce the differential effect of varying LET in the equivalent photon dose range below 1 Gy, which usually applies in beam margins. Clinically, RBE and weighting factor values would be lower in the beam margins than in the target volume, and this may necessitate increasing the field size in high LET therapy to compensate for the reduced effect.

I–1. INTRODUCTION

Relative biological effectiveness (RBE) for a radiation type, beam or configuration under test is traditionally defined as the ratio of a dose of a standard low linear energy transfer (LET) X ray beam (D_X) to the dose of the

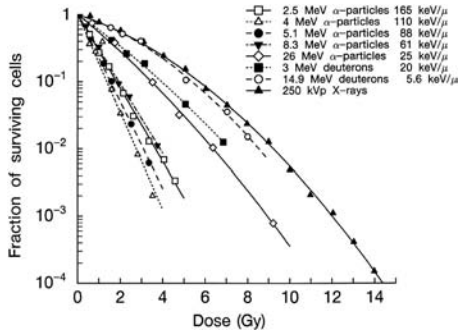

FIG. I–1. Survival of human kidney cells exposed in vitro to radiations of different LET (from Barendsen [I–1]).

test radiation type or configuration (D_T), required to cause the same biological level of effect. Thus:

$$RBE = D_X/D_T \tag{I–1}$$

This paper summarizes how the RBE depends on the dose (D_X or D_T), which corresponds to the level of biological isoeffect at which the dose comparison is made. We point out the general form of this RBE versus dose relationship in the normal clinical radiotherapy dose range and discuss how this general form should be modified when prescribing small doses to the target or when considering the RBE in the beam margins where the dose delivered will be much smaller than the dose to the planning target volume.

I–2. GENERAL FORM OF THE RBE VERSUS DOSE RELATIONSHIP

As an example of this relationship, Fig. I–1 compares dose response curves for human kidney cells as described in the classical study of Barendsen [I–1] on the response to deuteron and α particle beams covering a wide range of LET. Such a set of cell survival curves might be representative of the target cells in a normal tissue or a tumour undergoing radiotherapy.

Compared with the response to 250 kVp X rays, the responses to higher LET radiations demonstrate two universal features: lower doses are needed to give similar levels of response; as the LET increases the cell survival curves demonstrate less curvature. It is the latter property which confers the general shape of all RBE versus dose relationships, which is that RBE (as defined in Eq. (I–1)) increases with decreasing dose delivered; e.g. Fig. I–2 shows the RBE of 4 MeV α particles derived from the data in Fig. I–1.

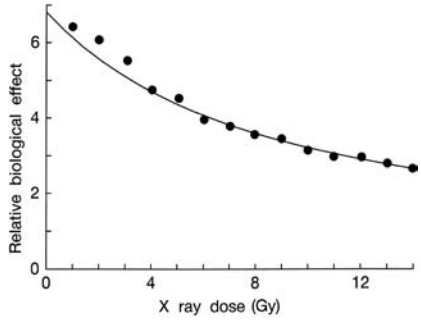

FIG. I–2. RBE of 4 MeV α particles increases for decreasing dose for cell lines irradiated in vitro. RBE values were calculated from the cell survival data shown in Fig. I–1. The full line is given by Eq. (I–4).

When applied to clinical or in vivo situations in which the radiation therapy is delivered as a number of fractions, n (the same number for both radiations), the RBE is calculated as:

$$RBE = D_X/D_T = d_X/d_T \qquad \text{(I–2)}$$

where D_X and D_T are now *total* doses ($D_X = nd_X$, $D_T = nd_T$), each delivered to cause the same biological effect. This is shown by the examples in Fig. I–3, where (a) shows dose response curves for renal clearance in mice following exposure to either 240 kVp X rays or d(4)-Be neutrons [I–2] with dose mean lineal energy 65.6 keV μm^{-1}, and HVL 3.0 cm in ICRU muscle. RBE values are calculated from these dose response curves using Eq. (I–2), by comparing pairs of high and low LET dose response curves in which the number of fractions is the same. In these examples, neutron dose alone is quoted and used in the calculations, excluding the gamma component that is typically 12% of the total neutron plus gamma dose for these irradiations. The right panel (b) shows these data that conventionally are plotted against *dose per fraction*, since it is dose per fraction which determines the single dose equivalent point on the underlying cell survival curve for the target cells. Figure I–3 again demonstrates the increasing RBE with decreasing dose per fraction; this increase reflects the greater sparing effect of fractionating the low LET (reference) X ray treatment compared with the high LET test treatment which, in the example in Fig. I–3, shows little or no sparing with fractionation.

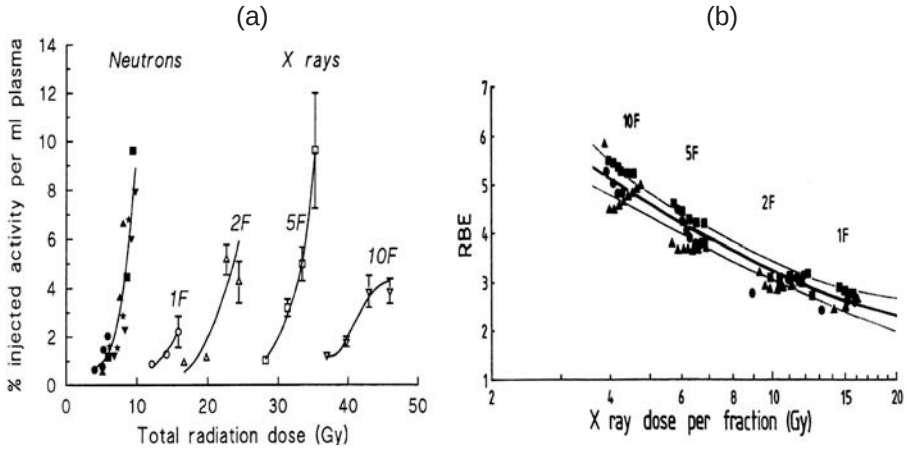

FIG. I–3. RBE for renal damage in mice increases with decreasing dose per fraction. RBE for in vivo end points are derived from dose response curves similar to (a) which shows examples of dose effect curves for ^{51}Cr-EDTA clearance following irradiation with 1, 2, 3, 5 or 10 fractions of d(4)-Be neutrons compared with 1, 2, 5 or 10 fractions of X rays. RBE values in (b) were obtained by comparing isoeffective neutron and X ray total doses given in the same number of fractions (Eq. (I–2)), for isotope clearance shown in (a) (circles) and two additional renal damage end points: reduction in haematocrit (squares) and increase in urination frequency (triangles) [I–2].

I–3. LINEAR QUADRATIC DESCRIPTION OF THE RBE VERSUS DOSE RELATIONSHIP

The linear quadratic (LQ) model is well established as a mathematical tool used to manipulate total dose and dose per fraction to maintain clinical isoeffectiveness and to predict and plan modified fractionation for any type of ionizing radiation therapy including both high and low LET radiations. Its routine use is well explained in recent textbooks [I–3 to I–5]. The exact shape of the underlying target cell survival response, for example, the curves in Fig. I–1, is determined by the parameters α and β in the LQ model. The *ratio* of the parameters α/β provides a measure of the curvilinearity of the survival response. As LET increases, the α/β ratio increases, which describes less curved responses when cell survival is plotted on a graph of log (surviving fraction) versus dose as in Fig. I–1, and which also reflects *less* change in total dose with fractionation. For example, the response to high LET neutrons, shown in Fig. I–3, changes very little with the number of fractions used to give the total dose, and has a high α/β ratio (21 Gy versus 3 Gy for the X ray response).

Joiner and Johns [I–2] and Joiner [I–6] show in detail how to derive the full RBE versus dose per fraction relationship mathematically, using three LQ parameters: the α/β ratios for the two radiations being intercompared (i.e. α_X/β_X and α_T/β_T) and the ratio of α for the two radiations (i.e. α_T/α_X). Briefly, if X ray (d_X) and high LET (d_T) doses per fraction given in the same number of fractions cause the same effect, then using the LQ model:

$$\alpha_T d_T + \beta_T d_T^2 = \alpha_X d_X + \beta_X d_X^2 \tag{I–3}$$

Replacing d_T by d_X/RBE in Eq. (I–3), dividing through by α_X, collecting terms and defining the parameters $K = \alpha_T/\alpha_X$, $V = \alpha_X/\beta_X$, $C = \alpha_T/\beta_T$, produces a quadratic equation in RBE which is then solved by the standard method to give RBE as a function of the (reference) X ray dose (or dose per fraction), d_X, as:

$$RBE = \frac{K + \sqrt{K^2 + 4Kd_X\left(1 + d_X/V\right)/C}}{2\left(1 + d_X/V\right)} \tag{I–4}$$

Similarly, replacing d_X by $d_T \times$ RBE in Eq. (I–3) enables RBE to be expressed as a function of the test (high LET) dose, d_T, as given by:

$$RBE = \frac{-V + \sqrt{V^2 + 4VKd_T\left(1 + d_T/C\right)}}{2d_T} \tag{I–5}$$

Equations I–4 and I–5 can be used to directly fit RBE versus dose measurements using non-linear least squares regression, to obtain the parameters K, V and C; examples of such direct fits are the solid lines in Figs I–2 and I–3. Alternatively, the parameters K, V and C can be derived from the α and β values obtained from LQ analyses of the isoeffective doses of the individual radiation types, then these 'calculated' parameters can be used to reconstruct the RBE relationship mathematically. The latter approach is shown using the example by Joiner [I–6] in the intercomparison of acute (skin) and late (kidney) damage following low or high energy fast neutron therapy. The summary of that study (Fig. I–4) shows the general feature of increasing RBE with decreasing dose per fraction for both radiation beams, but in both cases the relationship is steeper for the late damage in the kidney because of the lower value of α_X/β_X compared with the skin. An interesting feature of Fig. I–4 is that the X ray dose per fraction at which the skin and kidney RBE plots intersect is greater than 2 Gy for the low energy neutrons (generated by the original Hammersmith cyclotron), but lower than 2 Gy for modern high energy

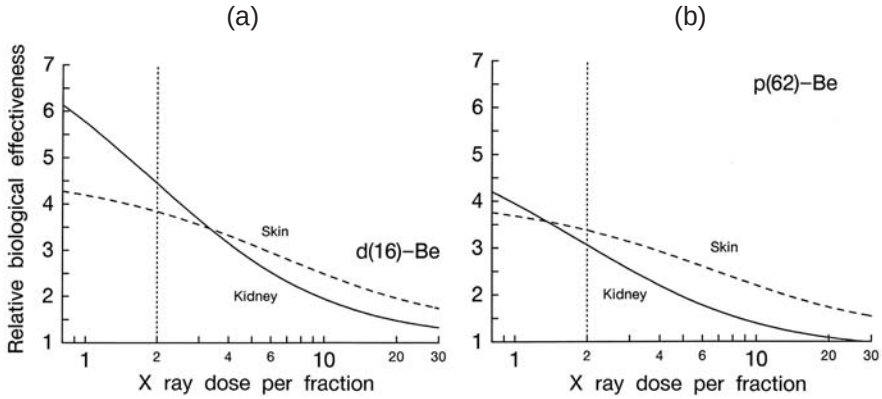

FIG. I–4. The RBE for renal damage in the mouse: (a) exposed to p(62)-Be; or (b) exposed to d(16)-Be neutrons relative to 240 kVp X rays as defined in Eq. (I–2). RBE was calculated using Eq (I–4), from the LQ parameters of the response to fractionation for each radiation. The dotted vertical lines mark a standard 2 Gy per fraction clinical photon dose; at this dose renal RBE is higher than skin RBE for d(16)-Be neutrons and lower than skin RBE for p(62)-Be neutrons.

neutron therapy beams indicating that with the latter, late renal damage should not be worse than with conventional photon therapy for the same level of acute damage or tumour effect. However, at higher LET, typical of light ion beams, RBE for late normal tissue reactions would be expected to remain higher than for acute reactions or for malignant tissues, necessitating the more precise dose delivery of which ion beams are capable.

The value of parameter K in Eqs (I–4) and (I–5) would be derived at the same time as V and C, in a simultaneous analysis of the total dose versus dose per fraction relationships for both radiations in the RBE comparison using the LQ model to determine the relative values of α_X, β_X, α_T and β_T. However, it is also possible to generate K from known or assumed values of V and C plus one single measurement (RBE_{ref}) at any dose d_{Xref} or d_{Tref}. From Eq. (I–1), $RBE_{ref} = d_{Xref}/d_{Tref}$, and substituting $d_{Tref} = d_{Xref}/RBE_{ref}$ for d_T and d_{Xref} for d_X in Eq. (I–3) gives:

$$\alpha_T d_{Xref} / RBE_{ref} + \beta_T d_{Xref}^2 / RBE_{ref}^2 = \alpha_X d_{Xref} + \beta_X d_{Xref}^2$$

Dividing through by $\alpha_X d_{Xref}$, multiplying through by RBE_{ref}^2, then substituting K, V and C gives:

$$K = \frac{RBE_{ref}^2 \left(1 + d_{Xref}/V\right)}{RBE_{ref} + d_{Xref}/C} \qquad \text{(I–6)}$$

Similarly, by substituting $d_{Xref} = RBE_{ref} \times d_{Tref}$ for d_X and d_{Tref} for d_T in Eq. (I–3) gives:

$$K = \frac{RBE_{ref}\left(1 + RBE_{ref} d_{Tref}/V\right)}{1 + d_{Tref}/C} \tag{I–7}$$

These equations circumvent the need to have an analysis of both X ray and high LET responses at a common isoeffect, and allow previous and separately generated values of the α/β ratios for the two radiations to be used to define the full RBE versus dose relationship from a single RBE and dose combination. This would be useful in clinical situations where high LET or proton therapy is already being used successfully and so a good estimate of the practical RBE is already available at the high LET dose prescribed. An estimate of the full RBE versus dose relationship can then be deduced for a given tissue (or tumour) by supplying the α/β ratio for conventional photon treatment (which is usually known) together with the α/β ratio for the high LET or proton beam. Where heavy ions are used, their α/β ratios (C) will be very large compared with the α/β ratios for the photon reference (V). In this case, Eqs (I–4) and (I–5) reduce to:

$$RBE = \frac{K}{\left(1 + d_X/V\right)} \tag{I–8}$$

$$RBE = \frac{-V + \sqrt{V^2 + 4VKd_T}}{2d_T} \tag{I–9}$$

And Eqs (I–6) and (I–7) reduce to:

$$K = RBE_{ref}\left(1 + d_{Xref}/V\right) \tag{I–10}$$

$$K = RBE_{ref}\left(1 + RBE_{ref} d_{Tref}/V\right) \tag{I–11}$$

To summarize, Eqs (I–4 to I–11) enable the complete RBE versus dose relationships to be constructed for a damage end point in a tissue, given the α/β ratios for the two radiations for that end point and the 'reference' value of RBE at one specified dose. The value of this approach lies in its ability to simply calculate an RBE at any dose per fraction which may be required in clinical therapy, from a lookup table of these three parameters. However,

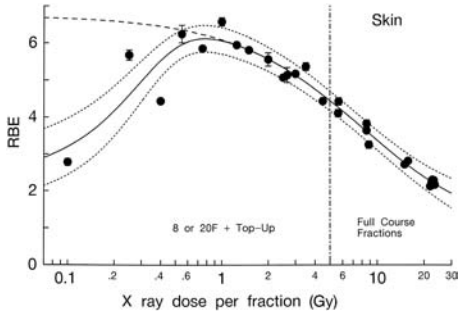

FIG. I–5. RBE for d(4)-Be neutrons referenced against 240 kVp X rays, for early reactions in the skin of the foot of the mouse. Doses less than 5 Gy per fraction were used, and the experiments compared 8 or 20 fractions of X rays with 8 or 20 fractions of neutrons, with each schedule followed by a top-up dose of neutrons to elicit comparable damage. The data were reanalysed and replotted from Joiner et al. [I–7]. Solid line: direct fit of Eq. (I–14) to the data, with 95% confidence intervals (dotted lines). Dashed line is an extrapolation using the simple LQ model, without the low dose correction.

careful attention should be paid to the uncertainty on the three parameters, particularly the reference RBE, which will determine the quality of the final RBE estimate calculated.

I–4. RBE AT LOW DOSES

It is clear that as the X ray dose (or dose per fraction) is decreased down to about 1 Gy, RBE increases for radiation beams with LET greater than the LET of the photon reference beam. However, in 1986, Joiner published the first study [I–7, I–8] indicating that below 1 Gy, RBE can *decrease* with decreasing dose (or dose per fraction). Figure I–5 shows this 'inverse' relationship between RBE and decreasing dose per fraction in mouse skin, in an intercomparison between 240 kVp X rays and d(4)-Be neutrons. A repeat study in skin also demonstrated a very similar pattern [I–9].

Skin is an early reacting tissue but, importantly, this *decreasing* RBE with decreasing dose per fraction has also been demonstrated in an experimental late reacting tissue. Figure I–6 shows the RBE versus dose profile for three end points assessing late renal damage in mice. These data show clearly the possibility of decreasing RBE in whole tissue systems as the dose per fraction is lowered below 1 Gy X ray equivalent. A decrease in RBE with decreasing dose per fraction is also implied by the data in the mouse lung [I–12, I–13] although not explicitly noted in those papers. Examination of the data for all three end

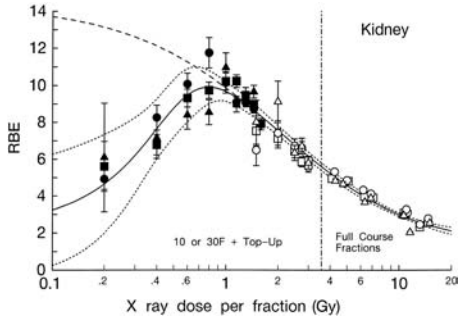

FIG. I–6. Data from a comparison between d(4)-Be neutrons and 240 kVp X rays for effects in the kidney of the mouse. Closed symbols from Joiner and Johns [I–10]; open symbols from Joiner and Johns [I–2]; squares: reduction in EDTA clearance; circles: reduction in haematocrit; triangles: increase in urination frequency; solid line: direct fit of Eq. (I–14) to the data, with 95% confidence intervals (dotted lines); dashed line is an extrapolation using the simple LQ model, without the low dose correction.

points (skin, kidney, lung) revealed that the decreasing RBE at X ray doses per fraction less than 1 Gy was due to greatly increased sensitivity to X rays below this dose, compared with the higher dose X ray sensitivity, while the sensitivity of the tissues to low doses of high LET neutrons remained similar to the sensitivity to high doses. The term 'low dose hyper-radiosensitivity' was introduced to describe this newly discovered phenomenon of increased X ray effectiveness when delivered in small doses per fraction [I–10].

To investigate the cellular basis for low dose hyper-radiosensitivity to X rays and, hence, the apparent convergence of the effectiveness of high and low LET radiations at low doses, an intensive study of the response of the V79 hamster cell line to 240 kVp X rays and d(4)-Be neutrons was carried out [I–11]. Measurements were focused on the dose region less than 1 Gy equivalent of X rays where increased sensitivity to X rays had been found in the animal normal tissue studies. In the X ray arm, 364 measurements were made with 84% of those at doses less than 1 Gy and 76% at doses less than 0.5 Gy. In parallel, 140 measurements of cell survival were made following a range of doses of d(4)-Be neutrons, in the dose range 0.02–3 Gy. This important data set demonstrates, at a cellular level, the increased sensitivity to X rays that had been seen in the animal normal tissue studies. The data are shown as survival curves in Fig. I–7 and as RBE in Fig. I–8. The parallel between Fig. I–8 and Figs I–5 and I–6 is clear and the form of the survival curve at low doses, shown in Fig. I–7, confirms the cellular basis for the decreased RBE with decreasing dose as an increase in sensitivity to X rays.

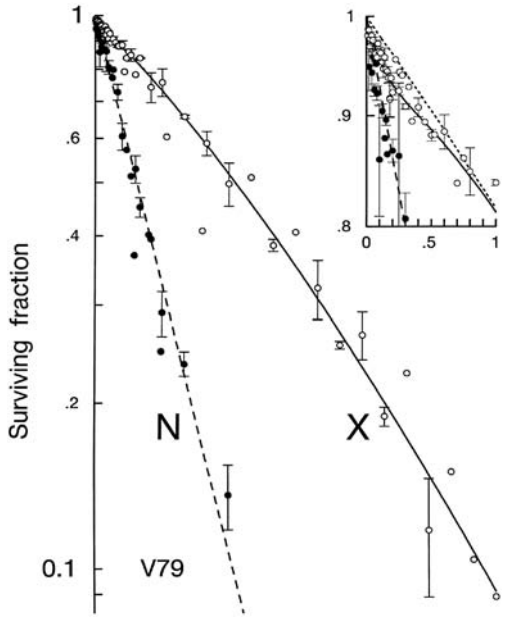

FIG. I–7. Comparison of cell survival after exposure to 240 kVp X rays or d(4)-Be neutrons in Chinese hamster V79 cells. The inset shows the low dose region; note convergence of the X ray and neutron responses below 0.5 Gy (from Marples and Joiner [I–7]).

The convergence of X ray and high LET cell survival responses is shown even more clearly in the human HT29 colon carcinoma cell line (Fig. I–9). In this case, the RBE values approach 1 at X ray doses less than 0.2 Gy [I–14]. Joiner et al. [I–15] and Marples et al. [I–16] have indicated that low dose hyper-radiosensitivity is the usual response of human cell lines to small doses of radiation, with approximately 80% of cell lines tested exhibiting the effect. Marples et al. [I–17] have shown that the mechanism for low dose hyper-radiosensitivity to low LET radiations is related to inefficient damage sensing below 0.5 Gy and, hence, reduction in a consequent G2 phase cell cycle block that, at higher doses, allows G2 irradiated cells to repair before undertaking mitosis. Since low dose hyper-radiosensitivity is then a process associated with the G2 phase of the cell cycle, it will be especially apparent and important to consider when the cells are in active proliferation, as is certainly the case for epithelia or in malignant tumours. However, Fig. I–6 demonstrates how important this effect can be, even in late responding tissues, if damage progresses from the destruction of a critical proliferating cell population, as in the case of the renal tubular epithelium.

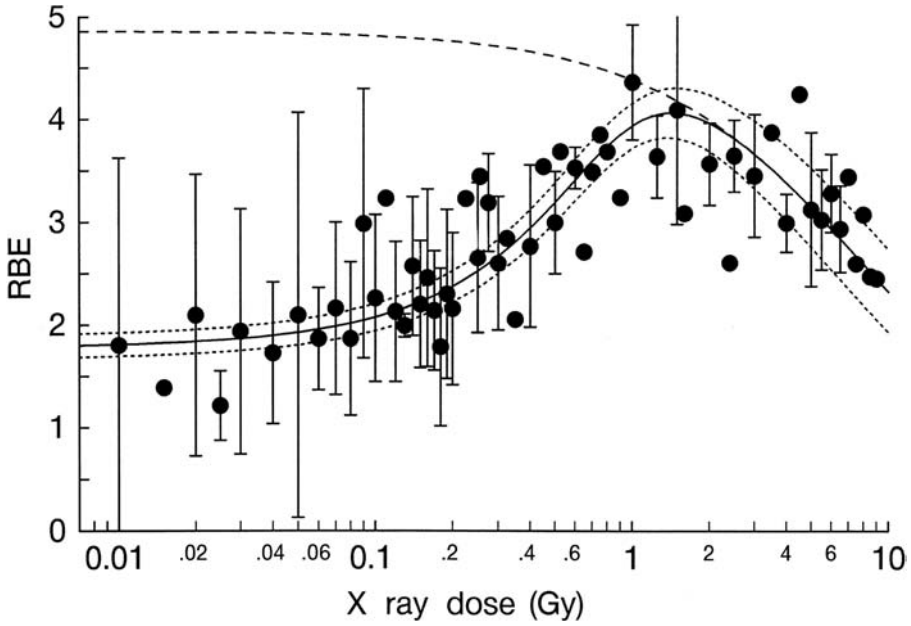

FIG. I–8. The data from Fig. I–7 shown as RBE; below an X ray dose of 1 Gy, the RBE decreases with decreasing dose per fraction in the Chinese hamster V79 cells; dashed line extrapolates the simple LQ model, without the low dose correction (from Marples and Joiner [I–11]).

The degree to which the low and high dose radiation responses differ depends on the LET. This can be inferred as probable since Figs I–7 and I–9 demonstrate no significant low dose subs tructure in the survival curves following irradiation with d(4)-Be neutrons (dose mean lineal energy 65.6 keV μm^{-1}) yet highly significant low dose substructure in the X ray survival curve. Marples et al. [I–18] showed that the low dose substructure was not only associated with the X ray response, but also that it was present in the survival curve after higher LET radiations. However, as LET increased, the substructure was gradually masked by the irreparable damage produced at higher LET. Figure I–10 shows these data.

I–5. MATHEMATICAL FORMULATION FOR LOW DOSE HYPER-RADIOSENSITIVITY

Joiner et al. [I–10] introduced a mathematical model of the low dose substructure in the cell survival curve which has remained robust to the present

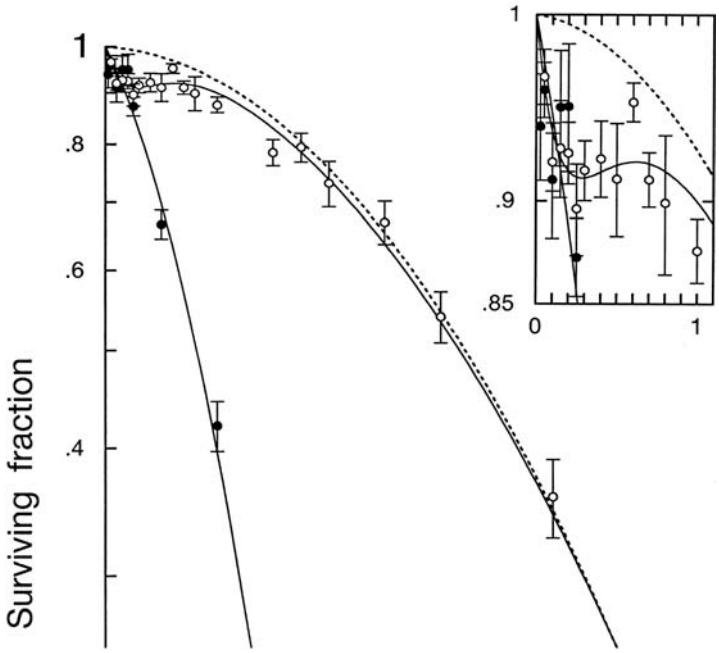

FIG. I–9. Comparison of cell survival following exposure to 240 kVp X rays or d(4)-Be neutrons in human HT29 cells. The inset shows that RBE is 1.0 below 0.2 Gy in this cell line. The dotted line shows the fit of the simple LQ model to the X ray data, without correcting for low dose hyper-radiosensitivity (from Lambin et al. [I–14]).

day. Taking the X ray response as an example, the assumption underlying the model is that the α term in the LQ description of the surviving fraction (S) versus dose (d_X) relationship (Eq. (I–12)) is expanded according to Eq. (I–13). In Eq. I–13, if d_X is much larger than d_C, then α tends to α_X, the value of α representing the high dose radioresponse. As d_X approaches zero, α tends to α_S, representing the enhanced response at low doses. Thus d_C represents the dose transition between hypersensitivity and increased resistance, with a value typically in the range 0.1–0.5 Gy, and α_S/α_X is the ratio by which low doses are more effective per unit dose than higher doses.

$$S = \exp\left(-\alpha d_X - \beta_X d_X^2\right) \tag{I–12}$$

$$\alpha = Q\alpha_X \text{ where } Q = 1 + \left(\frac{\alpha_S}{\alpha_X} - 1\right) e^{-d_X/d_C} \tag{I–13}$$

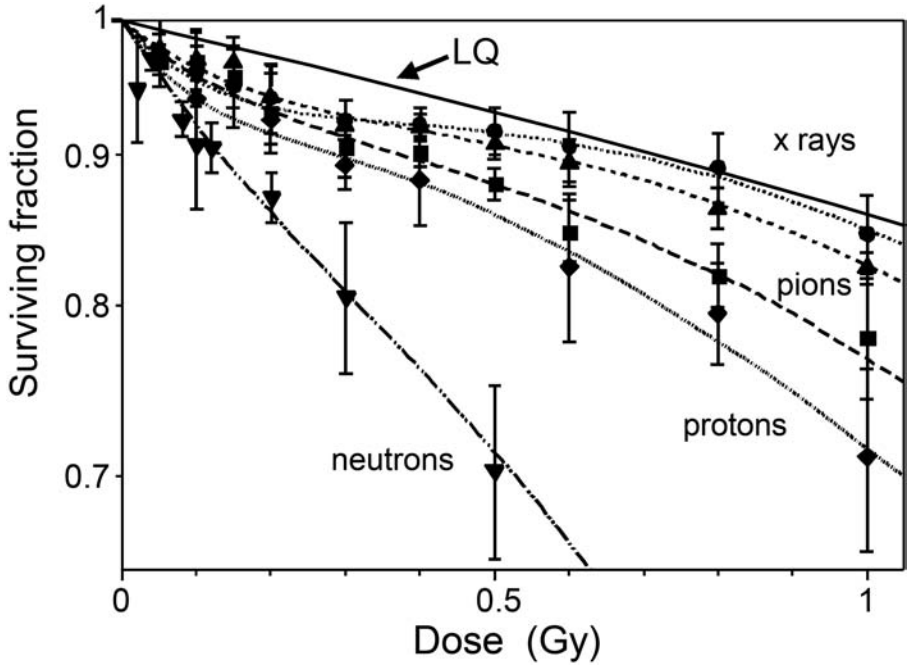

FIG. I–10. Survival curves (mean ± SD) for V79-379A cells irradiated with 250 kVp X rays, plateau (10–20 keV μm^{-1}) and peak (35 keV μm^{-1}) pions (200 MeV at TRIUMF, Canada, Marples et al. [I–19]), 70 MeV protons (at TRIUMF, Canada, Wouters et al. [I–20]) and d(4)-Be neutrons (60–70 keV μm^{-1} at Gray Laboratory, United Kingdom, Marples and Joiner [I–11]). Converging survival responses were obtained at doses below ~0·2 Gy for all the radiations. However, at higher doses (>0·2 Gy), the survival curves diverge: a near exponential response was observed for the high LET neutrons. The mathematical fits (broken lines) were obtained using Eqs (I–12) and (I–13). The solid line is the predicted response to X rays back-extrapolated from the fit of the LQ model to high dose data.

Equations (I–12) and (I–13) were used to fit the cell survival data in Figs I–9 and I–10. Then, Eq. (I–4) becomes:

$$RBE = \frac{K + \sqrt{K^2 + 4Kd_X\left(Q + d_X/V\right)/C}}{2\left(Q + d_X/V\right)} \qquad \text{(I–14)}$$

Note that Eq. (I–14) has been used to directly fit the data in Figs I–5, I–6 and I–8.

Equation (I–8) becomes:

$$RBE = \frac{K}{\left(Q + d_X / V\right)} \tag{I–15}$$

If Eqs (I–6, I–7, I–10 or I–11) are used to derive K from a single RBE measurement (RBE_{ref}) at a dose d_{Xref} (or d_{Tref}), then provided d_{Xref} (or $d_{Tref} \times RBE_{ref}$) is much larger than d_c (which would usually be the case), those equations can be used as they stand. Note that when low dose hypersensitivity is present in the response to the low LET radiation, then unique equations expressing RBE as a function of the *test* radiation dose (d_T) cannot be constructed because of the possibility of more than one isoeffective low LET radiation dose, corresponding to a value of d_T in the low dose region of the survival curve.

I–6. CONSEQUENCES OF LOW DOSE HYPER-RADIOSENSITIVITY — RBE IN THE FIELD EDGE

Since low dose hyper-radiosensitivity is a feature of the response to lower LET radiations, then if high LET radiations or light ions are deployed, then no corrections need to be made to those high LET doses. For example, if the prescribed dose at the tumour is D Gy, and at some point in the edge of the field the physical dose is D/10 Gy, then the biologically effective dose of that smaller physical dose is one tenth of the biologically effective dose to the tumour.

However, with a low LET radiation, this proportionality breaks down and smaller doses in the field edge may be more effective per unit dose than expected because of low dose hyper-radiosensitivity. Figure I–11 shows an example, using the survival response of HT29 cells in Fig. I–9 to model the effect of a non-uniform dose distribution. In this example, the effect at each position is expressed as an equivalent dose in 2 Gy fractions. In the low dose 'skirt' of the dose distribution, the example shows that this biologically effective dose equivalent of X ray irradiation is up to three times greater than the physical dose delivered.

In comparing the effects of a high and low LET treatment to identical fields, if the low and high LET physical dose distributions are identical, then the high LET treatment would be more effective per unit dose in the target than in the field edge. Thus, if the high LET dose to the target is chosen to be similarly effective to a low LET treatment, then the edge of the field could be underdosed. This can be understood as a consequence of the lowered RBE in

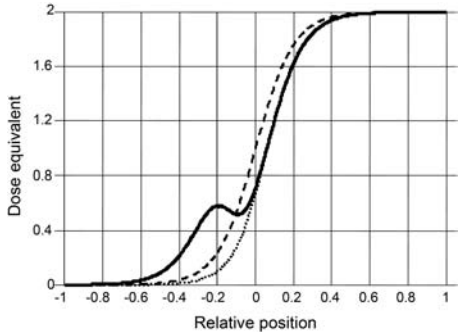

FIG. I–11. Predicted field edge effects in an imaginary HT29 tumour, based on the X ray survival curve shown in Fig. I–9. The dashed line shows a hypothetical physical dose transition from zero up to 2 Gy. The dotted line shows the 'biological effect' of this dose (in equivalent 2 Gy fractions), based on an LQ extrapolation from high doses. The solid line shows the true 'biological effect' (in equivalent 2 Gy fractions), based on the low dose hyper-radiosensitivity observed at low X ray doses.

the field edge and is because the low LET radiation is more effective than expected in the field edge. Thus, low dose hyper-radiosensitivity implies that high LET dose distributions might need to be deliberately broadened so as not to lose the extra effect that would have been delivered by a photon treatment.

I–7. EXTENSION OF THE FORMULAS TO UNEQUAL NUMBERS OF FRACTIONS

All of the preceding description of RBE applies to the case where comparisons are made between either single doses of two radiations, or fractionated treatments delivered with the same number of fractions for both radiations. In the latter case, a generalization to *unequal* numbers of fractions for the two radiations being compared can be made using the concept of a weighting factor. The weighting factor, W_T, for a test radiation relative to a low LET reference, is the ratio of the total doses to give the same effect regardless of the number of fractions each radiation treatment is given in. Thus:

$$W_T = \frac{n_X d_X}{n_T d_T} \tag{I–16}$$

where d_X is the low LET reference dose given n_X times and d_T is the test radiation dose given n_T times. For the case of unequal fractions, the isoeffect relationship described by Eq. (I–3) now becomes:

$$n_T\left(\alpha_T d_T + \beta_T {d_T}^2\right) = n_X\left(\alpha_X d_X + \beta_X {d_X}^2\right) \tag{I–17}$$

Using Eq. (I–16) to substitute for d_T in Eq. (I–17) gives:

$$W_T = \frac{K + \sqrt{K^2 + 4K d_X\left(n_X/n_T\right)\left(1 + d_X/V\right)/C}}{2\left(1 + d_X/V\right)} \tag{I–18}$$

Using Eq. (I–16) to substitute for d_X in Eq. (I–17) gives:

$$W_T = \frac{-V + \sqrt{V^2 + 4VK d_T\left(n_T/n_X\right)\left(1 + d_T/C\right)}}{2d_T\left(n_T/n_X\right)} \tag{I–19}$$

Note that when $n_T = n_X$ or when $n_T = n_X = 1$, then $W_T = RBE$ and Eqs (I–18) and (I–19) reduce to Eqs (I–4) and (I–5), respectively.

I–8. CONCLUSIONS

In the photon dose range above 1 Gy or 1 Gy per fraction, the relationship between RBE and dose is straightforward. In this dose range, RBE increases with decreasing dose or dose per fraction and does so more rapidly for late responding tissues than for acutely responding tissues or tumours. This acute versus late tissue differential, and the shape of the RBE versus dose curves, is dominated by the shape of underlying response to the low LET photon exposures that are conventionally used as a reference radiation for RBE calculations.

At photon doses or doses per fraction less than 1 Gy, the process of low dose hypersensitivity may play a substantial role. This causes the RBE to *decrease* with further decreases in dose, because the photon exposures become *more* effective per unit dose. However, low dose hyper-radiosensitivity, although a prevalent effect, is unpredictable in magnitude and, in approximately 20% of cell lines screened, is not detectable.

The effects of low dose hyper-radiosensitivity are masked as LET increases, because of the dominant effect of high LET induced irreparable damage. A simplification to dose and RBE reporting, therefore, would be to

standardize on a high LET radiation source as a reference. This is unlikely to be practical because of the need to have a reference radiation type readily accessible in all radiotherapy facilities and the desire to relate outcomes of new treatment modalities to those obtained using conventional photon irradiations.

ACKNOWLEDGEMENTS

We thank the many colleagues who have contributed and collaborated with us in the study of RBE in vivo and low dose hyper-radiosensitivity over many years. In particular, the early studies with low doses on mouse tissues would not have been possible without input from R. Maughan and B. Michael. P. Lambin is a co-worker on the first studies on low dose hyper-radiosensitivity in human cell lines; B. Wouters and K. Skov have collaborated with us on the study of the mechanisms underlying low dose effects. Thanks and appreciation go to J. Fowler and the late J. Denekamp for providing early encouragement to always finding something different.

REFERENCES

[I–1] BARENDSEN, G.W., "Responses of cultured cells, tumours and normal tissues to radiations of difference linear energy transfer", Current Topics in Radiation Research (EBERT, M., HOWARD, A., Eds), Vol. 4, North-Holland, Amsterdam (1968), 293–356.

[I–2] JOINER, M.C., JOHNS, H., Renal damage in the mouse: The effect of d(4)-Be neutrons, Radiat. Res. **109** (1987) 456–468.

[I–3] JOINER, M.C., VAN DER KOGEL, A.J., "The linear-quadratic approach to fractionation and calculation of isoeffect relationships", Basic Clinical Radiobiology (STEEL, G.G., Ed.), Arnold, London (1997) 106–122.

[I–4] HALL, E.J., GIACCIA, A.J., Radiobiology for the Radiologist, 6th edn, Lippincott Williams and Wilkins, Philadelphia, PA (2006).

[I–5] JOINER, M.C., BENTZEN, S.M., "Time–dose relationships: The linear-quadratic approach", Basic Clinical Radiobiology (STEEL, G.G., Ed.), Arnold, London (2002).

[I–6] JOINER, M.C., A comparison of the effects of p(62)-Be and d(16)-Be neutrons in the mouse kidney, Radiother. Oncol. **13** (1988) 211–224.

[I–7] JOINER, M.C., DENEKAMP, J., MAUGHAN, R.L., The use of 'top-up' experiments to investigate the effect of very small doses per fraction in mouse skin, Int. J. Radiat. Biol. **49** (1986) 565–580.

[I–8] JOINER, M.C., DENEKAMP, J., The effect of small radiation doses on mouse skin, Br. J. Cancer **53** Suppl. VII (1986) 63–66.

[I–9] JOINER, M.C., MARPLES, B., JOHNS, H., The response of tissues to very low doses per fraction: A reflection of induced repair? Recent Results Cancer Res. **130** (1993) 27–40.
[I–10] JOINER, M.C., JOHNS, H., Renal damage in the mouse: The response to very small doses per fraction, Radiat. Res. **114** (1988) 385–398.
[I–11] MARPLES, B., JOINER, M.C., The response of Chinese hamster V79 cells to low doses: Evidence of enhanced sensitivity of the whole cell population, Radiat. Res. **133** (1993) 41–51.
[I–12] PARKINS, C.S., FOWLER, J.F., Repair in mouse lung of multifraction X-rays and neutrons: Extension to 40 fractions, Br. J. Radiol. **58** (1985) 1097–1103.
[I–13] PARKINS, C.S., FOWLER, J.F., MAUGHAN, R.L., ROPER, M.J., Repair in mouse lung for up to 20 fractions of X-rays or neutrons, Br. J. Radiol. **58** (1985) 225–241.
[I–14] LAMBIN, P., MARPLES, B., FERTIL, B., MALAISE, E.P., JOINER, M.C., Hypersensitivity of a human tumour cell line to very low radiation doses, Int. J. Radiat. Biol. **63** (1993) 639–650.
[I–15] JOINER, M.C., MARPLES, B., LAMBIN, P., SHORT, S.C., TURESSON, I., Low-dose hypersensitivity: Current status and possible mechanisms, Int. J. Radiat. Oncol. Biol. Phys. **49** (2001) 379–389.
[I–16] MARPLES, B., WOUTERS, B.G., COLLIS, S.J., CHALMERS, A.J., JOINER, M.C., Low-dose hyper-radiosensitivity: A consequence of ineffective cell cycle arrest of radiation-damaged G2-phase cells, Radiat. Res. **161** (2004) 247–255.
[I–17] MARPLES, B., WOUTERS, B.G., JOINER, M.C., An association between the radiation-induced arrest of G2 phase cells and low-dose hyper-radiosensitivity: A plausible underlying mechanism? Radiat. Res. **160** (2003) 38–45.
[I–18] MARPLES, B., ADOMAT, H., KOCH, C.J., SKOV, K.A., Response of V79 cells to low doses of X-rays and negative pi-mesons: Clonogenic survival and DNA strand breaks, Int. J. Radiat. Biol. **70** (1996) 429–436.
[I–19] MARPLES, B., LAM, G.K., ZHOU, H., SKOV, K.A., The response of Chinese hamster V79-379A cells exposed to negative pi-mesons: Evidence that increased radioresistance is dependent on linear energy transfer, Radiat. Res. **138** (1994) 81–84.
[I–20] WOUTERS, B.G., et al., Measurements of relative biological effectiveness of the 70 MeV proton beam at TRIUMF using Chinese hamster V79 cells and the high-precision cell sorter assay, Radiat. Res. **146** (1996) 159–170.

Annex II

MODELLING THE INCREASED BIOLOGICAL EFFECTIVENESS OF HEAVY CHARGED PARTICLES FOR TUMOUR THERAPY TREATMENT PLANNING

M. SCHOLZ, W. WEYRATHER, M. KRÄMER, G. KRAFT
Gesellschaft für Schwerionenforschung mbH, Biophysics,
Darmstadt, Germany

Abstract

The complex dependencies of RBE on the parameters under consideration, such as particle type and energy, dose level and cell or tissue type, require careful consideration in treatment planning for applications of charged particle beams in tumour therapy. For the precise quantitative description of these dependencies, models are required. An example of such a model, the local effect model (LEM), is described in this report, and it has been tested by comparison with a wide variety of biological end points from in vitro cell survival to tumour control probabilities from clinical studies. The application of this model in treatment planning requires detailed knowledge of the physical parameters that permit derivation of the microscopic energy deposition pattern for the individual components of the radiation field. In the case of active beam delivery techniques such as raster scanning, these data are available from the physical optimization in treatment planning. An important feature of the approach presented here is that it allows prediction of the response of a biological object to high LET radiation from its response to low LET radiation. Therefore, the experience with conventional photon treatment represents an important resource for the estimation of clinical RBE values. Up to now, the LEM has been implemented in treatment planning for carbon ion irradiation. The clinical results obtained up to now at GSI are consistent with the predicted RBE values in that there is at least no significant overestimation or underestimation of RBE. Otherwise, either more severe normal tissue complications or a higher recurrence rate should have been observed. Further refinements of the LEM as well as experimental verifications for other modalities (protons, helium, oxygen) will make it generally applicable to light ion therapy.

II–1. INTRODUCTION

The relative biological effectiveness (RBE) of charged particle beams depends on several factors, such as particle type and energy, dose level, position in the treatment field and the cell or tissue type under consideration [II–1 to II–4]. These systematic dependencies of the RBE have to be considered when

using charged particle beams for therapy. As a consequence, RBE values are expected to be patient specific and probably cannot be adequately represented by a single number for conversion of physical/absorbed dose to biologically effective or photon equivalent dose.

For treatment planning, RBE values have thus to be estimated as precisely as possible. In principle, two strategies can be thought of: an experimental approach and a modelling approach. For the experimental approach, the systematics of RBE have to be measured with high accuracy for a large number of different irradiation conditions. However, it will be impossible to represent all clinically relevant conditions with respect to beam energies, size of the target volume, dose levels, etc. Thus, interpolation or extrapolation of the data is required. Moreover, since the systematics can be measured only with sufficient precision for in vitro systems, procedures have to be defined to transform the systematic of RBE observed in in vitro systems into the corresponding systematic of clinical RBE values.

The second strategy is based on biophysical modelling. The goal is to develop a model which should be able to predict the response to charged particle radiation from the known response of the biological object to photon radiation. This will ultimately allow linkage of the treatment planning for charged particle beams to the clinical experience with photon radiation.

The two facilities worldwide that treat cancer patients with carbon ion beams use different strategies. At HIMAC in Chiba, Japan, an experimentally oriented approach is used. It is based on the precise measurements of RBE in vitro, which are used to determine the shape of the isoeffective depth dose profile. The clinical RBE value is then determined by a link to the clinical experience with neutrons, which show similar radiobiological characteristics to those of carbon beams at the end of their penetration depth [II–5, II–6]. At the GSI, a modelling approach is used, which will be described in more detail in the following sections [II–7 to II–10].

II–2. MODELLING THE INCREASED EFFECTIVENESS OF CHARGED PARTICLES

There are different classes of models described in the literature which aim to describe or predict the biological effects of high LET radiation.

One class of models is characterized by the precise simulation of all of the relevant fundamental processes, starting with the details of energy deposition in terms of secondary electrons, induction of different types of damage, such as single strand breaks, double strand breaks or base damage, followed by processing of these damage sites up to the final biological end point of interest.

There are approaches available (often called 'mechanistic models'), which are able to represent at least the first steps of that chain of events leading to the induction of the relevant damage sites [II–11, II–12]. However, these steps are essentially defined by the comparably simple geometric properties of the energy deposition distribution and DNA conformation, in combination with a proper definition of the (bio-)chemical status of the medium surrounding the critical target, i.e. the DNA. The real complexity of the response of a cell to radiation, however, is related to the steps following the damage induction, namely, the processing and repair or misrepair of the initial damage sites. These processes are characterized by an enormous complexity of highly regulated networks, consisting of hundreds of different interacting proteins. Only parts of these networks are understood up to now and, although attempts have been made to simulate parts of these networks in biophysical models [II–13], it is absolutely impossible, at least at present, to simulate the complete network with a precision sufficient for applications, for example, in tumour therapy. This is evident because numerous parameters would have to be used to describe the individual protein responses. Besides the fact that only little is known quantitatively about these processes, due to the high number of parameters and the interaction between all pathways, the solutions will depend critically on small variations of the parameters and thus will probably result in unstable solutions.

As a consequence, this type of mechanistic modelling is not expected to result in the precision required for clinical treatment planning. Therefore, in principle, simpler empirical approaches could be more appropriate here, approaches which are not based on ab initio calculations as described previously. The requirements for clinical modelling can be made less demanding by referring to the (clinical) experience with conventional low LET radiation. Then it would be sufficient to find a strategy allowing transformation of the known response of a biological object to photon radiation to predict the response to charged particle radiation. This represents a significant simplification, since then in principle all the complex processes described are included in the response of a cell to photon radiation and can thus be handled as a type of black box. The local effect model developed at the GSI belongs to this latter class of models.

II–2.1. Local effect model

The principal assumption of the local effect model (LEM) is that the expectation value of the local biological effect, i.e. the biological damage in a small subvolume of the cell nucleus, is solely determined by the expectation value of the energy deposition in that subvolume, but is independent of the particular radiation type leading to that energy deposition. This is similar to the

microdosimetric approach, but is applied to much smaller volumes compared to the micron dimensions of microdosimetry. For a given biological object, all the differences in the biological action of charged particle beams should then be attributed to the different spatial energy deposition pattern of charged particles compared to photon irradiation, i.e. on track structure.

The energy deposition pattern of charged particles is determined essentially by the secondary electrons (delta electrons) liberated by the primary particle when penetrating matter. Depending on the energy spectrum of delta electrons, energy can be transferred from the trajectory of the primary particle to 'distant locations'. Experimental data as well as model calculations have revealed that the average energy deposition as a function of the distance, r, from the trajectory, the radial dose profile, follows a $1/r^2$ law. According to the kinematics of the secondary electron emission, the maximum transversal range of the electrons is restricted and the corresponding track radius can be described by a power law of the form [II–14]:

$$R_{Max} = 0.05 \cdot E^{1.7} \qquad \text{(II–1)}$$

where E is the specific energy of the projectile. Details of the particular representation of the track structure and the radial dose profile as used in the LEM can be found in Ref. [II–10].

Figure II–1 illustrates the influence of track structure on the microscopic dose distribution in the typical dimensions of a cell nucleus; the dose distribution is defined as the average energy deposited at a certain location for a given, fixed set of impact parameters of the incoming particles. For comparison, the distribution expected for photon irradiation is shown as an ideally flat plane; this is based on the fact that photons deposit their energy in a very large number of small energy depositions. Thus, in a first approximation, the average energy deposition is homogeneously distributed throughout the cell nucleus. In contrast, low energy (1 MeV/u) particles show a completely different pattern. Since their track radius is very small, their energy deposition is restricted to very small subvolumes along the particle trajectory, but in between there is no energy deposition at all. With increasing particle energy, the track radius increases, and the gap between the tracks is closed; here also considerable overlap between individual particle tracks contributes to the dose deposition. With increasing particle energy, the heterogeneity of the microscopic dose distribution decreases and increasingly resembles the photon dose distribution. This figure already qualitatively explains why very high energy carbon ions act similarly to photon radiation.

In order to determine the biological effect of these heterogeneous dose distributions, a reference to the photon dose response curve is made. This will

be explained here first for the effect of cell survival; the transfer to other biological end points will be described later. In our model, cell inactivation is assumed to be due to the production of lethal events. The biochemical nature or the precise molecular structure of these lethal events, however, does not have to be specified; only their number is relevant. A lethal event is assumed to be a *local* modification of the sensitive target (DNA) in a small subvolume of the critical cellular target, i.e. the cell nucleus. In particular, it is assumed that no interactions of sublethal damage sites over large distances in the order of micrometres are required to produce lethal events. Therefore, the approach was termed the *local effect* model.

For photon radiation, if the average number of lethal events per cell is given by $\overline{N_{l,X}}$, the *distribution* of the induced number of lethal events can be described by a Poisson distribution, since according to the energy deposition pattern of photons the lethal events will be randomly distributed among the individual cells of a population. The number of surviving cells is given by the fraction of cells carrying no lethal event, and according to the Poisson distribution we get:

$$S_X = e^{-\overline{N_{l,X}}} \tag{II–2}$$

and therefore:

$$\overline{N_{l,X}} = -\log S_X \tag{II–3}$$

From this number, a dose dependent event density $\nu_X(D)$ can be derived:

$$\nu_X(D) = \frac{\overline{N_{l,X}(D)}}{V_{Nucleus}} = \frac{-\log S_X(D)}{V_{Nucleus}} \tag{II–4}$$

where $V_{Nucleus}$ is the volume of the cell nucleus and D represents the dose. In this definition, no particular form of the photon dose response curve is required.

The calculation of the biological effects of charged particle radiation is based on their different microscopic pattern of energy deposition compared to photon radiation. The basic variable for the calculation is the *expectation value* of the dose deposited at a given point (x,y,z) in the nucleus for a given set of incoming primary photons or particles; we call this quantity *local dose* and denote it by *d(x,y,z)*. For photons at the dose levels relevant for our purposes, the spatial distribution of the *local dose* can be assumed to be homogeneous even down to nanometre volumes, although the actual energy deposition

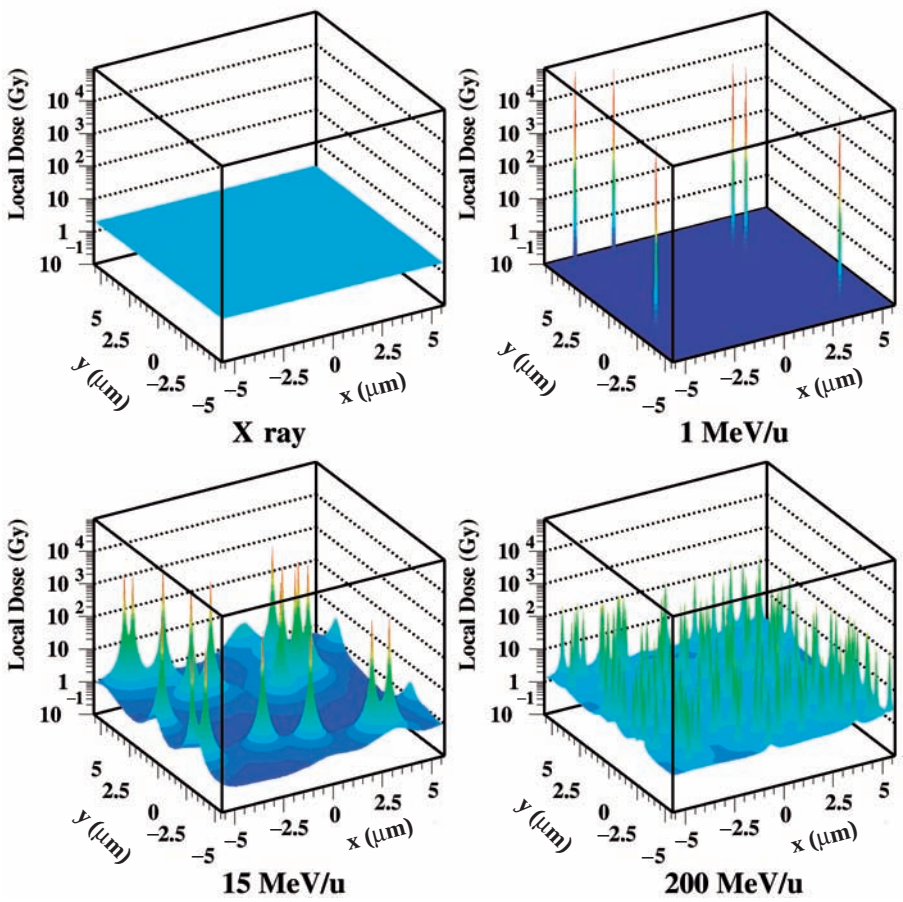

FIG. II–1. Local dose distribution of X rays and carbon ions at different specific energies. The average dose is 2 Gy in each case. The size of the area is 10 ×10 μm² and corresponds to the typical size of mammalian cell nuclei.

pattern is dominated by the stochastics of secondary electrons. In contrast, for particle radiation, the distribution is characterized by the extreme heterogeneity due to the $1/r^2$ distribution of local dose within the particle tracks (Fig. II–1).

Given the local dose distribution according to the impact parameters of a given set of impinging ions, the average number of lethal events induced per cell by heavy ion irradiation can then be obtained by integration of the local density $\nu_{Ion}(d(x,y,z))$:

$$\overline{N_{l,Ion}} = \int \nu_{Ion}(d(x,y,z))dV_{Nucleus} \qquad \text{(II–5)}$$

The fundamental assumption of the LEM is that the local biological effect is determined by the local dose, but is independent of the particular radiation type leading to a given local dose, i.e. the event densities for particle and photon radiation are identical for the same local dose:

$$\nu_{Ion}(d) = \nu_X(d) \tag{II–6}$$

Thus, equal local doses correspond to equal local biological effects, and Eq. (II–5) can be rewritten as:

$$\begin{aligned} \overline{N_{l,Ion}} &= \int \nu_X(d(x,y,z))dV_{Nucleus} \\ &= \int \frac{-\log S_X(d(x,y,z))}{V_{Nucleus}} dV_{Nucleus} \end{aligned} \tag{II–7}$$

This formula clearly demonstrates the theoretical link between the biological effect of photon radiation and ion radiation. The integrand is completely determined by the low LET response of the object under investigation; the particle effect is 'hidden' in the inhomogeneous local dose distribution *d(x,y,z)*. The concept of the LEM is illustrated in Fig. II–2. For a given pattern of particle traversals, the survival probability for a cell is then given by:

$$S_{Ion} = e^{-\overline{N_{l,Ion}}} \tag{II–8}$$

Equation (II–7) is the most general formulation of the LEM; it does not rely on any particular representation of the photon dose response curve. It can be applied even if only numerical values of $S_X(D)$ are available. However, for practical reasons, we have chosen the linear quadratic approach for the description of the low LET dose response curve. The average number of lethal events can then be identified with:

$$\overline{N_{l;X}} = \log S_X(D) = \alpha_X D + \beta_X D^2 \tag{II–9}$$

A modified version of the linear quadratic approach is used, since for many biological objects a transition from the shouldered to an exponential shape of the dose response curve is observed at high doses. This transition is described by a parameter D_t, representing the transition dose to the exponential shape with slope $s_{\max} = \alpha + 2\beta D_t$, so that the dose response is finally given by:

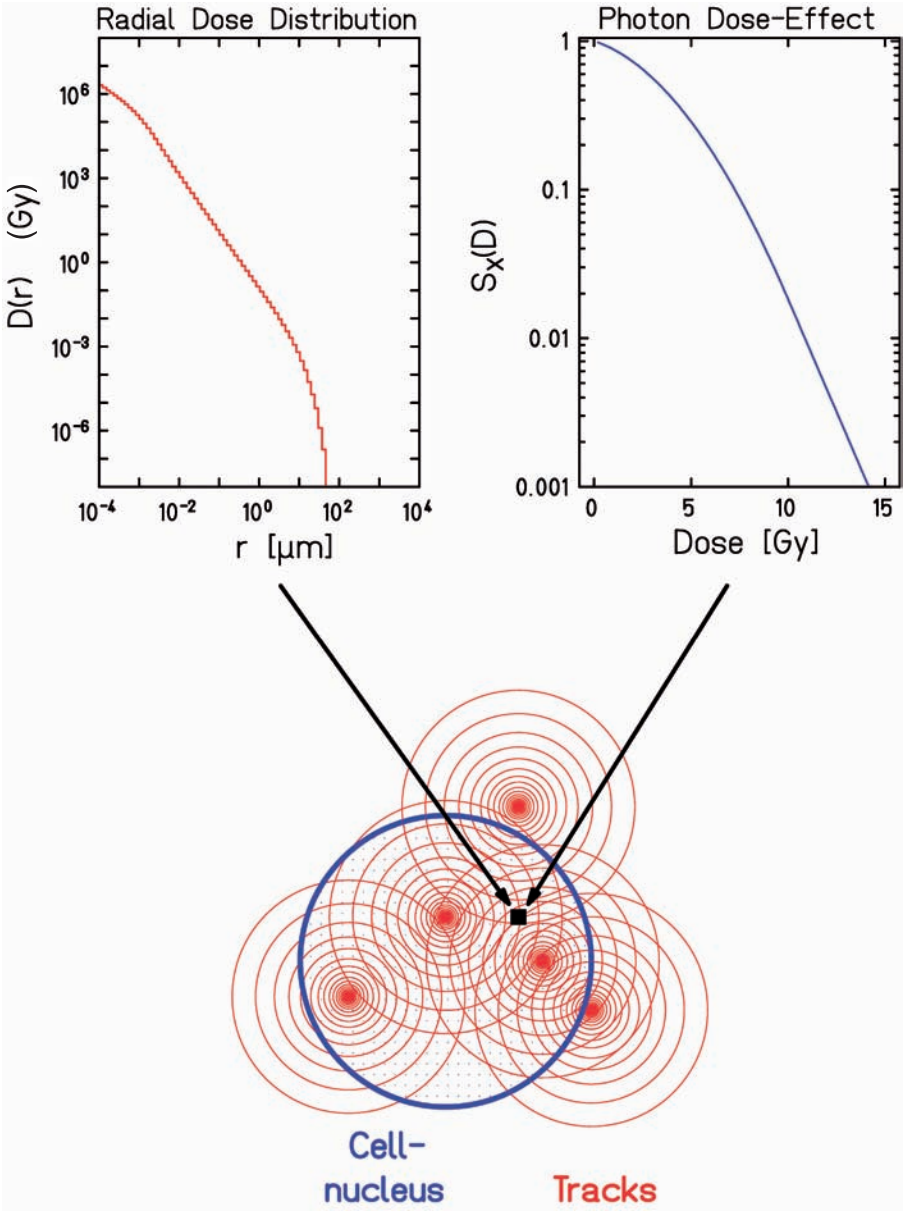

FIG. II–2. Representation of the local effect model.

$$S_X(D) = \begin{cases} e^{-(\alpha_X D + \beta_X D^2)} & : D \le D_t \\ e^{-(\alpha_X D_t + \beta_X D_t^2 + s_{\max}(D - D_t))} & : D > D_t \end{cases} \qquad \text{(II–10)}$$

The dose D_t often cannot be directly derived from experimental data, since survival curves can be measured only down to 10^{-3} for most mammalian cell lines; D_t represents thus a semifree parameter of the model. The value of D_t can be estimated, however, based on the finding that differences in sensitivity between different cell lines are expressed in general in a variation of the initial slope (α term), whereas the β term and thus the final slope s_{max} are very similar. In general, values for s_{max} in the order of 2 Gy^{-1} and the corresponding value for D_t — resulting from the particular α and β values — allow consistent descriptions of the experimental data.

In order to perform the numerical integration given in Eq. (II–7) for a random distribution of particle traversals, a small grid has to be used in order to cope with the rapid, position dependent variation according to the $1/r^2$ distribution of the radial dose profile. This leads to unacceptable computing times not compatible with the needs of treatment planning. Therefore, approximation procedures have been developed. The approximations are related to the estimation of the β parameter of the dose response curve; the α parameter always can be calculated exactly according to Eq. (II–7), since the initial slope corresponds to the effect at very low doses and thus fluences. In this case, the dose response is defined by single particle effects, and no overlap of contributions from different particles has to be taken into account. A more detailed discussion would be beyond the scope of this report; details of the approximation can be found in Ref. [II–10].

II–2.2. Comparison with experimental data

Figure II–3 compares survival curves calculated according to the approximations given in Ref. [II–10] with experimental data for carbon, oxygen and neon ion irradiation. The higher energies for the experiments were chosen so that the penetration depth is similar for all three ion beams; they represent the situation in the entrance channel. The lower energies represent the effectiveness in the Bragg peak region. A good agreement between model prediction and experimental data is observed: the transition from shouldered survival curves at high energies to exponential survival curves at low energies, as well as the most pronounced increase of RBE from high to low energies for carbon ions, are well represented by the model calculations.

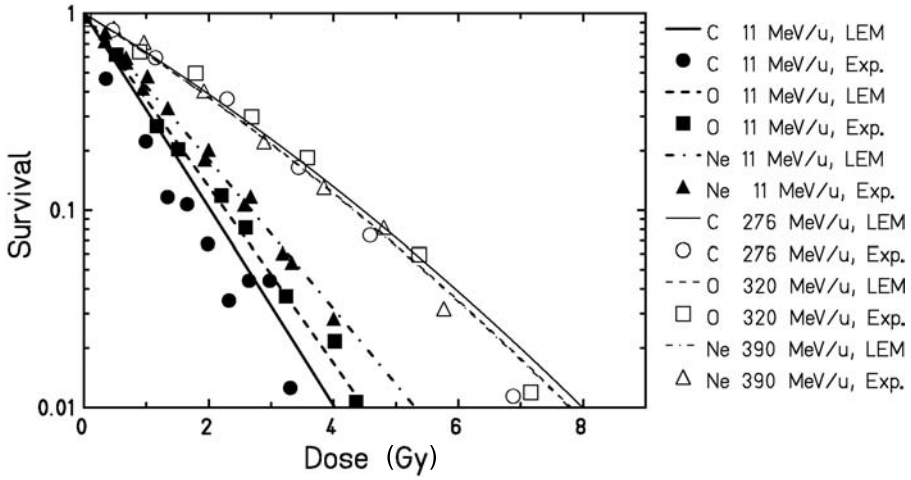

FIG. II–3. Comparison of model calculations with experimental data for CHO cells: C, O, Ne ions at high and low energies.

Figure II–4(a) compares the predictions of the LEM concerning the cell line specificity of RBE (LET) dependence for carbon ion irradiation. Here, the significantly higher RBE for V79 cells as compared to CHO and XRS cells is well reproduced. Furthermore, the near unity RBE for the repair deficient cell line XRS is also correctly reproduced by the model. The RBE apparently correlates with the α/β ratio of the photon dose response curves, which are shown for comparison in Fig. II–4(b), and thus with the repair capacity of the cell.

II–2.3. Transfer to complex tissues in vivo

Figure II–4 already demonstrates that different cell types are characterized by different RBE values, and the same is also expected to hold true in the in vivo and clinical situation. Therefore, normal tissues and tumour tissues might show different RBEs, but also within the groups of normal and tumour tissues a significant variation of RBE can be expected. Therefore, the question arises how to transfer the RBE values determined in vitro to the in vivo or clinical situation.

The LEM as described previously is based on the knowledge of the photon dose response curve. However, representative photon survival curves are not available for all tissues under consideration and, even if available, the correlation between cell survival and the clinically relevant tissue response remains unclear, at least on a quantitative level. Therefore, the question arises

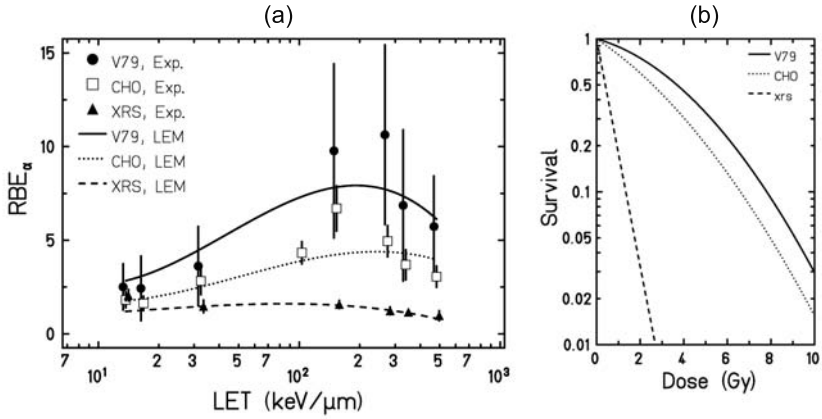

FIG. II–4. (a) Comparison of model calculations with experimental data: RBE_α versus LET for three different cell lines (XRS, CHO, V79); (b) photon dose response curves for the three cell lines.

as to which characteristic of the photon dose response curve is the most relevant for the determination of RBE.

According to Eqs (II–7) and (II–9) and in line with the results shown in Fig. II–4, the non-linearity of the photon dose response curve is a prerequisite for the prediction of RBE values greater than 1.0. If the photon dose response curve is purely exponential, N_{lethal} obeys a linear function of dose, and in that case the integral Eq. (II–7) corresponds to a simple averaging procedure of the local dose. As a consequence, RBE is expected to be equal to 1.0. In contrast, in the case of a shouldered X ray dose response curve, a higher effectiveness is expected and, according to that systematic, the increase in effectiveness should increase with the slope ratio $r = s_{max}/\alpha$ of the photon dose response curve, since the highest effectiveness of the very high local doses in the centre of the charged particle track is determined by the final slope of the photon dose response curve. The RBE_α for maximally effective particles should thus essentially correspond to the ratio of the final slope to the initial slope of the photon dose response curve, which in turn can be expressed in terms of the α/β ratio of the coefficients of the LQ model.

$$r = \frac{s_{max}}{\alpha} = \frac{\alpha + 2\beta D_t}{\alpha} = 1 + 2\frac{\beta}{\alpha} D_t \qquad \text{(II–11)}$$

Figure II–5 demonstrates this dependence of RBE on the slope ratio of the photon dose response curve by means of calculated RBE values as a

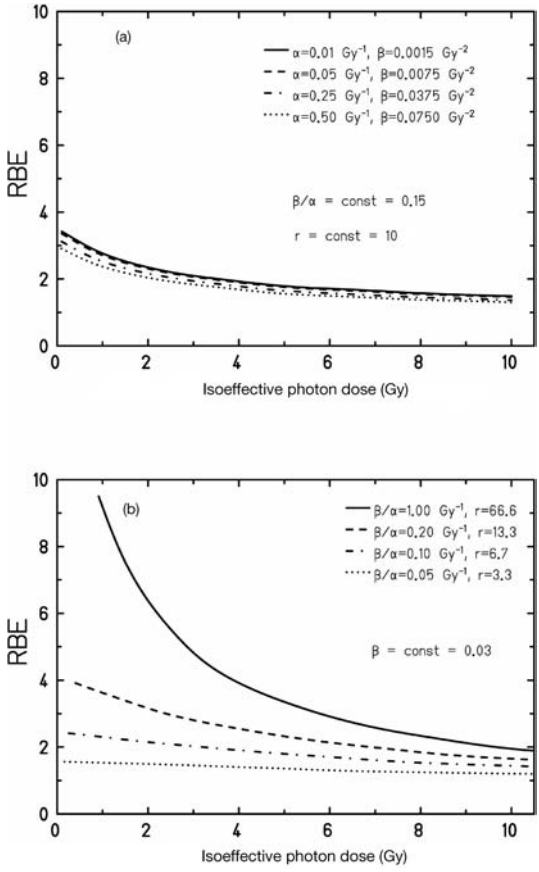

FIG. II–5. Comparison of predicted RBE values in the middle of a 4 cm extended Bragg peak: (a) constant α/β ratio, variation of absolute values of α and β; (b) constant β, variation of α and thus α/β.

function of dose for irradiation in an extended Bragg peak. In Fig. II–5(a), constant values for β/α and D_t and thus also for r are assumed, but the absolute values of α and β are varied by a factor of 50. Despite this large variation, the expected RBE values only show minor differences. In sharp contrast, for a variation of the slope ratio, r, expressed here through the corresponding variation of the β/α ratio and simultaneous adjustment of D_t to achieve the same final slope of 2 Gy^{-1}, an extreme variation of RBE is expected. In line with the qualitative description above, the RBE is highest in the case of a large β/α ratio.

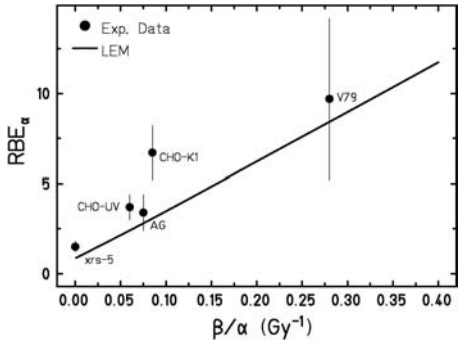

FIG. II–6. Correlation between shoulder width of the photon dose response curve as expressed by the ratio β/α and RBE$_\alpha$ (the initial low dose RBE) for different cell lines.

These dependencies of RBE are also in good agreement with experimental data as shown in Fig. II–6. Here, RBE values for the initial slope of survival curves for a panel of different cell lines irradiated with 11 MeV/u carbon ions as a function of their β/α value, which is directly proportional to the slope ratio (see Eq. (II–11)). The increasing RBE with increasing β/α becomes obvious and is well represented by the model calculation, supporting the hypothesis mentioned previously. Furthermore, this finding is in agreement with other reports, suggesting that radioresistant cell lines (characterized by a large β/α ratio) in general show a more significant enhanced RBE than do sensitive cell lines [II–15 to II–17].

The systematics mentioned previously also open up the application of the LEM to more complex normal tissue effects. This is done by drawing an analogous conclusion: if two biological end points are characterized by the same β/α ratio of the photon dose response curve, they should also show the same RBE for a given type of radiation. Since β/α ratios are known for many normal tissues, these can be used to estimate the RBE. In other words, the model calculation is performed using a photon survival curve, having the same β/α ratio as the tissue end point under consideration, and then assuming that both the survival curve and the tissue end point will show the same RBE at a given dose level. Therefore, if no detailed information about the absolute values of α and β for the tissue under consideration is available, RBE values for treatment planning are based on the β/α ratio for the specific tissue and end point under consideration. According to Fig. II–5(a), the calculated RBE does not critically depend on the particular choice of the absolute values for α and β. Therefore, an arbitrary value of α — of course within the range of otherwise observed values — is chosen, and the corresponding β value is derived from the β/α ratio.

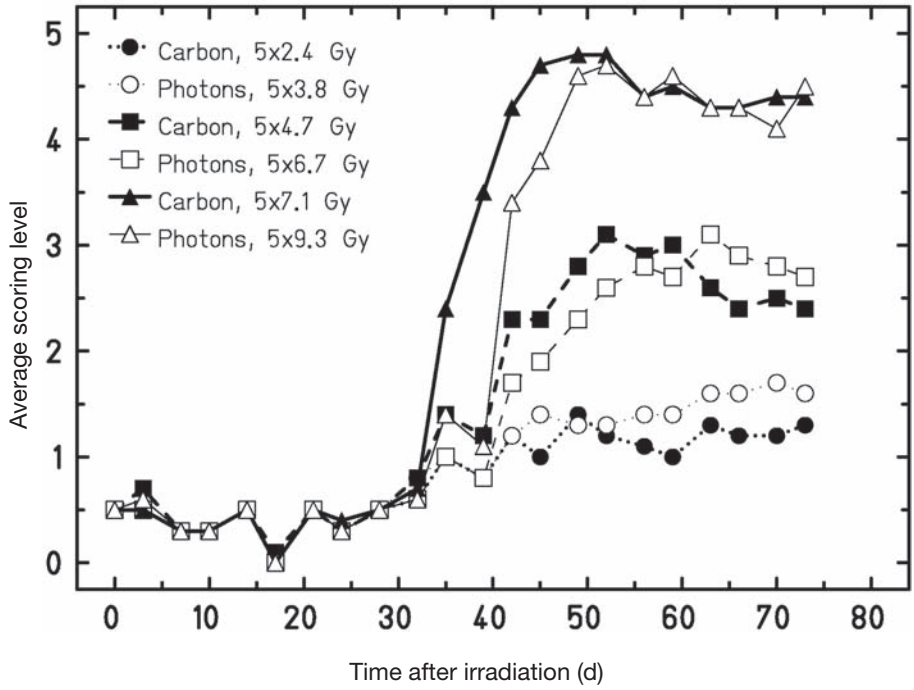

FIG. II–7. Skin reaction after irradiation with X rays and carbon ions. Using the LEM, the doses for carbon ion irradiation were adjusted to result in the same biological effect as the photon fields applied simultaneously. Redrawn after Ref. [II–18].

An example of the application of the LEM to normal tissue effects is given in Fig. II–7 [II–18], where the model has been used prospectively to predict the RBE for skin reactions in minipigs after fractionated irradiation (5 fractions) with carbon ions. Here, the primary aim was to determine the absorbed dose levels for carbon ions, which would result in the same skin reaction as the photon dose fields given to the same animals at the same time as the carbon fields. The model calculations were based on β/α values for skin reactions after photon irradiation obtained from in vivo studies; Fig. II–7 demonstrates that isoeffectiveness has been achieved with good precision.

2.2.4. Implementation in treatment planning

As shown above, the LEM is able to predict dose response curves for end points in vitro and in vivo with good precision. It has thus been implemented in the biological optimization module of the treatment planning procedure TRiP

[II–19, II–20] for the carbon ion therapy trial at GSI. In view of the complexity of the dose calculation and optimization in general, and the radiobiological model in particular, a means of overall verification of the planning procedures is indispensable. For this purpose, we have developed a 'head phantom' set-up that allows measurement of cell response under patient-like conditions [II–19, II–21]. Narrow plastic slides covered with cells are inserted into a cylindrical vessel of 30 cm diameter filled with cell culture medium in variable two-dimensional arrangements. The set-up is irradiated with one or more ion fields in configurations similar to real patients. Target volume definition and dose optimization are performed the same way as for patients. The fraction of surviving cells is measured and compared with the planning predictions.

Figure II–8 shows an example where phantom measurements have been used to investigate the role of dose ramping for the superposition of different treatment fields. As demonstrated by the comparison with the expectation from treatment planning, the effects in the region of the extended Bragg peak are well reproduced, whereas in the entrance channel, the model calculation slightly overestimates the biological effectiveness.

The role of biological optimization in carbon ion therapy treatment planning is demonstrated in Fig. II–9, showing depth dose profiles for single fields applied to patients within the carbon ion trial at GSI. A significant patient-to-patient variation of the RBE is seen, which is due to the different conditions, such as depth of the field, extension of the field and dose level. The full lines are calculated assuming a homogeneous distribution of sensitivity across the field, which corresponds to the sensitivity of the spinal cord and slow growing, radioresistant tumours. For comparison, arrows indicate the predicted effective dose for skin damage in the entrance channel. According to the systematics described in Section 2.3, the higher α/β ratio for skin damage leads to a lower RBE and, thus, to a lower biologically effective dose for skin reactions as compared to, for example, spinal cord damage.

More complete information is given in Fig. II–10, showing a dose distribution in one plane of a typical treatment field (b) and the resulting biologically effective dose distribution (a); in Fig. II–10(c) and (d), the spatial distribution of RBE for this plan is compared with the dose distribution. All quantities have been calculated voxel by voxel for the complete CT image. Besides an increase in RBE with increasing penetration depth, particularly high RBE values are also observed at the border of the treatment field. However, these arise from the dose dependence of RBE and can be attributed to the low dose levels at these positions, so that the biologically effective dose at these positions is still quite small. Up to now, more than 200 patients have been planned and successfully treated since 1997.

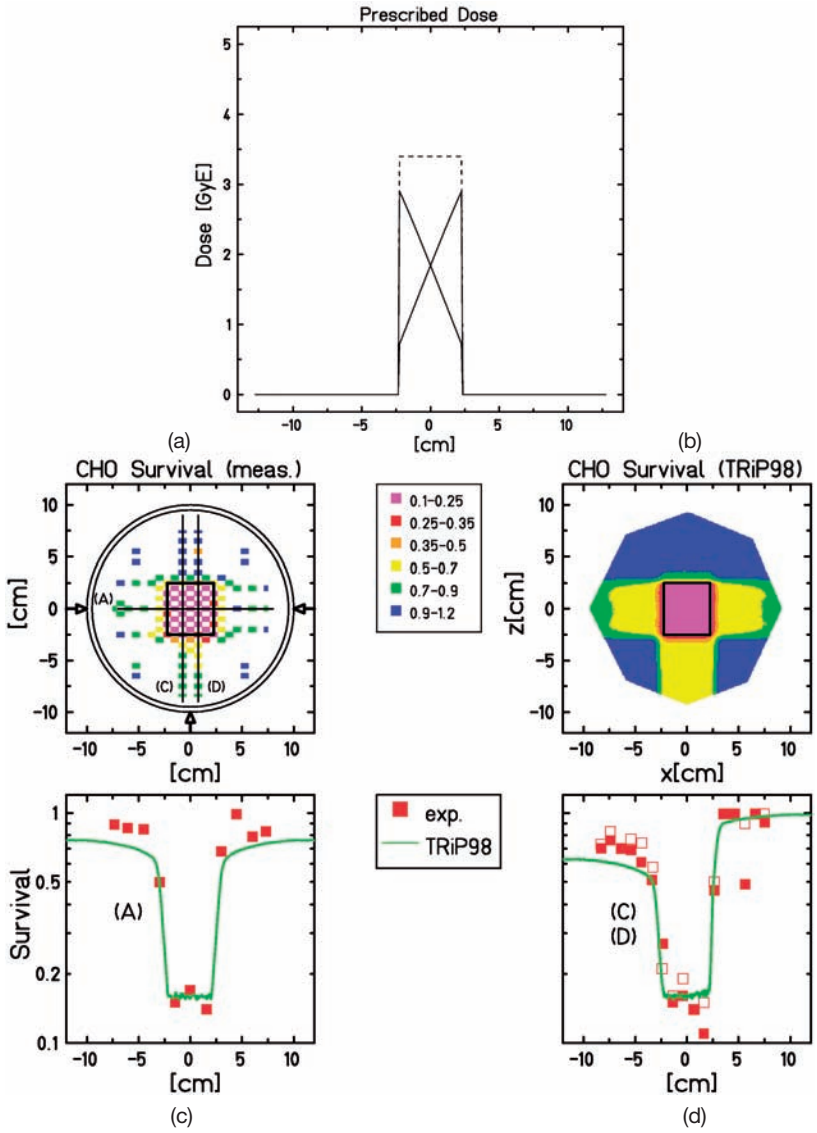

FIG. II–8. Biological verification of treatment planning using CHO cell survival in a cylindrical 'head phantom'. Upper panel: dose distributions of two opposing, ramped fields and a third constant field. Lower panel: (a) measured two-dimensional cell survival distribution; the colour code for the survival level is indicated in the legend; (b) corresponding calculated survival fraction distribution based on the TRiP98 treatment planning programme; (c) comparison of measured (symbols) and calculated survival fraction profiles (full lines) along the line 'A' indicated in the upper left panel; (d) same as (c), but for line 'C' (open symbols) and line 'D' (full symbols) in the upper left panel.

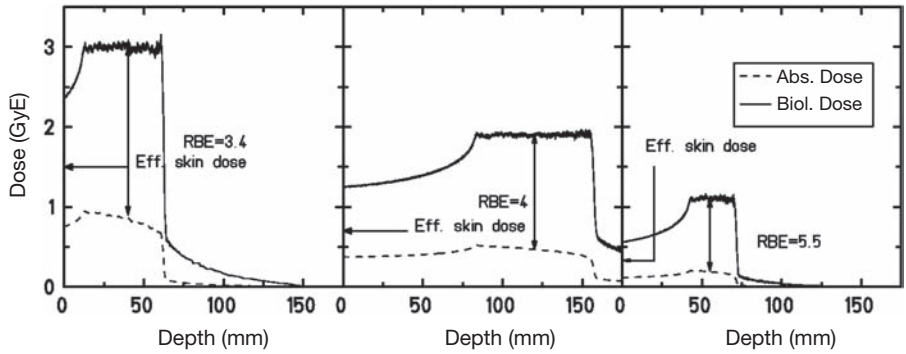

FIG. II–9. Depth dose profiles (in a water equivalent system) for different chordoma patients with different prescribed biologically effective dose levels. Different treatment situations and their consequences for RBE are shown. As expected, lower dose levels result in higher RBEs. Also included are the effective dose levels for the side effects of erythema.

II–2.5. Application to clinical data

Although the clinical data reported from the carbon ion trial at GSI are essentially consistent with the expectations from treatment planning, they have not yet been analysed in detail with respect to the estimation of clinical RBE values. But from HIMAC, excellent results for the irradiation of non-small cell lung cancer were reported [II–22], which allow a direct test of the predictive power of the LEM concerning clinical data. The application of the LEM was facilitated by a detailed analysis of the dose response curve obtained for conventional photon treatment of non-small cell lung cancer as described by Kanai et al. The TCP curves were analysed after photon irradiation with respect to heterogeneity of the radiosensitivity parameter α while keeping the β value constant. According to this analysis, the shallow slope of the photon dose response curve is due to a significant patient-to-patient variation of the α parameter; the distribution (Fig. II–11(a)) can be described by:

$$\begin{aligned} &\bar{\alpha}_X = 0.331 \\ &\sigma(\alpha_X) = 0.18 \\ &\bar{\alpha}_X/\beta_X = 5.585 \end{aligned} \qquad \text{(II–12)}$$

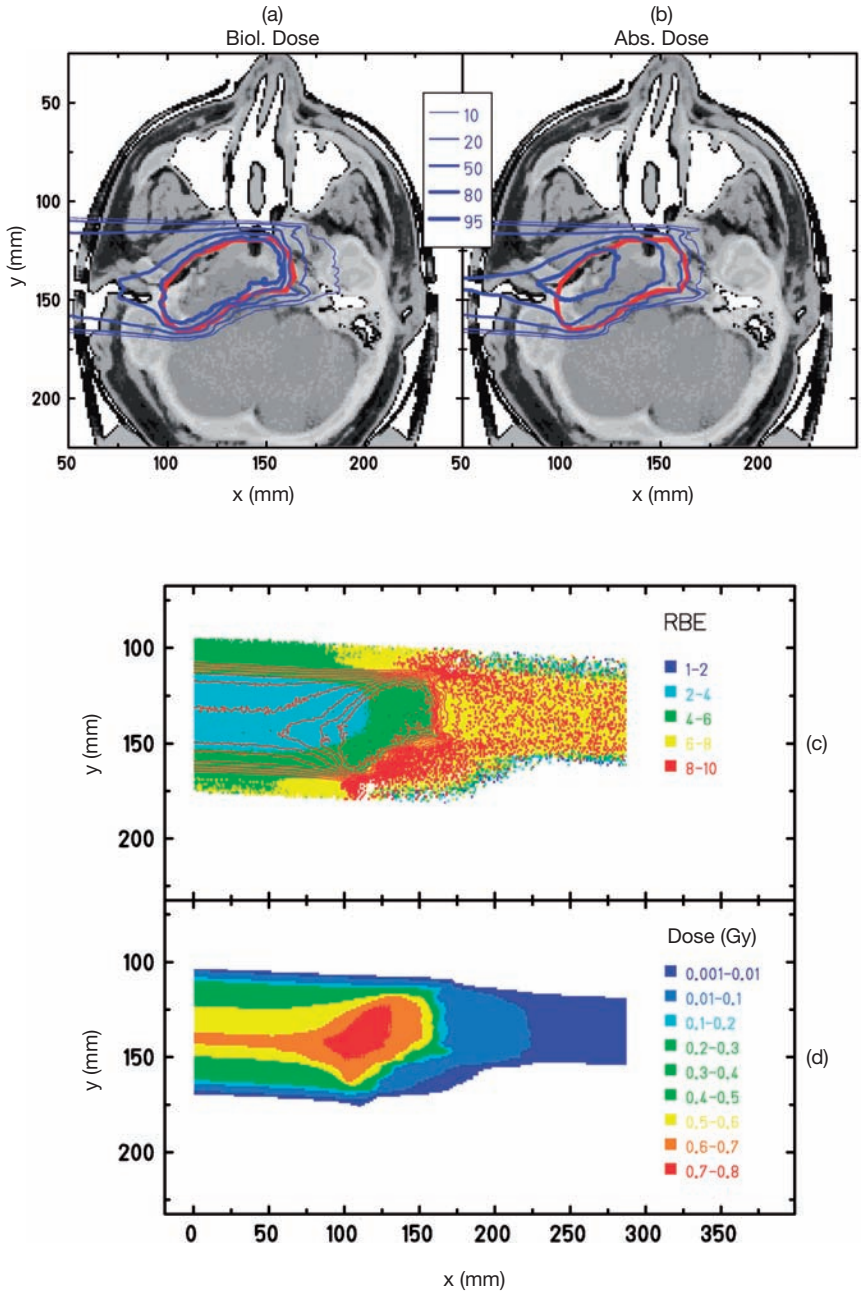

FIG. II–10. Comparison of (a) biological effective dose distribution and (b) absorbed dose distribution for a typical treatment plan. The corresponding RBE distribution in comparison to the absorbed dose distribution is shown in (c) and (d).

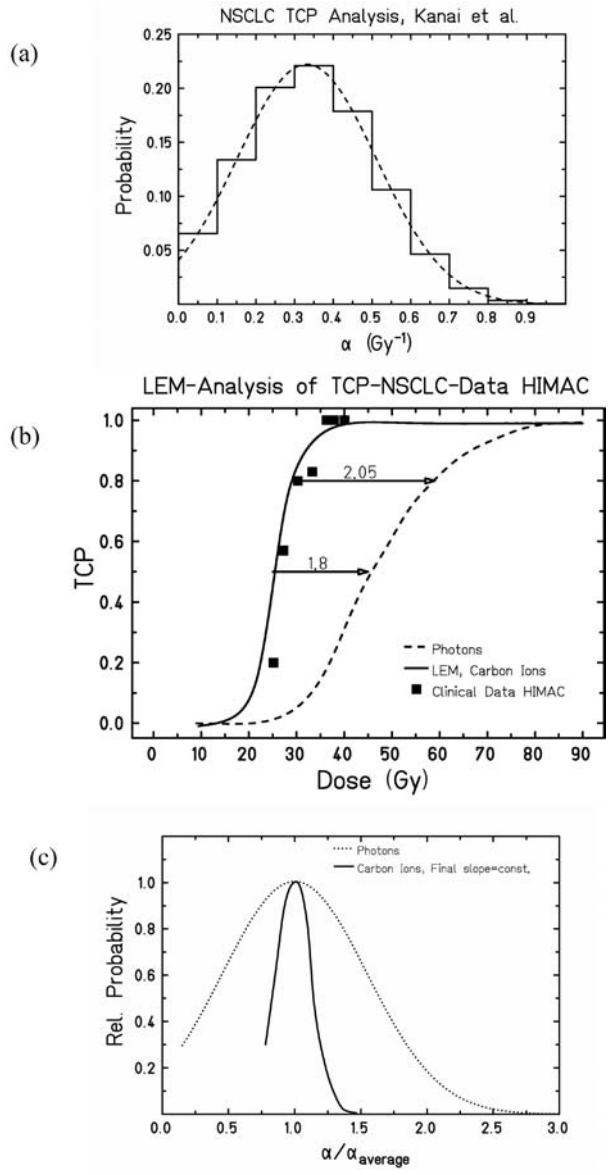

FIG. II–11. (a) Distribution of α parameter values derived from the TCP curves after photon treatment of non-small cell lung cancer patients (courtesy T. Kanai); (b) comparison of the predicted TCP curve for carbon treatment of non-small cell lung cancer with the TCP curve for photon radiation based on the distribution shown in (a); (c) relative distribution of α parameter values for dose response curves after photon radiation (dashed line) and carbon ion radiation assuming a constant value of D_t (full line) or a constant value of the final slope of the photon dose response curve (Scholz, unpublished).

These values correspond to a β_X value of 0.06; for reasons of simplicity, for the application of the LEM the continuous curve was replaced by a histogram with 10 different classes for α; the corresponding values are summarized in Table II.1. The value of β_X has been kept constant for the 10 subpopulations, in line with the general finding that variation of sensitivity is mostly related to variations in the α term, whereas the β term is found to be more or less constant. (The focus here is on the influence of the patient-to-patient variation of intrinsic radiosensitivity; the impact of other parameters such as differences in hypoxia remains to be elucidated.) The dose, D_t, describing the transition to the linear part of the survival curve according to Eq. (II–10) has been chosen according to the assumption that the dose response curves for the different α/β ratios are characterized by the same final slope of 2.1 Gy^{-1} (this value was chosen according to the empirical finding that it gives also consistent results for other end points). Additional input data required for the calculation is the cell nuclear size, defining the integration volume for application of Eq. (II–7); the nuclear radius of the cells was assumed to be 5 μm.

TABLE II–1. NUMERICAL VALUES FOR PHOTON RADIOSENSITIVITY PARAMETERS α_X AND β_X FOR PHOTON RADIATION CORRESPONDING TO THE DISTRIBUTION SHOWN IN FIG. II.11(a)
(D_T values were chosen according to the assumption of the same final slope for all subpopulations; P represents the fraction of the corresponding subpopulation; α_C, β_C and RBE_α represent the linear quadratic parameters for carbon ion irradiation predicted on the basis of the LEM)

α_X (Gy^{-1})	β_X (Gy^{-1})	D_t (Gy)	p	α_C (Gy^{-1})	β_C (Gy^{-2})	RBE_α
0.05	0.06	17.1	0.07	0.64	0.039	12.8
0.15	0.06	16.25	0.14	0.70	0.039	4.67
0.25	0.06	15.4	0.20	0.76	0.039	3.04
0.35	0.06	14.6	0.22	0.83	0.039	2.37
0.45	0.06	13.8	0.18	0.90	0.039	2.00
0.55	0.06	12.9	0.11	0.94	0.040	1.71
0.65	0.06	12.1	0.05	1.01	0.040	1.55
0.75	0.06	11.3	0.02	1.08	0.041	1.44
0.85	0.06	10.4	0.006	1.13	0.041	1.33
0.95	0.06	9.6	0.002	1.20	0.042	1.26

Based on the parameters given above, cell survival curves were calculated using the LEM. The calculation was performed for a position in the middle of an extended Bragg peak of carbon ions ranging in depth from 6 cm to 10 cm. For a first estimate, the calculations were based on the primary carbon ions alone and fragmentation of the beam when passing through tissue has not yet been taken into account; however, the corresponding effects can be expected to be minor and will not significantly influence the results reported below.

The α and β parameters for the calculated dose response curves after carbon irradiation are also given in Table II–1, together with the RBE_{α} values calculated for the initial slope of the survival curves. From these linear quadratic parameters, TCP curves were calculated using an initial cell number of $N_c = 3 \times 10^9$. According to the weighting factors given in Table II–1, the effective TCP curve was then calculated and compared to the clinical data obtained at the HIMAC and the photon dose response curve in Fig. II–11(b). A remarkably good agreement is found when comparing the model prediction with the actual clinical outcome; the TCP_{50} as well as the extreme steepness of the TCP curve after carbon radiation are well reproduced. This steepness is puzzling particularly at first glance, since it apparently is in contradiction to the dose dependence of RBE reported for in vitro systems. In the latter, RBE decreases with dose, whereas for the lung TCP curves, RBE is lowest at low doses and correspondingly low TCP values. With increasing dose, the photon and carbon curves diverge more and more, leading to an increase in RBE with dose and thus an 'inverse' dose dependence of RBE.

According to the analysis described previously, the steepness of the TCP curve after carbon irradiation can be attributed to the reduced variance of the sensitivity parameters after carbon compared to photon radiation. Whereas the coefficient of variation of the α parameter is 55% for photon radiation, it is reduced to only 13% in the case of carbon radiation (see Fig. II–11(c)). The reduced variance is a consequence of the systematics of α/β ratios for the different subpopulations. When keeping the β value constant, variation of the α parameter results in a variation of the α/β ratio. For the highest α values and thus the most sensitive tumours, the α/β ratio is high and thus the RBE is expected to be small. In contrast, for the lowest α values, corresponding to the resistant tumour population, the α/β ratio is small, and the expected RBE is very high. As a consequence, the range of sensitivities, expressed in terms of the α parameter after ion irradiation, is 'compressed' compared to the values for photon radiation. Therefore, the dispersion of sensitivity against photon radiation at least allows a consistent description of the difference in tumour response between photon and carbon ion treatment, although the influence of other factors such as differences in hypoxia cannot be excluded by this analysis.

This reduction of heterogeneity is very specific for high LET radiation. It cannot be mimicked by giving, for example, correspondingly higher doses of proton (or photon) radiation. This is because protons show RBE values close to unity in any case, and thus will not show the differential RBE effect described above, which is necessary to obtain the reduction in heterogeneity.

II–2.6. Critical issues in LEM

As demonstrated previously, the LEM is able to reproduce the systematics of high LET radiation for a wide variety of different end points from in vitro cell survival up to tumour control probabilities. Further support comes from applications to strand break induction [II–23] and even from transfer of the principle to physical applications such as film response to charged particle radiation [II–24]. Nevertheless, there is still need for further developments and optimizations of the model, which will be briefly summarized here.

As indicated in Fig. II–8, the model tends to slightly overestimate the biological effectiveness in the entrance channel. This is further supported by studies of the spinal cord response after fractionated irradiation with carbon ions. From the clinical point of view, this discrepancy is uncritical, since doses are on the safe side, if according to a higher estimated RBE the effects in normal tissue of the entrance channel should be actually somewhat lower than expected. This is at least true, as long as it does not lead to underdosage of the tumour as a consequence of the normal tissue tolerance limits. However, this still needs more systematic comparisons in order to draw definite conclusions. The tendency of overestimation seems to be more pronounced in the case of lighter ions at high energies. Therefore, procedures for further optimization of the LEM are considered for a general application of the model in light ion therapy.

A further point of discussion is the particular representation of the photon dose response curves according to Eq. (II–10). In particular, the dose, D_t, often cannot be directly derived from experimental data, since survival curves can be measured only down to 10^{-3} for most mammalian cell lines. D_t represents thus a semifree parameter of the model, where ‘semifree’ describes a situation where, according to the comparison of model predictions with experimental data, the values of D_t should be restricted to a comparably narrow range in the order of 15–30 Gy. According to the principle of the LEM, it is essentially the final slope of the photon dose response curve which determines the effectiveness of the high local doses in the charged particle track. The interplay between the α/β ratio, the ratio of initial to final slope and the corresponding dependence on D_t will thus need to be investigated in more detail.

II–3. COMPARISON TO OTHER APPROACHES

II–3.1. Katz model

The approach proposed by Katz and co-workers [II–25, II–26] also focuses on the role of track structure, but it significantly differs from the approach presented here, in particular with respect to its application to extended targets such as mammalian cells. The essential differences are only briefly summarized in the following (a detailed discussion can be found in [II–27]):

— The Katz approach is based on the average energy deposition in targets of micrometer size. Therefore, the details of track structure are blurred in that approach.
— The Katz approach uses two different inactivation modes, which are explicitly introduced to handle the different shapes of dose response curves after low LET and high LET radiation. In contrast, the LEM only uses the photon dose response as input, and the transition from linear quadratic to linear dose response curves is a resulting prediction of the LEM.
— The target size and structure ('beans' of micrometre size in a 'bag' of cell nuclear size) is incompatible with the experimental results obtained for very high LET radiation such as uranium ions.
— The approximations introduced in the Katz approach are based on the multitarget formulation of the photon dose response curve. Because this is connected with a vanishing slope of the photon dose response at low doses, it is incompatible with most experimental data and leads to RBE values of infinity for D->0.

II–3.2. Microdosimetry

Microdosimetry has been widely used within the framework of fast neutron therapy, where it has been proven to be useful for the physical characterization of neutron beams [II–28]. This was important, since different facilities were using different neutron energies, collimators, etc. so that they differed considerably with respect to their secondary charged particle spectra. It could be demonstrated that the measured y spectra for different neutron beams also give an indication of the RBE values [II–29, II–30].

The situation is different in the case of accelerated charged particles. These particle beams are very well characterized with respect to the interaction of the primary particles and the distributions of secondary fragments. This is a

prerequisite for physical optimization of treatment plans, since precise depth dose profiles can be obtained only if the underlying charged particle spectra are known for each voxel in the treatment field. Therefore, microdosimetric measurements are not expected to lead to a significant gain in the precision of the description of particle spectra in a given voxel.

Furthermore, the application of microdosimetric methods to predict RBE values within the framework of light ion therapy is limited by the following factors:

— According to the analysis given in this report, details of the spatial distribution of energy deposition far below micrometre dimensions are required for the description of the systematics of increased RBE for charged particle beams. Microdosimetric spectra are obtained, however, from measurements corresponding to micrometre dimensions and thus do not reflect track structure characteristics with the precision required.
— The estimation of RBE from microdosimetric spectra requires knowledge of the biological weighting function, which is strictly valid only for one given biological end point at one given dose level. Since weighting functions are obtained from experimental data, huge efforts would be required to establish the corresponding database of weighting functions for all clinically relevant situations.
— Microdosimetric spectra are based only on lineal quantities and thus mainly reflect the LET of the particles. However, particles with the same LET, but different atomic number differ substantially with respect to their biological effectiveness [II–31]. This can be explained only in terms of their different three-dimensional, spatial energy deposition pattern, which is not adequately represented by lineal variables such as LET.

II–4. CONCLUSIONS

The complex dependencies of RBE on parameters, such as particle type and energy, dose level and the cell or tissue type under consideration, require careful consideration in treatment planning for the applications of charged particle beams in tumour therapy. For the precise quantitative description of these dependencies, models are required. An example of such a model, the LEM, is described in this report, and it has been tested by comparison with a wide variety of biological end points from in vitro cell survival to tumour control probabilities from clinical studies.

The application of this model in treatment planning requires detailed knowledge of the physical parameters that permit derivation of the microscopic

energy deposition pattern for the individual components of the radiation field. In the case of active beam delivery techniques, such as raster scanning, these data are available from the physical optimization in treatment planning.

An important feature of the approach presented here is that it allows the prediction of the response of a biological object to high LET radiation from its response to low LET radiation. Therefore, the experience with conventional photon treatment represents an important resource for estimation of clinical RBE values.

Up to now, the LEM has been implemented in treatment planning for carbon ion irradiation. The clinical results obtained up to now at GSI are consistent with the predicted RBE values in that there is at least no significant overestimation or underestimation of RBE. Otherwise, either more severe normal tissue complications or a higher recurrence rate should have been observed. Further refinements of the LEM as well as experimental verifications for other modalities (protons, helium, oxygen) will make it generally applicable to light ion therapy.

REFERENCES

[II–1] BLAKELY, E.A., "Biology of BEVALAC beams", Pion and Heavy Ion Radiotherapy: Pre-Clinical and Clinical Studies (SKARSGARD, L.D., Ed.), Elsevier Science Publishing Co., Inc., New York (1982) 229–250.

[II–2] FURUSAWA, Y., et al., Inactivation of aerobic and hypoxic cells from three different cell lines by accelerated ^{3}He-, ^{12}C- and ^{20}Ne-ion beams, Radiat. Res. **154** (2000) 485–496.

[II–3] KRAFT, G., Radiobiological effects of very heavy ions: Inactivation, induction of chromosome aberrations and strand breaks, Nucl. Sci. Appl. **3** (1987) 1–28.

[II–4] WEYRATHER, W.K., RITTER, S., SCHOLZ, M., KRAFT, G., RBE for carbon track-segment irradiation in cell lines of different repair capacity, Int. J. Radiat. Biol. **75** (1999) 1357–1364.

[II–5] KANAI, T., et al., Irradiation of mixed beam and design of spread-out Bragg peak for heavy-ion radiotherapy, Radiat. Res. **147** (1997) 78–85.

[II–6] KANAI, T., et al., Biophysical characteristics of HIMAC clinical irradiation system for heavy-ion radiation therapy, Int. J. Radiat. Oncol. Biol. Phys. **44** (1999) 201–210.

[II–7] SCHOLZ, M., KRAFT, G., Calculation of heavy ion inactivation probabilities based on track structure, x-ray sensitivity and target size, Radiat. Prot. Dosim. **52** (1994) 29–33.

[II–8] SCHOLZ, M., KRAFT, G., Track structure and the calculation of biological effects of heavy charged particles, Adv. Space Res. 5–14 (1996).

[II–9] SCHOLZ, M., Calculation of RBE for normal tissue complications based on charged particle track structure, Bull. Cancer Radiother. **83** Suppl. (1996) 50–54.
[II–10] SCHOLZ, M., KELLERER, A.M., KRAFT-WEYRATHER, W., KRAFT, G., Computation of cell survival in heavy ion beams for therapy — the model and its approximation, Radiat. Environ. Biophys. **36** (1997) 59–66.
[II–11] OTTOLENGHI, A., MERZAGORA, M., PARETZKE, H.G., DNA complex lesions induced by protons and alpha-particles: Track structure characteristics determining linear energy transfer and particle type dependence, Radiat. Environ. Biophys. **36** (1997) 97–103.
[II–12] FRIEDLAND, W., JACOB, P., BERNHARDT, P., PARETZKE, H.G., DINGFELDER, M., Simulation of DNA damage after proton irradiation, Radiat. Res. **159** (2003) 401–410.
[II–13] CUCINOTTA, F.A., DICELLO, J.F., NIKJOO, H., CHERUBINI, R., Computational model of the modulation of gene expression following DNA damage, Radiat. Prot. Dosim. **99** (2002) 85–90.
[II–14] KIEFER, J., STRAATEN, H., A model of ion track structure based on classical collision dynamics, Phys. Med. Biol. **31** (1986) 1201–1209.
[II–15] WEYRATHER, W.K., KRAFT, G., RBE of carbon ions: Experimental data and the strategy of RBE calculation for treatment planning, Radiother. Oncol. **73** Suppl. 2 (2004) 161–169.
[II–16] TOBIAS, C.A., BLAKELY, E.A., CHANG, P.Y., LOMMEL, L., ROOTS, R., Response of sensitive human ataxia and resistant T-1 cell lines to accelerated heavy ions, Br. J. Cancer Suppl. **6** (1984) 175–185.
[II–17] SLABBERT, J.P., THERON, T., ZÖLZER, F., STREFFER, C., BÖHM, L., A comparison of the potential gain of p(66)/Be neutrons and d(14)/Be neutrons, Int. J. Radiat. Oncol. Biol. Phys. **47** (2000) 1059–1065.
[II–18] ZACHARIAS, T., et al., Acute response of pig skin to irradiation with 12C-ions or 200 kV X-rays, Acta Oncol. **36** (1997) 637–642.
[II–19] KRÄMER, M., WANG, J.F., KRAFT-WEYRATHER, W., Biological dosimetry of complex ion radiation fields, Phys. Med. Biol. **48** (2003) 2063–2070.
[II–20] KRAMMER, M., SCHOLZ, M., Treatment planning for heavy-ion radiotherapy: Calculation and optimization of biologically effective dose, Phys. Med. Biol. **45** 11 (2000) 3319–3330.
[II–21] MITAROFF, A., KRAFT-WEYRATHER, W., GEISS, O.B., KRAFT, G., Biological verification of heavy ion treatment planning, Radiat. Environ. Biophys. **37** (1998) 47–51.
[II–22] MIYAMOTO, T., et al., Carbon ion radiotherapy for stage I non-small cell lung cancer, Radiother. Oncol. **66** (2003) 127–140.
[II–23] BRONS, S., TAUCHER-SCHOLZ, G., SCHOLZ, M., KRAFT, G., A track structure model for simulation of strand breaks in plasmid DNA after heavy ion irradiation, Rad. Environ. Biophys. **42** (2003) 63–72.
[II–24] SPIELBERGER, B., SCHOLZ, M., KRAMER, M., KRAFT, G., Calculation of the x-ray film response to heavy charged particle irradiation, Phys. Med. Biol. **47** (2002) 4107–4120.

[II–25] BUTTS, J.J., KATZ, R., Theory of RBE for heavy ion bombardment of dry enzymes and viruses, Radiat. Res. **30** (1967) 855–871.
[II–26] KATZ, R., ACKERSON, B., HOMAYOONFAR, M., SHARMA, S.C., Inactivation of cells by heavy ion bombardment, Radiat. Res. **47** (1971) 402–425.
[II–27] SCHOLZ, M., KRAFT, G., The physical and radiobiological basis of the local effect model: A response to the commentary by R. Katz, Rad. Res. **161** (2004) 612–620.
[II–28] MENZEL, H.G., PIHET, P., WAMBERSIE, A., Microdosimetric specification of radiation quality in neutron radiation therapy, Int. J. Radiat. Biol. **57** (1990) 865–883.
[II–29] PIHET, P., MENZEL, H.G., SCHMIDT, R., BEAUDUIN, M., WAMBERSIE, A., Biological weighting function for RBE specification of neutron therapy beams: Intercomparison of 9 European centers, Rad. Prot. Dosim. **31** (1990) 437–442.
[II–30] GUEULETTE, J., MENZEL, H.G., PIHET, P., WAMBERSIE, A., Specification of radiation quality in fast neutron therapy: Microdosimetric and radiobiological approach, Recent Results Cancer Res. **150** (1998) 31–53.
[II–31] BELLI, M., et al., RBE–LET relationship for the survival of V79 cells irradiated with low energy protons, Int. J. Radiat. Biol. **55** (1989) 93–104.
[II–32] GOODHEAD, D.T., et al., Direct comparison between protons and alpha-particles of the same LET: I. Irradiation methods and inactivation of asynchronous V79, HeLa and C3H 10T1/2 cells, Int. J. Radiat. Biol. **61** (1992) 611–624.

Annex III

MEASUREMENT OF RBE OF CARBON IONS FOR CELLS, TUMOUR RESPONSE AND TISSUE REACTIONS IN EXPERIMENTAL SYSTEMS

K. ANDO, M. AOKI, Y. FURUSAWA
National Institute of Radiological Sciences,
Chiba, Japan

Abstract

More than 10 cell lines were collected for human malignant melanomas and another 10 cell lines for squamous cell carcinomas, and dose responses were compared between carbon ions and X rays. The distribution of α values for malignant melanomas was wider than that for squamous cell carcinomas. However, squamous cell carcinomas tended to possess larger β values for carbon ions than malignant melanomas. The results indicated that the α/β ratio is an important discriminator to characterize tumour type specificity of carbon ion sensitivities. Also, a direct comparison of RBE values was made for tumour growth delay and skin reactions. The RBE values of carbon ions decreased with an increase in dose per fraction. The RBE values of lower LET carbon ions (14 and 20 keV/μm) were not different between the tumour growth delay and the skin reaction end points. However, for higher LET carbon ions (42 and 77 keV/μm) with a large dose per fraction, an apparent difference between the RBE for tumour growth delay and the skin reaction was observed. It was concluded that high LET radiotherapy could achieve a therapeutic gain not only because of its dose localization but also by minimizing the difference in either the repair capacity or the oxygen status between the tumour and normal tissue. The ratio α/β depends on the type of cell or tissue, and the values of this ratio are critical for assessing the benefits of fractionated irradiations using carbon ion therapy.

III–1. INTRODUCTION

Biological responses in vitro and in vivo were investigated for heavy ions, including carbon ions. Biological questions involved in clinical carbon ion therapy consist of two items: (a) how the biological gain of carbon ions could be increased; and (b) whether the biological effectiveness of carbon ions depends on tumour type. The first question arose from the anxiety that high LET radiotherapy would cause severe normal tissue damage and reduce therapeutic gain. As RBE values of different cells in vitro are not unity, as has been demonstrated in extensive studies conducted by E. Blakely [III–1], a comparison of

RBE between tumour response and normal tissue reactions would clarify the biological gain of carbon ions. A direct comparison was made of RBE values between tumour growth delay (TGD) and skin reaction. The second question comes from initial observations of clinical trials at Chiba, Japan. Malignant melanomas and adenocystic carcinomas of head and neck respond well to HIMAC carbon ion radiotherapy, while squamous cell carcinomas of the head and neck show only a moderate response to carbon ions [III–2]. This implies that malignant melanomas in general could have larger RBE for carbon ions than squamous cell carcinomas. More than 10 cell lines were collected for human malignant melanomas and another 10 cell lines for squamous cell carcinomas, and dose responses were compared between carbon ions and X rays.

III–2. MATERIALS AND METHODS

III–2.1. Human cells

Malignant melanomas (MM) used here were HMV-I, HMV-II, G361, C32TG, Mewo, Colo679, OMM-1, OCM-1, 92-1 and GAK. Squamous cell carcinomas used were SAS, SQ-20B, SQ-5, HSQ-89, FaDu, Sa3, HO-1-u-1, HSC-2, HSC-3, BOKU and T.Tn. All cells were irradiated in the exponentially growing phase.

III–2.2. Mouse skin and tumour

C3H/HeMsNrsf mice aged 12–18 weeks were used: males for the tumour study and females for the skin study. The animals were produced and maintained in specific pathogen free (SPF) facilities. The tumour was a syngeneic NFSa fibrosarcoma, and its 16th through 18th generations were transplanted intramuscularly into the right hind legs of mice 7 d before the first irradiation [III–3].

Hairs on the right hind leg of female mice were removed by applying a depilatory agent (Shiseido, Tokyo) 7–8 d before the first irradiation [III–4].

A total of 881 male mice for the tumour experiment and 2323 female mice for the skin reaction experiment were used with 5 mice for each irradiation dose point [III–5]. All of the data collected from repeated experiments were combined.

III–2.3. Irradiation

Carbon-12 ions were accelerated by the HIMAC synchrotron to 290 MeV/u. The desired LET was obtained by inserting a given thickness of polymethyl methacrylate (PMMA) upstream of the culture bottles and mice. Carbon beams with 14 and 20 keV/μm LET were obtained at the entrance of the plateau, while those with 40–100 keV/μm LET were within the 6 cm SOBP. A desired irradiation field was obtained by the simultaneous use of an iron collimator and a brass collimator. For cell irradiation, the central position of the SOBP with a LET of 50 keV/μm was used. With pentobarbital anaesthesia (50 mg/kg) and taping, five mice were immobilized on a Lucite plate to place their right hind legs in a rectangular field of 28 mm × 100 mm, and received either a single dose or daily fractionated doses. The foot was excluded from the irradiation field. The tumour diameter at the first irradiation time was 7.5 ± 0.5 mm (mean ± range). Cs-137 γ rays with a dose rate of 1.6 Gy/min at an FSD of 21 cm were used as a reference beam for determining the RBE of tumour response and skin reactions. The LET of ^{137}Cs γ rays was assumed to be 1 keV/μm. Daily fractionation was given with equal daily doses using an inter-fractional interval of 24 ± 1 h. Several graded doses were used to determine an isoeffect dose, and animals assigned to a given dose group received equal daily doses. The reference beam used for cell survival determinations was 200 kVp X rays.

III–2.4. End points and data analysis

Cell survivals were determined by the colony formation assay commonly used to determine in vitro reproductive cell death. All cells, exponentially growing in Ham's F12 medium supplemented with 10% FBS were irradiated with seven different doses of either carbon beams or X rays. Irradiated cells were trypsinized, diluted and seeded in medium to form colonies for 2–3 weeks. Experiments were triplicated, at least, for all cell survival determinations.

Tumours were transplanted into the hind legs of the animals 7 d before the first irradiation, and a tumour volume measurement was used for a TGD assay. The tumour volume was plotted against days after irradiation, and the growth delay was calculated by subtracting the days for a non-irradiated control tumour to reach five times the initial volume from the days for an irradiated tumour to reach five times the initial volume of irradiation. The tumour growth (TG) time, i.e. the time required for each tumour to become five times as large as the initial volume, was calculated from the first irradiation day, and the TG times obtained for all animals were averaged for each dose

group. The difference between the TG time of an experimental group and that of an unirradiated control was defined as the TGD time.

Irradiated legs were observed for skin reaction scoring every other day up to five weeks. The five highest scores in an individual mouse were averaged, and this averaged score was designated as the averaged peak reaction.

To analyse the effectiveness of various fractionation schemes, a dose–response curve was constructed by plotting either the TGD time or the averaged peak reaction as a function of the radiation dose for each scheme. This dose–response curve was used to obtain an isoeffect dose that was defined as the radiation dose necessary to produce either a TGD time of 15 d or a skin reaction score of 3.0. The data for each dose–response curve were fitted to a cubic polynomial function using a least squares method. The 95% confidence limit around the isoeffect dose (TGD time of 15 d and skin reaction score of 3.0) was calculated using the Maharanobis distance.

The Fe plot proposed by Douglas and Fowler [III–6] was used as a multi-fraction linear quadratic (LQ) model. A plot between the reciprocal of the isoeffect dose and the dose per fraction resulted in a straight line with a slope of β/E, and a y axis intercept of α/E, where E is the isoeffect, which is the negative natural logarithm of the surviving fraction at a given isoeffect, i.e. a TGD time of 15 d and a skin reaction score of 3.0. The RBE value (mean ± 95% confidence limits) was obtained by using:

$$\text{RBE}\ (A/B) = (A/B) \pm (A/B) \times \sqrt{\{(a/A)^2 + (b/B)^2\}}$$

where A and B are the mean dose for γ rays and carbon ions, respectively, and a and b are the 95% confidence limits for γ rays and carbon ions, respectively.

III–3. RESULTS

Survival curves were obtained for cell lines of 10 malignant melanomas (Fig. III–1(a), Fig. III–1(b)) and 11 squamous cell carcinomas (Fig. III–1(c), Fig. III–1(d)) irradiated with X rays (Fig. III–1(a), Fig. III–1(c)) and the carbon ion beam (Fig. III–1(b), Fig. III–1(d)). Fitting survival data to the α–β model, α values were plotted for each cell line for X rays and carbon ions on the x and y axis, respectively (Fig. III–2). The relation between X rays and carbon ions for malignant melanomas was similar to that for squamous cell carcinomas, even though distribution of α values for malignant melanomas was wider than that for squamous cell carcinomas. However, squamous cell carcinomas tended to possess larger β values for carbon ions than malignant melanomas

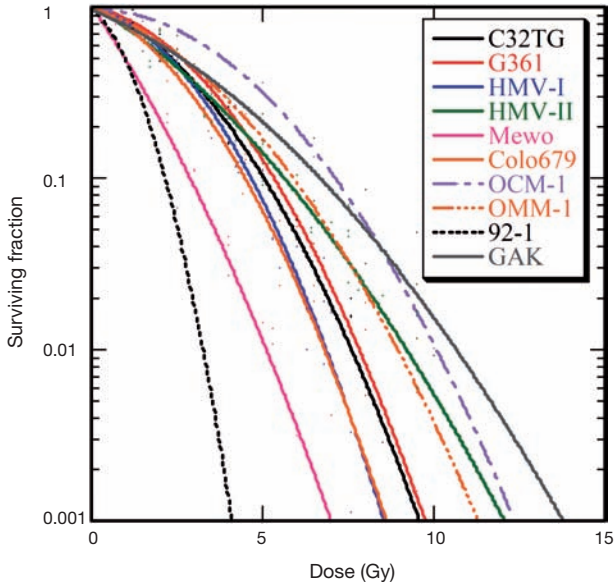

FIG. III–1(a). Survival curves of ten malignant melanoma cell lines after X irradiation, showing the wide spectrum of response to photons.

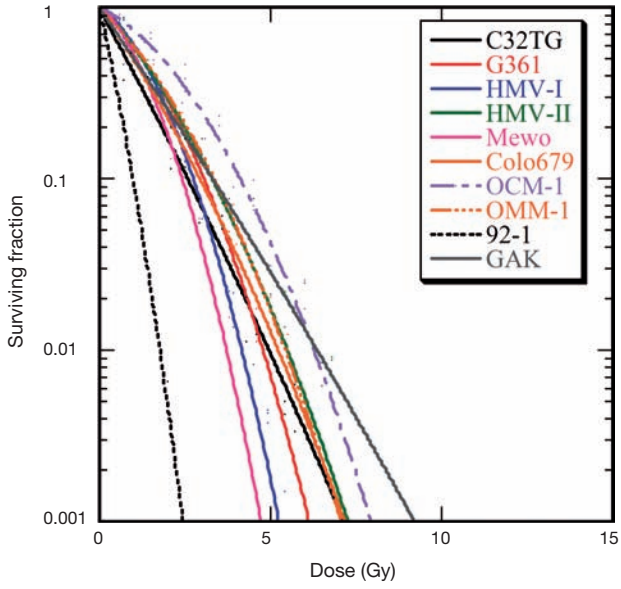

FIG. III–1(b). Survival curves of ten malignant melanomas after carbon ion radiation, showing the narrower spectrum of response to ions compared to the response to photons (compare with Fig. III–1(a)).

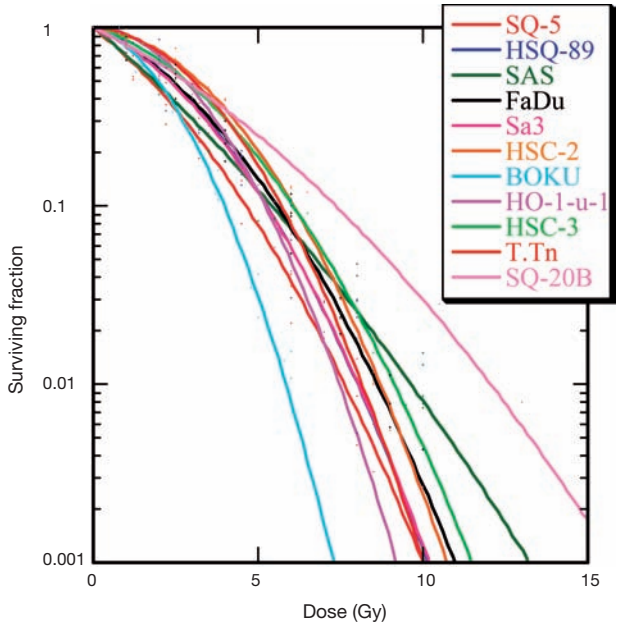

FIG. III–1(c). Survival curves of 11 squamous cell carcinomas after X irradiation, showing the wide spectrum of response to photons.

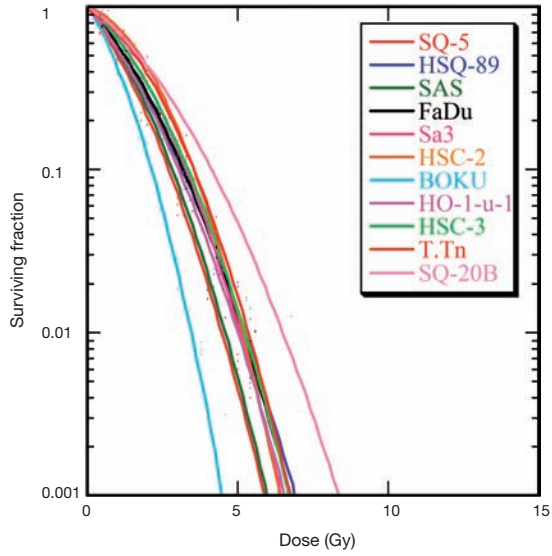

FIG. III–1(d). Survival curves of 11 squamous cell carcinomas after carbon ion irradiation, showing the narrower spectrum of response to ions compared to the response to photons (compare with Fig. III–1(c)).

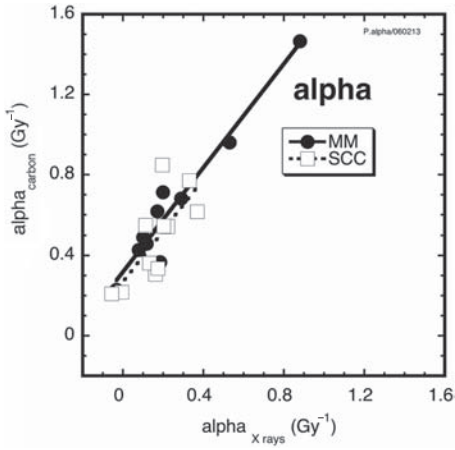

FIG. III–2. α values of carbon ions and X rays. α values for carbon ions are plotted on the vertical scale while those for X rays are on the horizontal scale. Closed circles (•) are for malignant melanomas and open squares (□) for squamous cell carcinomas.

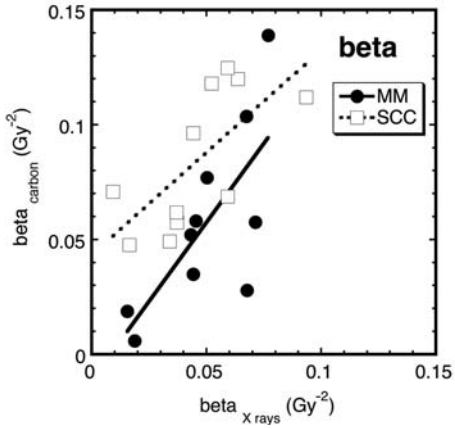

FIG. III–3. β values of carbon ions and X rays. β values for carbon ions are plotted on the vertical scale while those for X rays are on the horizontal scale. Symbols are the same as those in Fig. III–2.

(Fig. III–3). When α/β ratios were plotted, the difference between malignant melanomas and squamous cell carcinomas was most prominently detected (Fig. III–4). The distribution of X ray sensitivities for squamous cell carcinomas, i.e. 1.9–40.3 Gy^{-1}, was wider than that of carbon ions, 1.7–9.5 Gy^{-1}.

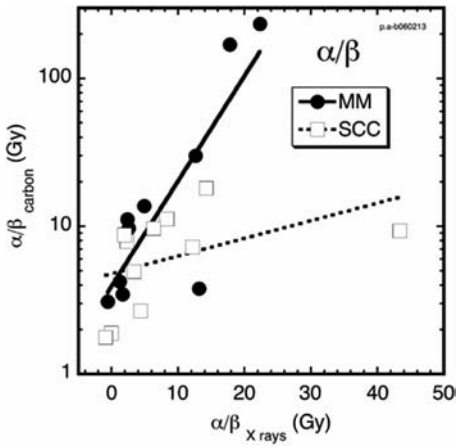

FIG. III–4. α/β ratios of carbon ions and X rays. α/β ratios for carbon ions are plotted on the vertical scale while those for X rays are on the horizontal scale. Symbols are the same as those in Fig. III–2.

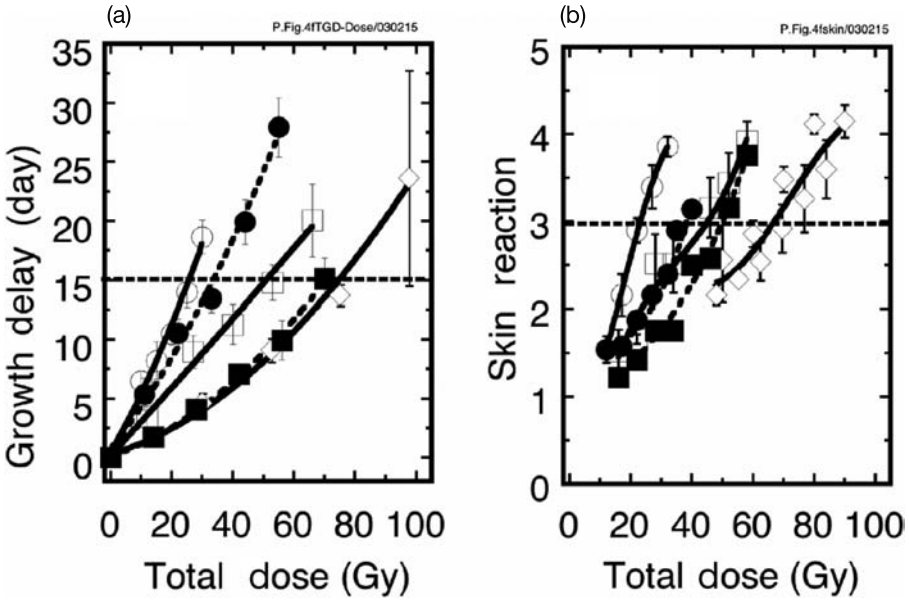

FIG. III–5. (a) Tumour; (b) skin. Dose–response relation for the growth delay of NFSa tumour and for the skin reaction after 4 daily fractionated irradiation. The symbols and bars are the means and the 95% confidence limits for mice irradiated with either γ rays (◇) or carbon ions of 14(■), 20(□), 42(●) or 77 (○) keV/μm, respectively.

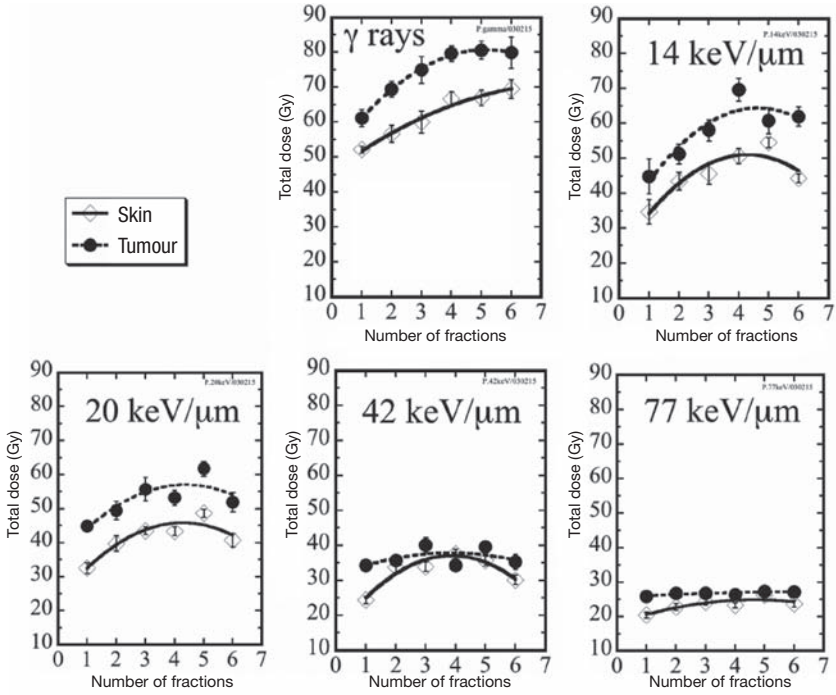

FIG. III–6. Relation between the isoeffect dose and the number of fractions. Isoeffect doses to produce a TGD time of 15 d (•) and skin reaction score of 3.0 (◇) were calculated from the dose–response curves. The mean values with 95% confidence limits are plotted against the number of fractions.

This means that heterogeneity of α/β ratios between different squamous cell carcinomas for carbon ions is smaller than that for X rays. On the contrary, the distribution of X ray sensitivities for malignant melanomas was 1.2–15.6 Gy^{-1}, and similar to that for carbon ions of 3.0–19.6 Gy^{-1}. These results indicate that the α/β ratio is an important discriminator to characterize tumour type specificity of carbon ion sensitivities.

Figure III–5 shows the TGD and skin reactions against the total dose for γ rays or carbon ions of 14–77 keV/μm. As the LET increased, the dose–response curves for both TGD and skin reactions shifted to the left. Dose responses were obtained for 1–6 fraction irradiations, and the isoeffect doses were calculated for the TGD and the skin reaction data (Fig. III–6). The isoeffect dose of γ rays after a single dose was 50 Gy and 60 Gy for skin reactions and TGD, respectively. Overall, the variation in isoeffect total dose was smaller for carbon ions compared with that for γ rays. This was LET

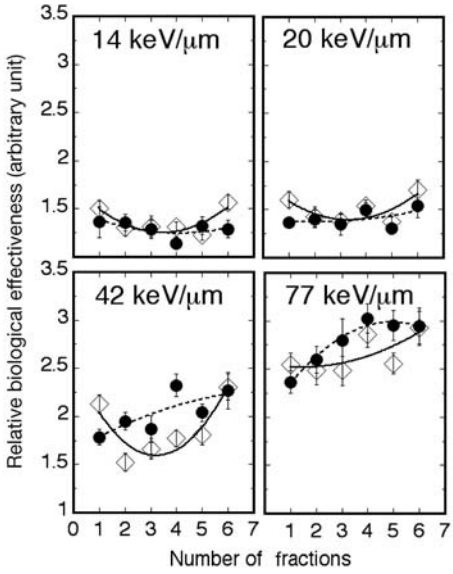

FIG. III–7. Biological effectiveness of carbon ions relative to γ rays, plotted against the number of fractions. The ratio of the isoeffect dose for γ rays to that for carbon ions at a given number of fractions, i.e. RBE, is plotted against the number of fractions. The symbols and bars are the same as those in Fig. III–6.

related, and the higher the LET, the smaller the total isoeffect dose. The isoeffect dose progressively increased with an increase in the number of fractions for both the skin reactions and TGD, but the increase was less prominent, or reached a plateau, when the number of fractions exceeded 4. This was true for γ rays as well as lower LET carbon ions, such as 14 and 20 keV/μm. For higher LET carbon ions of 42 and 77 keV/μm, not only was the isoeffect dose further reduced, but the difference between the skin reaction and the TGD also diminished. No fractionation effect was observed for 77 keV/μm carbon ions. The RBE values of lower LET carbons (14 and 20 keV/μm) ranged from 1.2 to 1.7, and did not show any apparent dependence on the number of fractions (Fig. III–7). When the LET of carbon ions increased to 42 keV/μm, the RBE values became large. The RBE values of TGD, but not the skin reaction, increased with an increase in the number of fractions. The RBE values for TGD at 2 and 4 fractions were significantly larger ($P < 0.05$) than those for skin reaction. When the RBE values were compared for the TGD versus the RBE values for the skin reaction, the resulting ratio or therapeutic gain of carbon ions was 1.16 ± 0.09 (95% confidence limits) and 1.31 ± 0.09 at 2 and 4 fractions, respectively (Fig. III–8). The therapeutic gain was also

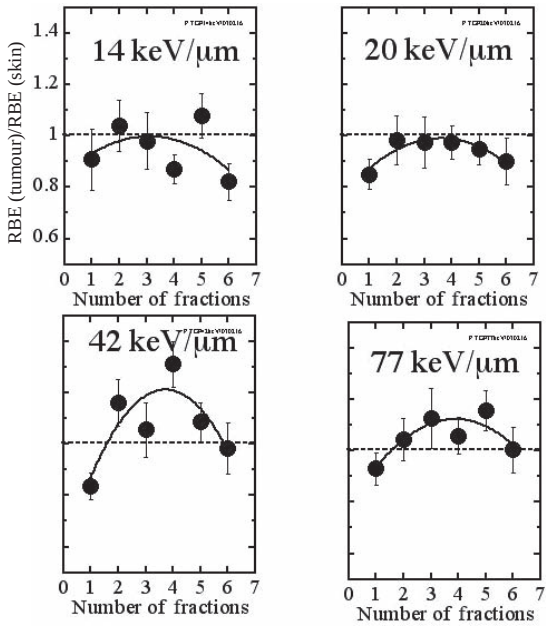

FIG. III–8. The therapeutic gain. The therapeutic gain is the ratio of the tumour RBE to the normal tissue (skin) RBE, and is of benefit when the RBE ratio exceeds 1.0.

larger than 1.0 at 3 and 5 fractions with 77 keV/μm. The RBE of charged particles depends on the dose per fraction. The RBE values of carbon ions decreased with an increase in dose per fraction (Fig. III–9). The RBE values of low LET carbon ions (14 and 20 keV/μm) were not different between the TGD and the skin reaction. Although an apparent difference between the RBE for TGD and the skin reaction was observed, it was most apparent for RBE values of higher LET carbon ions (42 and 77 keV/μm) with a large dose per fraction.

Radiation damage to tissues is primarily caused by energy deposited in the critical target in cells, i.e. DNA. Because high LET radiation produces dense energy deposits, single hit or intratrack damage caused by high LET radiation is more prominent than that caused by low LET radiation, which produces dual hit or intertrack damage to DNA. Using an Fe plot, the isoeffect dose was used to evaluate the dependence of the intratrack damage (α term) and of the intertrack damage (β term) on LET (Fig. III–10). The reciprocal total dose for TGD and skin reaction also increased with an increase of the dose per fraction. When LET increased, the regression lines moved upward, which was more prominent for a higher LET. The slope of the line fitted to skin reaction was steeper for 80 keV/μm carbon ions {$(5.235 \pm 1.205) \times 10^{-4}$ Gy^{-1};

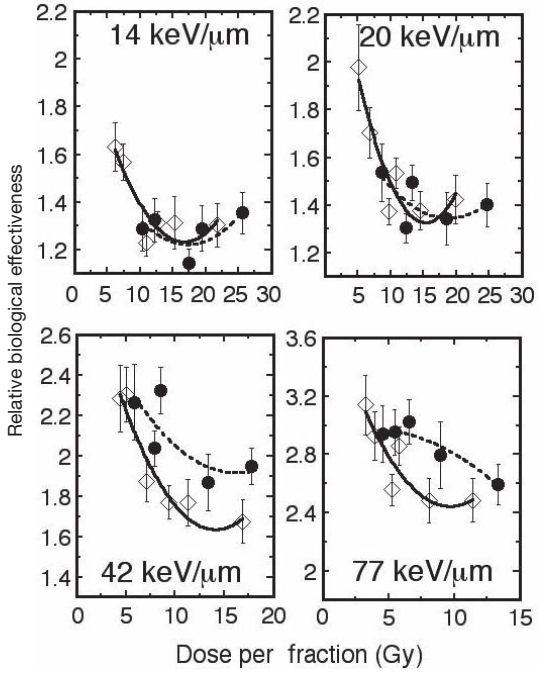

FIG. III–9. RBE plotted against the dose per fraction. The symbols and bars are the same as those in Fig. III–6.

mean and 95% confidence limit} than for γ rays {$(1.376 \pm 0.308) \times 10^{-4}$ Gy^{-1}}. The α and β terms of each regression line were calculated for all of the LET values shown in Fig. III–10 as well as for the skin reaction data of LET 50, 60 and 100 keV/μm. The α terms of the TGD and skin reaction also apparently increased with an increase in the LET (Fig. III–11); the increase in the α terms was slightly larger for the TGD than for the skin reaction, even though no statistical difference was detectable between the two tissues. On the other hand, the β terms of the two tissues depended differently on the LET; the β term of the skin reaction significantly ($r = 0.807$, $P = 0.015$) increased with LET, while that of the TGD was independent of LET. Using the α and β terms calculated from the regression lines shown in Fig. III–11, quasi-survival curves for tumour cells and skin cells were reconstructed. The α and β terms contain an isoeffective surviving fraction (E) that produces a given magnitude of TGD and skin reaction, namely, α/E and β/E. A value for E of 10^{-5} was used here for tumour cells which was experimentally obtained by using a transplantation assay [III–7], while it was empirically determined to be 10^{-6} for skin cells. The quasi-surviving fractions of skin cells after γ rays were lower than those of

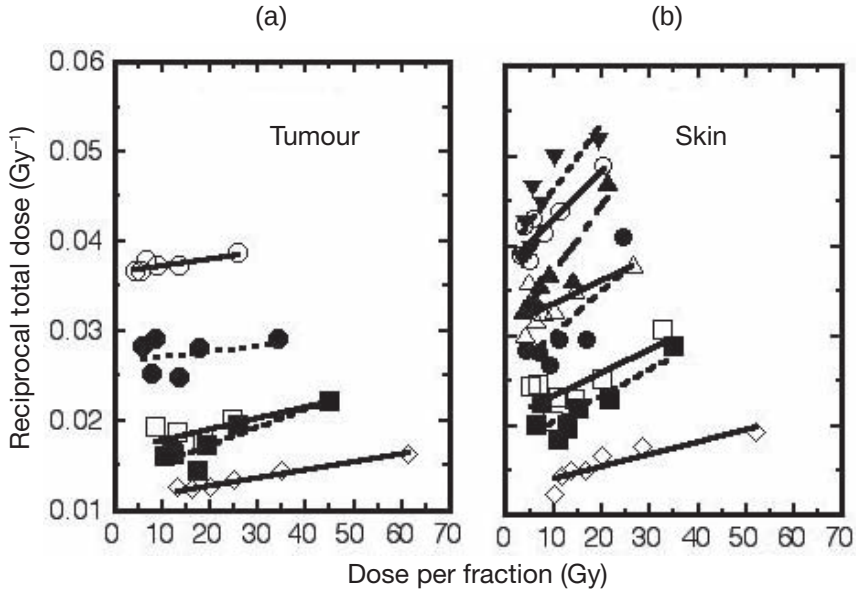

FIG. III–10. The reciprocal of the isoeffect dose plotted against the dose per fraction. The symbols in (a) represent tumours receiving (◇) γ rays and carbon ions of 14 (■), 20 (□), 44(●) and 74 (○) keV/μm, respectively. The symbols in (b) represent skin receiving (◇) γ rays and carbon ions of 14 (■), 20 (□), 40 (●), 50 (△), 60 (▲), 80 (○) and 100(▼) keV/μm, respectively. The intercept gives the intratrack damage (α term) while the slope gives the intertrack damage (β term).

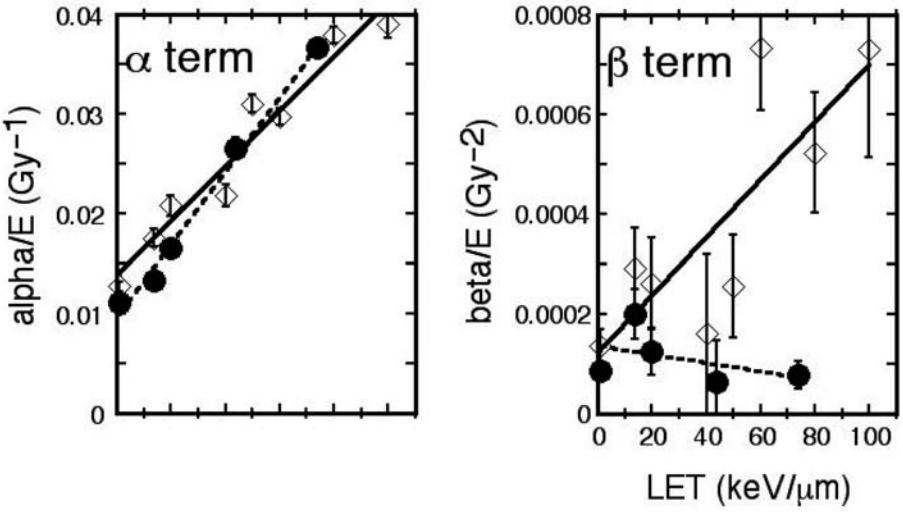

FIG. III–11. The α and β terms plotted against LET. The symbols and bars are the means and 95% confidence limits for the TGD (●) and the skin reaction (◇).

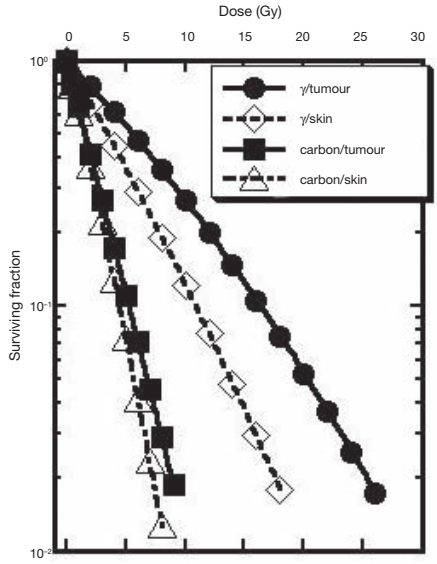

FIG. III–12. Quasi-survival curves of tumour cells and skin cells constructed by using the α and β terms obtained in Fig. III–11. The symbols are calculated values, and represent the tumour cells receiving γ rays (•), 77 keV/μm carbon ions (■), skin cells receiving γ rays (◇) and 77 keV/μm carbon ions (△).

tumour cells (Fig. III–12). Carbon ions of 77 keV/μm moved both the quasi-survival curves of the skin and tumour cells to the left. Because the move is more prominent for tumour cells than for skin cells, the two survival curves became indistinguishable.

III–4. CONCLUSIONS

High LET radiotherapy could achieve therapeutic gain not only because of its dose localization but also by minimizing the difference in either the repair capacity or the oxygen status between the tumour and normal tissue. The ratio α/β depends on types of cells/tissues, and would be critical for fractionated irradiation of high LET carbon ion therapy.

REFERENCES

[III–1] BLAKELY, E.A., NGO, F.Q.H., CURTIS, S.B., TOBIAS, C.A., Heavy-ion radiobiology: Cellular studies, Adv. Radiat. Biol. **11** (1984) 295–382.

[III–2] MIZOE, J., et al., Dose escalation study of carbon ion radiotherapy for locally advanced head and neck cancer, Int. J. Rad. Oncol. Biol. Phys. **60** (2004) 358–364.

[III–3] ANDO, K., et al., Accelerated reoxygenation of a murine fibrosarcoma after carbon ion radiation, Int. J. Radiat. Biol. **75** (1999) 505–512.

[III–4] ANDO, K., et al., Mouse skin reactions caused by fractionated irradiation with carbon ions, Int. J. Radiat. Biol. **74** (1998) 129–138.

[III–5] ANDO, K., et al., Biological gain of carbon-ion radiotherapy for the early response of tumor growth delay and against early response of skin reaction in mice, J. Radiat. Res. **46** (2005) 51–57.

[III–6] DOUGLAS, B.G., FOWLER, J.F., The effect of multiple small doses of X-rays on skin reactions in the mouse and a basic interpretation, Radiat. Res. **66** (1976) 401–426.

[III–7] ANDO, K., KOIKE, S., SATOH, S., Nonlinear survival curves for cells of solid tumors after large doses of fast neutrons and γ rays, Radiat. Res. **131** (1992) 157–161.

Annex IV

CLINICAL RBE DETERMINATION SCHEME AT NIRS–HIMAC

J. MIZOE, K. ANDO, T. KANAI, N. MATSUFUJI, H. TSUJII
National Institute of Radiological Sciences,
Chiba, Japan

Abstract

Clinical trials were started with carbon beams by establishing equivalency between carbon and neutron beams to make use of the experience in neutron therapy at the National Institute of Radiological Sciences (NIRS), Chiba, Japan. Through biological experiments, it was found that a carbon beam that possesses a dose averaged LET of 80 keV/μm causes equivalent biological responses to those from the neutron beams. The clinical RBE was defined as 3.0, the same as that used in neutron therapy at the point where the dose averaged LET value is 80 keV/μm. The physical dose distribution required in the SOBP was chosen to yield a constant biological response across the SOBP using parameters for HSG cells in the linear quadratic model. In 10 years, this scheme realized excellent clinical results. The TCP of lung cancer was well explained by taking into account the patient-to-patient variation of radiosensitivity. When comparing the '4 GyE' results with those estimated at the GSI, Germany, about 15% difference was found in clinical dose at the middle of the SOBP. It is indispensable in future to establish inclusive convertibility between GSI and other centres to make clinical experiences referable and, as a goal, to contribute in finding optimum heavy ion treatment protocols.

IV–1. INTRODUCTION

In the clinical application of a heavy ion beam, it is necessary to select the type of heavy ion, irradiation schedule, and dose for the treatments. In the beginning phase of a heavy ion clinical trial, there is a lack of pertinent biological data on the biological effects of the high LET radiation of the heavy ion beams. A carbon beam was selected because of its maximum peak to plateau dose ratio expected among any ion species. At the beginning, it seemed reasonable to start heavy ion radiotherapy by applying the treatment schedule used in neutron radiotherapy that had been carried out for more than 20 years at NIRS. NIRS strategy for the heavy ion radiotherapy was set up as follows:

(1) Equivalency between NIRS neutron and carbon beam in biological responses should be established.

(2) As a starting point, the treatment schedule of the neutron radiotherapy should be applied to heavy ion radiotherapy.

The optimum particle and treatment schedule for heavy ion radiotherapy should then be selected.

IV–2. RBE DETERMINATION SCHEME

The following briefly summarizes the clinical RBE determination scheme currently used at NIRS.

Beam model

Fragmentation of monoenergetic carbon ions in a patient's body is estimated with a simulation code, HIBRAC [IV–1]. Dose averaged LET value is deduced at each depth from the calculated LET spectra.

Design of biological SOBP

The human salivary gland (HSG) cell line, derived from an HSG tumour, was chosen as representative of various cell lines due to its moderate radiosensitivity. Dose–survival relationships of the HSG cells to carbon ions of various incident energies and LETs were characterized with two parameters, α and β, using the LQ model. The SOBP was designed to achieve constant survival probability (10%) for HSG cells over the entire SOBP region. Values of the coefficients α and β based on dose averaged LET were used for survival calculations at each depth.

Determination of clinical RBE

It is assumed that the carbon beam is clinically equivalent to fast neutrons at the point where the dose averaged LET value is 80 keV/μm, the neutron equivalent point. NIRS's enormous neutron therapy experience indicates that the NIRS neutron beam has a clinical RBE of 3.0. The clinical RBE of carbon is normalized to 3.0 at the point in the SOBP where the LET is 80 keV/μm. The clinical SOBP shape is deduced by multiplying the biological SOBP shape by a constant factor equal to the ratio of the clinical RBE to the biological RBE determined at the neutron equivalent point.

Each step is explained in detail in the following sections.

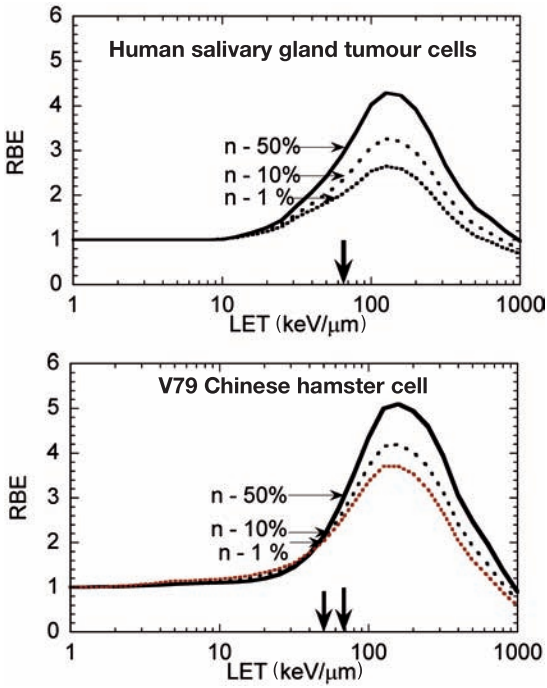

FIG. IV–1. LET dependency of RBE for colony formation of V79 and HSG cells at 1%, 10% and 50% survival levels. The RBE values were obtained using low energy carbon ions at the RIKEN ring cyclotron facility and NIRS cyclotron. The arrows indicate RBE values obtained using the neutron beam at the survival levels indicated.

IV–2.1. Beam model

The depth dose distribution and LET distributions of a monoenergetic carbon beam were calculated, including fragmentation effects, using the code HIBRAC [IV–1]. Here, the patient's body is regarded as water equivalent. The results were verified through comparisons with NIRS experimental results.

IV–2.2. Design of biological SOBP

Through biological experiments as shown in Fig. IV–1, it was found that the neutron RBE at several survival levels coincided with the RBE of the carbon beam at a dose averaged LET of around 65 keV/μm. It can thus be said that the neutron beam is nearly equivalent to a 65 keV/μm carbon beam.

Survival curves of mouse crypt cells for the neutron irradiation coincided with the survival curves for the irradiation in the proximal peak of the SOBP

carbon beam in both cases of single and fractionated irradiation [IV–2]. The dose averaged LET of the proximal peak of the SOBP was about 65 keV/μm. Even though the biological effects for the SOBP beam should be slightly different from those for the monoenergetic beam of the same LET, these results of the effects of single and fractionated irradiation on crypt cells have supported the assumptions that the NIRS neutron beam is nearly equivalent to a 65 keV/μm carbon beam. Consequently, the decision was made to select a carbon beam as the first heavy ion beam to start clinical trials of heavy ion radiotherapy.

It is assumed that cell survival versus dose for combined high and low LET beams could be expressed by an LQ model, in which new coefficients (α and β) for combined irradiation were obtained by dose averaging coefficients α and $\sqrt{\beta}$ for monoenergetic beams over the spectrum of the SOBP beam [IV–3]. Also, it has been shown that, using a SOBP designed to give uniform survival of HSG cells, the survival level of V79 Chinese hamster cells is successfully uniform throughout the SOBP. The biological responses for a range modulated beam were also examined for quite different biological samples, such as HSG cells [IV–4], MG 63 human osteosarcoma cells [IV–5] and crypt cells of mouse jejunum [IV–2].

In the design of the SOBP, data is needed concerning the LET dependence of the coefficients (α and β) in the LQ model of the survival curve for an appropriate cell line, which represents the response of tumour tissue. Referring to the work of Lyman et al. in the design of their ridge filter [IV–6] and the work by Ito et al. at the RIKEN ring cyclotron [IV–7], it was found the response of the HSG cells was in the middle of a variety of biological species. HSG cells have a small shoulder in their survival curve, typical of early responding tissues. In addition, RBE at D10 is found to be independent of cell type as shown in Fig. IV–2 [IV–8]. Therefore, data were adapted of the coefficients (α and β) of the HSG cell line as being representative of typical tumour responses in the design of the SOBP of the HIMAC beam.

The RBE of HSG cells against the dose averaged LET of the SOBP shows that at around 80 keV/μm, the carbon beam in the SOBP is equivalent to the NIRS neutron beam in terms of the biological responses (Fig. IV–3). The neutron equivalent LET of the spread out beam was higher than in the case of a monoenergetic carbon beam of 135 MeV/n. This may be because a spread out beam using 290 MeV/n carbon contains a large amount of low LET components, and the LET spectrum of the beam is spread over a very large range. The biological responses for the 6 cm SOBP of 290 MeV/n carbon beam were also slightly less effective than those for the 3 cm SOBP of 135 MeV/n carbon beams having low contaminations with fragmented light nuclei.

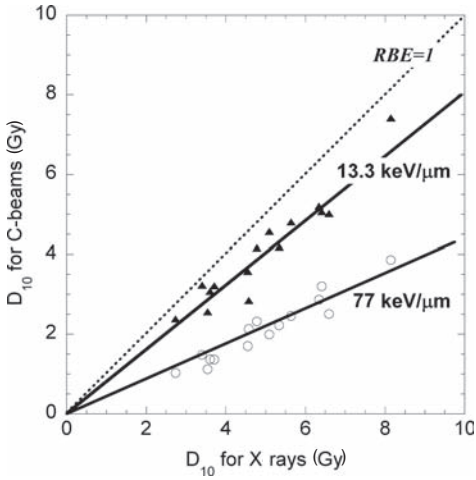

FIG. IV–2. Relationship between D_{10} values for X rays and carbon ions for various cell lines. RBE is largely categorized by the difference of LET, however, it is not dependent on the cell line [IV–8].

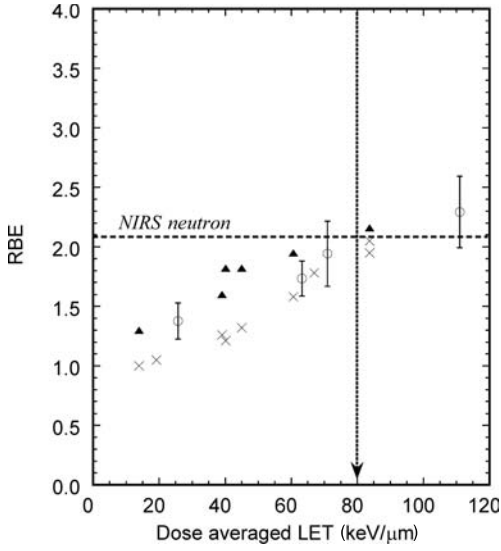

FIG. IV–3. LET dependency of the RBE for colony formation of HSG cells at the 10% survival level. The data for the RBE were obtained by exposures from a HIMAC carbon beam of 290 MeV/nucleon. The dashed line shows the RBE for the NIRS neutron beam for the HSG cells.

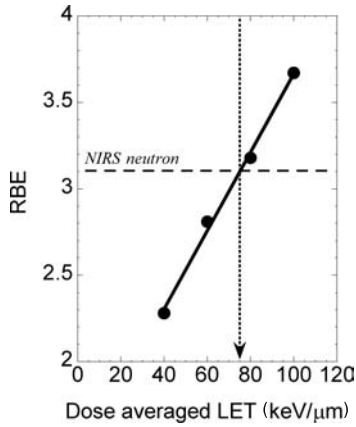

FIG. IV–4. LET dependency of the RBE for skin reaction of C3H mouse legs at the average skin reaction score of 2.5 (dry desquamation). Mouse legs were locally irradiated with either HIMAC carbon beam of 290 MeV/n (at around 80 keV/μm point of 6 cm SOBP) or ^{137}Cs γ rays for 4 fractions over 4 d.

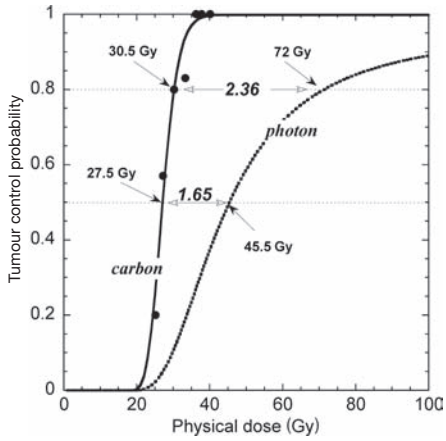

FIG. IV–5. Biological dose distribution of a therapeutic carbon beam, using several cell lines and theoretical prediction. The Bragg peak of a monoenergetic carbon beam of 290 MeV/n was spread out to 6 cm.

The results of an experiment on the early reaction of mouse skin also showed that at around 80 keV/μm, beams of carbon SOBP were equivalent to the NIRS neutron beam in the case of 4 fraction irradiation as shown in Fig. IV–4. Approximately constant responses were observed in the SOBP for various cell lines (Fig. IV–5).

IV–2.3. Determination of clinical RBE

The clinical RBE of the carbon beam was determined based on the RBE for the neutron beam at NIRS. From the experience involving neutron therapy, the clinically determined RBE for the neutron beam was 3.0 when the total number of fractionated doses was 18 and the neutron dose level of each fraction was 0.9 Gy. The clinical RBE value at the neutron equivalent position of the carbon SOBP was then determined to be 3.0. The relative biological and physical dose distributions obtained using the responses of the HSG cells were assumed to be maintained for the clinical cases.

Prescription of clinical dose:

(1) The effective dose level of the flat top of the clinical dose distributions is first chosen by a radiation oncologist.
(2) The corresponding physical dose at the neutron equivalent position is determined using an RBE value of 3.0.
(3) The physical dose distribution of the SOBP beam is then normalized to the dose at the neutron equivalent position.
(4) The physical dose at the centre of the SOBP is obtained and the RBE values at the centre of the SOBPs are then obtained by dividing the biological dose by the physical dose. To obtain the effective clinical dose, the biological dose at every depth is multiplied by the ratio of the biological and clinical RBEs at the neutron equivalent position.

Figure IV–6 schematically shows the method for determining the RBE at the centre of the SOBP for clinical situations. Usually, in a treatment planning system, the physical dose at the centre of the SOBP is given using an RBE table. In the procedure of dose calibration, the dose monitor is calibrated against the given physical dose at the centre of the SOBP. Table IV–1 gives the clinical RBE of carbon beams at the centre of various sizes of SOBP.

IV–3. CLINICAL EXAMPLE: NON-SMALL CELL LUNG CANCER [IV–9]

Ten years have passed since clinical trials began at NIRS with carbon ions at HIMAC. A tumour control probability (TCP) analysis for non-small cell lung cancer (NSCLC) is presented as an example of clinical results in terms of the clinical RBE determination scheme mentioned previously.

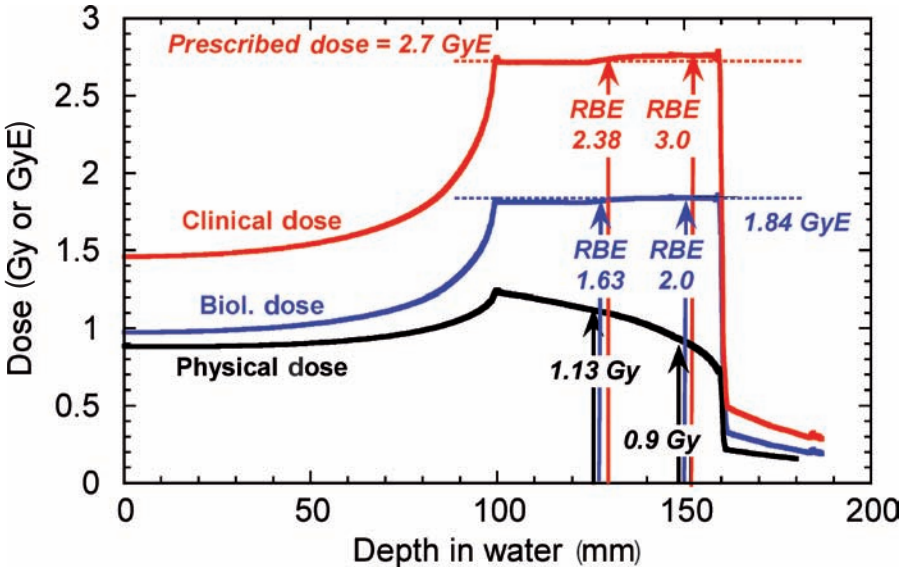

FIG. IV–6. Schematic method used to determine the RBE at the centre of the SOBP for the clinical situation.

TABLE IV–1. CLINICAL RBE OF THE CARBON BEAMS AT THE CENTRE OF THE VARIOUS SIZES OF SOBP

SOBP width (mm)	Clinical RBE
30	2.8
40	2.6
60	2.4
80	2.3
100	2.2
120	2.1

Miyamoto et al. [IV–9] analysed the clinical results of NSCLC treated by HIMAC beams. They depicted a very conspicuous dose dependency of local control rate. The dose escalation study was performed with a treatment schedule of 18 fractions in 6 weeks. As to photons, Hayakawa et al. [IV–10] and Choi et al. [IV–11] reported local control rate for NSCLC. In order to compare

both results, the dose dependency of the TCP with the photon beam was fitted by the following formula [IV–12]:

$$TCP = \sum_i \frac{1}{\sqrt{2\pi}\sigma}\left\{-\frac{(\alpha_i-\alpha)^2}{2\sigma^2}\right\} \times \exp\left[-N\exp\left\{-n\alpha d\left(1+\frac{d}{\alpha/\beta}\right)+\frac{0.693\left(T-T_k\right)}{T_p}\right\}\right] \quad \text{(IV–1)}$$

α and β are coefficients of the LQ model of cell survival curves. In the analysis, α and β values of HSG cells were used. σ is a standard deviation of the coefficient α, which reflects patient-to-patient variation of radiosensitivity. N is the number of clonogens in the tumour (a fixed value of 10^9 was used); n and d are total fraction number and fractional dose, respectively. T (42 d), Tk (0 d) and Tp (60 d) are overall times for treatment, 'kick-off' time for tumour cell repopulation, and average doubling time of tumour cells, respectively. Values used in the analysis are shown in brackets. The result is shown in Fig. IV–7. An analysis was carried out on the TCP with the carbon beam. Here, the width of the SOBP and dose averaged LET in the SOBP region were both fixed as 60 mm and 50 keV/μm, respectively, for simplicity. The result is also shown in the figure. It is clear from the figure that the TCP curve of the carbon beam is much steeper than that with the photon beam. The value of sigma in Eq. (IV–1) is 0.18 for the photon beam while for the carbon beam, the value is reduced to 0.11. The result suggests that the carbon beam provides equally excellent local tumour control regardless of individual radiosensitivity.

The difference of TCP slope shown in Fig. IV–7 suggests that, when TCP is regarded as an end point, the RBE value is dependent on the level of the TCP. It is found that NIRS biological RBE value coincides with RBE at 50% TCP whereas the clinical RBE value corresponds to that at 80% TCP.

Currently, the number of fractions used in the clinical trial of NSCLC has been reduced. By applying a σ value deduced from actual clinical results into Eq. (IV–1), it is possible to estimate the TCP of different treatment schedules. Figure IV–8 shows the result of TCP estimation using 1, 4, 9 and 18 fractions. TCP at 80% again coincides with prescribed dose in the clinical trials.

The plan is to extend the analysis to other tumour sites to verify the validity of this TCP analysis for carbon ion therapy. On the other hand, complications in normal tissue (skin reaction) must be also associated with LET and dose and analysed in terms of RBE.

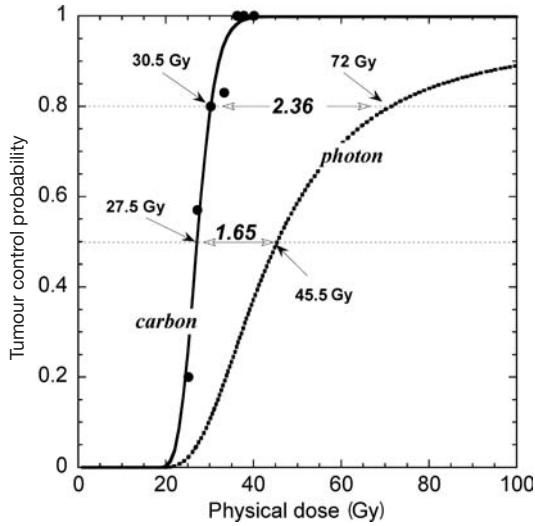

FIG. IV–7. TCP of NSCLC with photon (dashed line) and carbon ion (solid line) beams. Circles show the clinical result at HIMAC. For carbon TCP, the width of the SOBP and LET were fixed as 60 mm and 50 keV/μm, respectively. The values on the blue lines indicate RBE values for the respective TCPs. The theoretical TCP curves were calculated using Eq. (IV–1) and the parameter values shown.

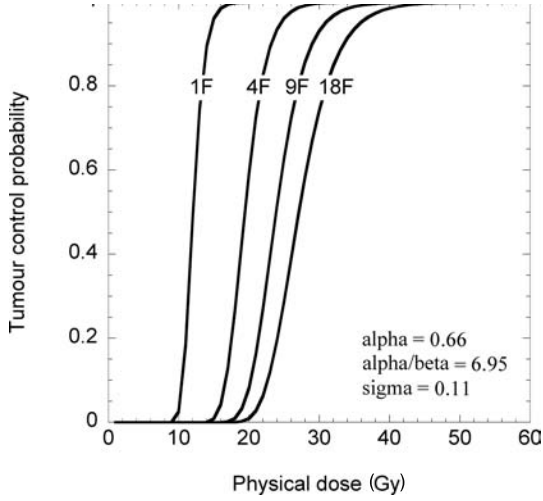

FIG. IV–8. Estimated TCP curves with carbon ion beam for 1 fraction (left curve), 4 fractions (second curve from left), 9 fractions (third curve from left), and 18 fractions (right hand curve).

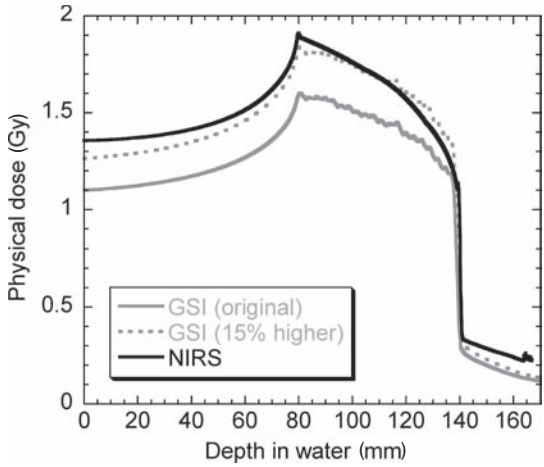

FIG. IV–9. Calculated physical dose distributions that correspond to 4 GyE in the SOBP region by NIRS and GSI methods.

IV–4. COMPARISON OF CLINICAL DOSE WITH GSI

The scheme of determining clinical RBE is different from that used in GSI. As a matter of course, the NIRS 'GyE' can be different from that of GSI. It is indispensable, however, to make both GyE interconvertible to make use of mutual clinical experiences.

As the first step toward achieving this resolution, physical dose distributions were calculated and compared between NIRS and GSI. Boundary conditions of the calculation were as follows:

— SOBP width: 60 mm;
— Prescribed clinical dose: 4 GyE:
  • Target: chordoma;
  • Distal energy: 290 MeV/n.

The SOBP was designed to provide a constant biological effect over the entire SOBP region. The result is shown in Fig. IV–9. It was found that the clinical dose at NIRS is about 15% higher than the technical dose at GSI. In other words, NIRS has a lower RBE value in comparison with GSI. The difference is mainly due to the differences in biological systems and model calculations. What has to be pointed out here is that if a single factor of 115% is applied to the GSI physical dose distribution, the two physical dose distributions are in good agreement. This suggests the potential feasibility of

converting GyE from one to another by multiplying by a single factor. However, the relationship will be affected by changing the dose level, SOBP width, tumour site, etc. It is strongly required, therefore, to extend the comparison for various conditions and tabulate the conversion factor to make both clinical results totally comparable.

IV–5. SUMMARY OF CLINICAL RBE SELECTION

Clinical trials with the carbon beam were started by establishing equivalency between carbon and neutron beams to make use of NIRS experience in neutron therapy. Through biological experiments, it was found that a carbon beam that possesses a dose averaged LET of 80 keV/μm causes equivalent biological responses to those from NIRS neutron beams.

The clinical RBE was defined as 3.0, the same as that used in neutron therapy at the point where dose averaged LET value is 80 keV/μm. The physical dose distribution required in the SOBP was chosen to yield a constant biological response across the SOBP using parameters for HSG cells in the LQ model.

In these 10 years, this scheme realized excellent clinical results. The TCP of lung cancer was well explained by taking into account the patient-to-patient variation of radiosensitivity.

When comparing NIRS '4 GyE' with those estimated at GSI, there was about 15% difference in clinical dose at the middle of the SOBP. It is indispensable in future to establish inclusive convertibility between GSI and other centres to make clinical experiences referable and, as a goal, to contribute in finding optimum heavy ion treatment protocols.

IV–6. CLINICAL STUDIES WITH CARBON IONS

IV–6.1. Fractionation, early versus late effects

The phase I/II dose escalation studies using different fractionation schedules were conducted for five sites of disease listed in Table IV–2. The patients' eligibility was the same in the protocol for each particular site of disease. The dosages were escalated in increments of 10% basically after careful observation of at least three cases treated to the same dose level. Three protocols are ongoing and two protocols are already completed. Results of the various trials are discussed in Section IV–7.

TABLE IV–2. COMPLETED PROTOCOLS OF PHASE I/II CLINICAL TRIAL OF CARBON IONS WITH SAME ELIGIBILITY CRITERIA FOR DIFFERENT FRACTIONATION REGIMES

Period	Fractionation	Pt.	Dose level (GyE)
Head and neck			
June 1994–Feb. 1996	18 fr./6 wks	7	5(48.6, 54.0, 59.4, 64.8, 70.2)
Apr. 1996–Feb. 1997	16 fr./4 wks	19	3(52.8, 57.6, 64.0)
NSCLC			
Oct. 1994–Aug. 1998	18 fr./6 wks	48	7(59.4, 64.8, 72.0, 79.6, 86.4, 90.0, 95.4)
Oct. 1997–Feb. 1999	9 fr./3 wks	34	4(68.4, 72.0, 75.9, 79.2)
Oct. 2000–Nov. 2003	4 fr./1 wk	69	2(52.8, 60.0)
Apr. 2003–	1 fr./1 d		
HCC			
Apr. 1995–Feb. 1997	15 fr./5 wks	24	6(49.5, 54.0, 60.0, 66.0, 72.0, 79.5)
Apr. 1997–Feb. 2001	12 fr./3 wks	33	4(54.0, 60.0, 66.0,69.6)
Apr. 2003–	8 fr./2 wks	22	3(48.0, 52.8, 58.0)
	4 fr./1 wk	28	2(48.0, 528)
	2 fr./1 wk		
UCC			
Apr. 1995–Nov. 1997	24 fr./6 wks	31	5(52.8, 57.6, 62.4, 67.2, 72.0)
Dec. 1997–Feb. 2000	24 fr./6 wks	15	2(68.6,72.8)
Apr. 2000–	20 fr./5 wks		
Pancreas			
Apr. 2000–Feb. 2003	16 fr./4 wks	22	2(44.8, 48.0)
Apr. 2003–	12 fr./3 wks		

IV–6.1.1. Skin reactions in head and neck cancer [IV–13]

Between June 1994 and January 1997, 36 patients with locally advanced, histologically proven, and new or recurrent cancer of the head and neck were treated with carbon ions. A dose escalation study was conducted, delivering 18 fractions through 6 weeks for 17 patients (Group A) and 16 fractions through 4 weeks for 19 patients (Group B). Eligibility and ineligibility criteria were the same in both groups. The dosages were escalated in increments of 10% after careful observation of at least three patients treated with the same dosages. The end points of the study were a grade 3 reaction of the skin and the mucous membrane or local control of the tumours. Follow-up time ranged from 77 to 108 months with a median of 90 months. Grade 3 acute reaction of the

skin was detected in one of the two patients in Group A who were treated with 70.2 GyE through 18 fractions for 6 weeks. In Group B, grade 3 acute skin reaction was detected in 20% (1/5), 27% (2/11) and 67% (2/3) of patients treated with 52.8 GyE, 57.6 GyE and 64.0 GyE through 16 fractions for 4 weeks, respectively. There was only one patient with a grade 3 acute reaction of the mucous membrane. Only one patient developed a grade 2 late reaction of the mucous membrane (superficial ulcer), which was located close to the tumour. No other grade 2 or greater late reaction was noted up to the time of analysis.

IV–6.1.2. Non-small cell lung cancer (NSCLC)

Ten years have passed since clinical trials on NSCLC were started using carbon ions at HIMAC. A discussion of the results is presented in Section IV–2.

IV–6.1.3. Hepatocellular carcinoma (HCC) [IV–14]

Between June 1995 and February 1997, 24 patients with histopathologically proven hepatocellular carcinoma were treated to 15 fractions within 5 weeks in a step-wise dose escalation study. The disease stage was Stage II in 10, IIIA in 6 and IVA in 8 patients. During a median follow-up of 71 months (range, 63–83 months), no severe adverse effects and no treatment related deaths occurred. The Child-Pugh score did not increase by >2 points after the start of therapy. In 78% and in 75% of all patients, the score did not increase by >1 point in the early and late phase, respectively.

Between April 1997 and February 2001, 86 patients with histologically proven hepatocellular carcinoma were enrolled into the prospective clinical study of short course carbon ion radiotherapy. The disease stage (UICC 5th edition) was Stage II in 27, IIIA in 37, and IVA in 22 patients. the Child-Pugh grade was A in 69, B in 14 and not evaluative in 3. Fifty-two patients (60%) had been treated before carbon ion radiotherapy by TAE (43 cases), PEI (31 cases), operation (9 cases) and HIMAC (6 cases), and 31 of them received a combination of these therapies for their hepatic cell carcinoma. The recurrent lesions of 52 patients consisted of local recurrence in 40 and regional recurrence in 12 patients. Thirty-four, 24 and 28 patients were treated to 12 fractions within 4 weeks, 8 fractions within 2 weeks, and 4 fractions within 1 week in a step-wise dose escalation study, respectively. During a median follow-up of 66 (42–87) months, no severe adverse effects and no treatment-related deaths occurred. The Child-Pugh score did not increase by more than 2 points after the start of therapy, except for three patients. In 95% and 78% of all patients, the score did not increase by >1 point in the early

and late phase, respectively. There were no differences among the fractionation schemes in the hepatic toxicity. The adverse effects occurred in the skin. Grade 3 acute skin reaction occurred in two patients (2%) treated with 52.8 GyE 4 fraction regimen and grade 3 late skin reaction was observed in the same two patients.

IV–6.1.4. Uterine cervical cancer (UCC) [IV–15]

A first phase I/II dose escalation study was conducted on 30 patients with locally advanced squamous cell carcinoma of the uterine cervix. In this protocol, the whole pelvis was irradiated with 35.2–48.0 GyE in 16 fractions followed by additional irradiation of 8 fractions to the primary site by carbon ions only. Consequently, the total dose to the primary site was between 52.8 GyE and 72.0 GyE in 24 fractions.

In a second phase I/II study on 14 patients, the pelvis was irradiated with 44.8 GyE in 16 fractions followed by 24.0 GyE or 28.0 GyE in 8 fractions (3.0 or 3.5 GyE per fraction) to the primary site. Consequently, the total dose to the primary site was 72.8 GyE or 68.8 GyE in 24 fractions. From these studies, the tolerance dose to the rectum and sigmoid colon was found to be around 60 GyE in 24 fractions delivered within 6 weeks.

IV–7. CLINICAL RESULTS

The following are clinical results of phase II clinical trials at NIRS.

IV–7.1. Head and neck cancer

Between April 1997 and October 2003, a total of 193 patients were treated with 64.0 GyE through 16 fractions for 4 weeks (20 cases), or 57.6 GyE through 16 fractions for 4 weeks when the dose to the skin was high and high grade skin reaction was expected (173 cases). They consisted of 97 nasal and paranasal sinus, 20 oral cavities, 19 salivary glands, 17 pharynx, 15 orbita, 12 thyroid glands, 5 ears and others. They also consisted of 71 mucosal malignant melanoma, 49 adenoid cystic carcinoma, 18 adenocarcinoma, 13 papillary adenocarcinoma, 10 squamous cell carcinoma, 6 osteosarcoma, 6 mucoepidermoid carcinoma, 3 rhabdomyosarcoma and others. The local control rate was 73% at five years. On the other hand, the overall survival rate was 36% at five years. From the above results, a new dose escalation protocol for bone and soft tissue sarcoma and another new combined protocol with chemotherapy for mucosal malignant melanoma were started from April 2002.

IV–7.2. Lung cancer

Between April 1999 and February 2001, a total of 50 patients with Stage I NSCLC were treated with 72 GyE through 9 fractions for 3 weeks. They consisted of 38 male and 12 female patients, and of 18 cases with squamous cell carcinoma and 32 cases with adenocarcinoma. The five year cause specific survival and overall survival rates were 78.5% and 60.7%, respectively.

IV–7.3. Hepatocellular carcinoma

Between April 2001 and February 2003, a total of 44 patients with hepatocellular carcinoma were treated with 52.8 GyE through 4 fractions for one week. They consisted of 30 male patients and 14 female patients. They consisted of 27 new patients and 17 recurrent and/or residual patients after various kinds of therapy other than radiotherapy. The three year local control rate was 95% and the three year overall survival rate was 72%.

IV–7.4. Prostate cancer

Between April 2000 and October 2003, a total of 176 patients with prostatic cancer were treated with 66 GyE through 20 fractions for 5 weeks or 63 GyE through 20 fractions for 5 weeks for the patients with severe diabetes mellitus. In the phase II trials, patients were divided into 2 groups. Combined carbon ion RT and hormone therapy was given to the high risk group (PSA > 20 ng/ml or Gleason score > 7 or Stage > T2b, 143 cases) and carbon ion radiotherapy alone to the low risk group (33 cases). The three year local control rate, biochemical relapse free rate, disease specific survival rate and overall survival rate were 100%, 90.5%, 95.7% and 91.6%, respectively.

IV–7.5. Bone and soft tissue tumours

Between April 2000 and November 2003, a total of 115 patients with bone and soft tissue tumours were treated with 70.4 GyE (105 cases) or 73.6 GyE (10 cases) through 16 fractions for 4 weeks. The two year local control rate was 90% and the two year overall survival rate was 75% [IV–5, IV–7].

IV–8. IMPLICATIONS FOR TREATMENT PLANNING: VOLUME EFFECTS

In the first phase I/II clinical trials for the prostate gland which consisted of a combination of carbon ion radiotherapy and hormonal therapy, 35 patients with locally advanced (T2b and T3) prostate cancer were treated between June 1995 and December 1997. The indicated dose was stepped up from the initial dose of 54.0 GyE through 20 fractions to 72.0 GyE through 20 fractions, in 10% increments. In this study, 7 out of 35 patients developed grade 3 late rectal and/or genitourinary morbidities, 6 of these were the patients treated with the highest dose of 72.0 GyE and one patient with 66.0 GyE. To address the high rate of grade 3 morbidities, an interim analysis was performed of the risk factors for these morbidities, including dose volume histogram (DVH) analysis. As a result, a high target dose (72.0 GyE) and a large irradiated volume of the rectum were extracted as risk factors. The decision was, therefore, taken to discontinue dose escalation and employ a field shrinkage technique in order to reduce the high dose volume of the rectum. Furthermore, the total dose was reduced to 66.0 GyE through 20 fractions since no local recurrence had been observed at the date of interim analysis. After applying these modifications in the irradiation regime, no grade 3 or higher grade morbidities were observed [IV–13].

REFERENCES

[IV–1] SIHVER, L., TSAO, C.H., SILBERBERG, R., BARGHOUTY, A.F., KANAI, T., Calculations of depth-dose distributions, cross sections and momentum loss, Adv. Space Res. **17** 2 (1995) 105–108.

[IV–2] FUKUTSU, K., KANAI, T., FURUSAWA, Y., ANDO, K., Response of mouse intestine after single and fractionated irradiation with accelerated carbon ions with a spread-out Bragg peak, Radiat. Res. **148** (1997) 168–174.

[IV–3] KANAI, T., et al., Irradiation of mixed beam and design of spreadout Bragg peak for heavy-ion radiotherapy, Radiat. Res. **147** (1997) 78–85.

[IV–4] FURUSAWA, Y., et al., "Difference in the LET-RBE and –OER response to heavy-ions revealed by accelerated ions and cell strains", in: Proc. 3rd Workshop on Physical and Biological Research with Heavy Ions, HIMAC report, NIRS Publication, NIRS-M-99, HIMAC-006, Chiba (1993).

[IV–5] KUBOTA, N., et al., A comparison of biological effects of modulated carbon-ions and fast neutrons in human osteosarcoma cells, Int. J. Radiat. Oncol. Biol. Phys. **33** (1995) 135–141.

[IV–6] LYMAN, J.T., HOWARD, J., KANSTEIN, L., ALONSO, J.R., "Radiological physics of heavy charged-particle beams used for therapy", Biological and Medical Research with Accelerated Heavy Ions at the Bevalac, 1977–1980 (PIRRUCCELLO, M.C., TOBIAS, C.A., Eds), LBL-11220, UC-48, University of California, Berkeley (1980) 319–324.
[IV–7] ITO, H., et al., Carbon beam irradiation of monolayer cells, Nippon Acta. Radiol. **53** (1993) 321–328.
[IV–8] SUZUKI, M., et al., Relative biological effectiveness for cell-killing effect on various human cell lines irradiated with heavy-ion medical accelerator in Chiba (HIMAC) carbon-ion beam, Int. J. Radiat. Oncol. Biol. Phys. **48** (2000) 241–250.
[IV–9] MIYAMOTO, T., et al., Carbon ion radiotherapy for stage I non-small cell lung cancer, Radiother. Oncol. **66** (2003) 127–140.
[IV–10] HAYAKAWA, K., et al., Definitive radiation therapy for medically inoperable patients with stage I and II non-small cell lung cancer, Radiat. Oncol. Invest. **4** (1996) 165–170.
[IV–11] CHOI, N.C.H., DOUCETTE, J.A., Improved survival of patients with unresectable non-small-cell Bronchogenic carcinoma by an innovated high-dose en-bloc radiotherapeutic approach, Cancer **48** (1981) 101–109.
[IV–12] WEBB, S., NAHUM, A.E., A model for calculating tumour control probability in radiotherapy including the effects of inhomogeneous distributions of dose and clonogenic cell density, Phys. Med. Biol. **38** (1993) 653–666.
[IV–13] MIZOE, J.E., et al., Organizing Committee for the Working Group for Head-and-Neck Cancer: Dose escalation study of carbon ion radiotherapy for locally advanced head-and-neck cancer, Int. J. Radiat. Oncol. Biol. Phys. **60** (2004) 358–364.
[IV–14] KATO, H., et al., Results of the first prospective study of carbon ion radiotherapy for hepatocellular carcinoma with liver cirrhosis, Int. J. Radiat. Oncol. Biol. Phys. **59** (2004) 1468–1476.
[IV–15] NAKANO, T., et al., The phase I/II clinical study of carbon ion therapy for cancer of the uterine cervix. cancer, J. Sci. Am. **6** (1999) 362–369.

CONTRIBUTORS TO DRAFTING AND REVIEW

Ando, K.	National Institute of Radiological Sciences, Japan
Andreo, P.	International Atomic Energy Agency
Blakely, E.	Lawrence Berkeley National Laboratory, United States of America
Debus, J.	Deutsches Krebsforschungszentrum, Germany
De Luca, P.	University of Wisconsin Medical School, United States of America
Gahbauer, J.	A. James Cancer Hospital, United States of America
Hendry, J.	International Atomic Energy Agency
Höppner, C.	Siemens Medical Solutions, Germany
Joiner, M.	Wayne State University, United States of America
Kanai, T.	National Institute of Radiological Sciences, Japan
Matsufuji, N.	National Institute of Radiological Sciences, Japan
Menzel, H.	European Organization for Nuclear Research, CERN
Michael, B.	Mount Vernon Hospital, United Kingdom
Mizoe, J.	National Institute of Radiological Sciences, Japan
Scholz, M.	Gesellschaft für Schwerionenforschung mbH, Germany
Wambersie, A.	Université Catholique de Louvain, Belgium
Whitmore, G.	Ontario Cancer Institute, Canada

Technical Meeting

Vienna, Austria, 23–24 June 2004

This report covers all the aspects of the relative biological effectiveness (RBE) of ion beams, including laboratory measurements of RBE and the important variables that influence it, dose related quantities and units, and approaches to the clinical use of the concept of RBE based on experimental findings, theoretical models, and previous clinical experience with fast neutrons and ions. RBE is a simple concept but its clinical application is complex. Future developments in ion therapy will require a coherent approach to the reporting of therapies and their outcomes, not only for comparison with other ion facilities but also with conventional and newly developing photon irradiation techniques. The report is the result of a joint initiative between the IAEA and the International Commission on Radiation Units and Measurements, and is the only current extensive review of ion RBE.

INTERNATIONAL ATOMIC ENERGY AGENCY
VIENNA
ISBN 978–92–0–107807–0
ISSN 0074–1914